

University of Nebraska - Lincoln

DigitalCommons@University of Nebraska - Lincoln

Civil Engineering Theses, Dissertations, and
Student Research

Civil Engineering

Spring 5-4-2012

Prestressed Concrete Wind Turbine Supporting System

Ibrahim Lotfy

University of Nebraska – Lincoln, ilotfy@unomaha.edu

Follow this and additional works at: <http://digitalcommons.unl.edu/civilengdiss>



Part of the [Civil Engineering Commons](#)

Lotfy, Ibrahim, "Prestressed Concrete Wind Turbine Supporting System" (2012). *Civil Engineering Theses, Dissertations, and Student Research*. 45.

<http://digitalcommons.unl.edu/civilengdiss/45>

This Article is brought to you for free and open access by the Civil Engineering at DigitalCommons@University of Nebraska - Lincoln. It has been accepted for inclusion in Civil Engineering Theses, Dissertations, and Student Research by an authorized administrator of DigitalCommons@University of Nebraska - Lincoln.

PRESTRESSED CONCRETE WIND TURBINE SUPPORTING SYSTEM

By

Ibrahim Lotfy

A THESIS

Presented to the Faculty of

The Graduate College at the University of Nebraska

In Partial Fulfillment of Requirements

For the Degree of Master of Science

Major: Civil Engineering

Under the Supervision of Professors Maher Tadros and George Morcous

Lincoln, Nebraska

May, 2012

PRESTRESSED CONCRETE WIND TURBINE SUPPORTING SYSTEM

Ibrahim Lotfy M.S.

University of Nebraska, 2012

Advisors: Maher Tadros and George Morcous.

Wind energy is one of the most commercially developed and quickly evolving renewable energy technologies worldwide. Wind turbines are commonly supported on tubular steel towers. As the turbines are growing and the towers are elevating, an increase in structural strength and stiffness is required to withstand the applied forces. Recent studies established concrete as a more economic and durable alternative to steel especially when the tower height exceed 240ft. Presently, concrete towers are not common due to their perceived heavy weight and assembly complexity. One of the systems that have been mentioned in the literature consists of precast rings that are post-tensioned together and assembled at the turbines site. While the tubular shape is compatible with wind variation and behavior, its construction process can be burdensome, demanding and expensive. In this thesis, an effort to reduce the construction cost is proposed by developing a precast prestressed concrete system that consists of vertical columns and horizontal panels. Composed of simple precast elements, this system is easy to transport, assemble and erect, plus it will reduce the post-tensioning costs. The proposed system has a triangular shaped cross-section that consists of three columns at each corner of the triangle connected together with commonly used precast concrete wall panels. The tower has a tapered profile to reduce the area subjected to wind thus lower the total weight and applied moment. It will also enhance the dynamic response of the tower and improve its overall stability. This thesis presents analysis and design of 240ft and 320ft high supporting systems under dead, wind and seismic loading. A comparison between the proposed system and current concrete and steel systems is also presented in terms of behavior, ease of construction and cost.

ACKNOWLEDGEMENTS

First, I would like to express my appreciation and gratitude to my advisor, Professor Maher Tadros, for his expertise, guidance and encouragement throughout my entire master's study in UNL. I would also like to express my appreciation to my co-advisor, Professor George Morcous, for his guidance throughout my courses and laboratory experiments and his help and support with my thesis. I feel privileged to have had the opportunity to study under both of their supervisions.

I also want to thank Professor Christopher Tuan for his help and support during my master's studies and for providing some modeling insights and advice with my thesis. My appreciation and gratitude goes to Professor Terri Norton for her contribution to my work and her guidance throughout the structural dynamics analysis in my thesis.

I thank the all of the aforementioned professors for serving on my Master's Thesis defense committee.

I would also like to thank Dr. Kromel Hanna for his early contribution and this important role in both my master's studies and my thesis.

I also want to thanks my fellow graduate students, Eliya Henin, Afshin Hatami, Jenna Hansen, Yaohua Deng, Peter Samir and Nathan Toenies for their friendship, their belief in me and their help throughout my time in UNL.

I also want to thank my family for believing in me and supporting me during my studies abroad.

CONTENTS

Contents	iv
List of figures	viii
List of Tables	xii
1. Introduction	1
1.1 Background.....	1
1.1.1 A window to the past	1
1.1.2 Status Quo.....	2
1.1.3 Future Development.....	6
1.2 Problem Statement.....	6
1.3 Research Objectives.....	7
1.4 Scope of this Research.....	8
1.5 Thesis Organization	8
2. Literature Review	10
2.1 Concrete vs. Steel	10
2.2 Current Concrete Applications	17
2.3 Concrete's Appeal.....	26

3. Proposed System	29
3.1 System Description	29
3.2 Construction Sequence	35
3.3 Expected Benefits	38
3.4 Design Procedures and Standards	40
3.5 Dynamic Concerns	42
3.5.1 Dynamic Properties Interpretation	44
4. Loading	47
4.1 Wind Turbine Generator	47
4.1.1 Wind Models	47
4.1.2 Safety Factors for Wind Turbine	48
4.2 Wind Turbine Loads	49
4.3 Direct Wind Pressure on the Tower	50
4.4 Fatigue Loads	56
4.4.1 S-N Curves	56
4.4.2 Dynamic Load Simulation	57
4.4.3 Damage Equivalent Load Method	58
4.5 Seismic Loading	58
4.5.1 Design Response Spectrum	60
4.5.2 Seismic Design load	61
4.6 Load Combinations	63

5. Analysis and Design	65
5.1 System Properties and Dimensions.....	65
5.2 Design Approaches	67
5.3 Modeling.....	67
5.3.1 Elements Role and Load Path	68
5.3.2 Tower's profile.....	69
5.3.3 Finite Element Models.....	70
5.3.4 Conclusions.....	73
5.4 Design	76
5.4.1 Concrete Design.....	76
5.4.2 Steel Design	98
5.4.3 Recommended design Procedures for the proposed system	101
6. Summary and Conclusions	102
6.1 Design Summary.....	102
6.2 Quantities.....	109
6.3 Systems Comparison.....	110
6.3.1 Comparing the 240ft systems.....	110
6.3.2 Comparing the 320ft systems.....	112
6.4 Conclusions.....	115

Bibliography	117
A. Wind Turbine Specifications and Loads	120
B. 240 ft Proposed Concrete System Design	122
C. 240 ft Steel Tower Design	172
D. Dynamic Analysis	190

LIST OF FIGURES

Figure 1-1: Development of wind turbines. (US department of energy, 2008).....	2
Figure 1-2: World's new and cumulative installed capacity [MW]. (WWEA, 2011).....	3
Figure 1-3: Expected growth of the world installed capacity [MW]. (WWEA, 2011)	4
Figure 1-4: United States installed capacities map [MW]. (AWEA, 2011)	5
Figure 1-5: Installed capacities by state [MW]. (AWEA, 2011)	5
Figure 2-1: Transportation of complete steel tube segments. (Sri, S., 2011)	11
Figure 2-2: Blades transportation. (Sri, S., 2011).....	11
Figure 2-3: Nacelle transportation. (Sri, S., 2011).....	12
Figure 2-4: Lifting of complete steel tube segments. (Sri, S., 2011).....	12
Figure 2-5: Erection of steel towers. (Sri, S., 2011)	13
Figure 2-6: Nacelle placement. (Sri, S., 2011)	14
Figure 2-7: Blade tipping using two cranes. (Sri, S., 2011).....	15
Figure 2-8: Blade lifting using two cranes. (Sri, S., 2011).....	16
Figure 2-9: Advanced Tower Systems hybrid tower. (Vries, 2009).....	18
Figure 2-10: 328ft concrete wind turbine with a power of 3.6MW. (LaNier, M.W., 2005)	20
Figure 2-11: Enercon wind turbine with rated power 7.5MW. (Enercon GmbH).....	22
Figure 2-12: The Concrete Center 328ft concrete tower. (The Concrete Center, 2007) ..	23

Figure 2-13: The Concrete Center 328ft construction. (The Concrete Center, 2007)	24
Figure 2-14: Construction of an Inneo Torres tower in Spain. (Jimeno, J., 2012)	25
Figure 3-1: Tower's cross section.....	30
Figure 3-2: Column's cross section.	31
Figure 3-3: Tower's vertical profile for 320ft (left) and 240ft (right) systems.	33
Figure 3-4: 240ft system's elevation.....	34
Figure 3-5: Segment 1 columns erection and slope control.....	36
Figure 3-6: Segment 1 panels installation.....	36
Figure 3-7: Segment 2 erection.....	37
Figure 3-8: Segment 3 erection.....	37
Figure 3-9: Nacelle and blades installation.....	38
Figure 3-10: Design procedures for proposed system.	41
Figure 3-11: Natural frequencies of different towers and operational frequency range... 43	
Figure 3-12: Mode shapes and natural periods for the 320ft proposed system.	46
Figure 4-1: Wind pressure profile along the 240ft tower height.	52
Figure 4-2: EN and AISC fatigue strength curve as shown in ASCE/AWEA RP2011. ..	57
Figure 4-3: Design response spectrum.....	61
Figure 5-1: Load path for direct wind pressure (S-N direction).	69
Figure 5-2: Axial forces in columns (left) and panels (right) (240ft tower).....	71
Figure 5-3: Panel represented as tie beams.....	72
Figure 5-4: Panel represented as X-bracing.....	73
Figure 5-5: SAP models: tie beam (left) shell (middle) X-bracing (right) (320ft tower). 74	

Figure 5-6: Free body, shear and moment diagrams for panels.....	75
Figure 5-7: Base segment column cross section.	79
Figure 5-8: Base segment column interaction diagram (240ft tower).	80
Figure 5-9: Straining actions on panels according to wind direction.	87
Figure 5-10: Linear strain distribution in normal beams. (Nawy, E., 2008).....	89
Figure 5-11: Nonlinear strain distribution in deep beams. (Nawy, E., 2008).....	89
Figure 5-12: Panel reinforcement details.....	90
Figure 5-13: Panel connection cross section details.	93
Figure 5-14: Panel connection elevation details.	94
Figure 5-15: Column splice details.	96
Figure 5-16: Base connection details.....	97
Figure 6-1: The 240ft proposed concrete system's design plan.	105
Figure 6-2: The 240ft Steel tower's design plan.....	106
Figure 6-3: The 320ft proposed concrete system's design plan.	107
Figure 6-4: The 320ft concrete circular tower's design plan. (LaNier, M.W., 2005).....	108
Figure B-1: Tower profile.....	123
Figure B-2: Tower cross section.	124
Figure B-3: Column cross section.....	124
Figure B-4: Velocity pressure along the tower height.	131
Figure B-5: Moment distribution in the X-direction.....	136
Figure B-6: Moment distribution in the Y-direction.....	136
Figure B-7: Design response spectrum.	138

Figure B-8: Segments 1 columns interaction diagram.....	142
Figure B-9: Segments 2 columns interaction diagram.....	148
Figure B-10: Segments 3 columns interaction diagram.....	154
Figure B-11: Panel connection cross section details.....	167
Figure B-12: Panel connection elevation details.	168
Figure C-1: Velocity pressure along the tower's height.	177
Figure C-2: Moment distribution along the tower's height.	181
Figure C-3: Design Response spectrum.....	182
Figure C-4: Demand to capacity ratio.....	189
Figure D-1: Lumped mass model.	191
Figure D-2: Modal and total top deflection for triangular (left) and circular (right) tower. (MATLAB model).....	194
Figure D-3: Modal and total top deflection for triangular (left) and circular (right) tower. (SAP model).....	195
Figure D-4: SAP model for the triangular system.	196
Figure D-5: Mode shapes and periods for the triangular system.....	197

LIST OF TABLES

Table 3-1: Natural frequencies of different towers and operational frequency range.	43
Table 3-2: Modal properties comparison for 320ft concrete systems.....	45
Table 4-1: Force coefficient for towers*.	54
Table 4-2: Force coefficient for the 240ft proposed concrete tower cross section.....	55
Table 4-3: Force coefficient for the 320ft proposed concrete tower cross section.....	55
Table 4-4: Force coefficient for the 240ft steel tower (smooth surface).	55
Table 4-5: ratio of the seismic force to the wind force.....	62
Table 4-6: ASCE 7-10 load combinations.....	63
Table 5-1: The 240ft concrete tower properties.....	65
Table 5-2: The 320ft concrete tower properties.....	66
Table 5-3: The 240ft steel tower properties.....	66
Table 5-4: Axial forces acting on the critical section of the columns.	74
Table 6-1: The 240ft systems design summary.	103
Table 6-2: The 320ft systems design summary.	104
Table 6-3 Material quantities and cost.....	109
Table A-1: Wind turbine specifications.....	120
Table A-2: Wind turbine loads.	121
Table A-3: Wind turbine fatigue loads.	121

Table B-1: Force coefficient for towers*	132
Table B-2: Force coefficient for proposed cross section ($h/D=8.776$)	132
Table B-3: Ultimate loads acting on segment 1 columns.	140
Table B-4: Segments 1 column properties.....	142
Table B-5: Service and operational loads check for segment 1 columns.	143
Table B-6: Shear check for segment 1 columns.	145
Table B-7: Ultimate loads acting on segment 2 columns.	147
Table B-8: Segment 2 column properties.	149
Table B-9: Service and operational loads check for segment 2 columns.	149
Table B-10: Shear check for segment 2 columns.	151
Table B-11: Ultimate loads acting on segment 3 columns.	153
Table B-12: Segment 3 column properties.	155
Table B-13: Service and operational loads check for segment 3 columns.	155
Table B-14: Shear check for segment 3 columns.	157
Table B-15: Panels properties.....	162
Table B-16: Panels design for out of plane bending (as slab).	163
Table B-17: Panels design for shear and in plane bending (as deep beam).....	164
Table B-18: Panels connection properties.	169
Table B-19: Panels connection design.....	169
Table B-20: Base connection design.....	171
Table C-1: Force coefficient for the circular tower*.	178
Table D-1: Lumped mass model properties.....	191

Table D-2: Modal properties..... 192

Table D-3: MATLAB and SAP result comparison..... 195

CHAPTER 1

INTRODUCTION

1.1 Background

1.1.1 A window to the past

Wind energy is abundant; it is a free source of renewable energy that has been used for decades. Ever since man decided to build ships and conquer the sea, wind energy was the force blowing those sails and driving these ships. And when he built windmills, either for grinding grains or pumping water, wind energy was the reason those windmills were turning. Still to this day, some farmers use wind energy for those small applications as oppose to using fossil-fueled engines. The introduction of wind turbines as means to generate electricity can be traced back to the late nineteenth century; however, they received little interest all throughout the twentieth century. In the mid-seventies, the spike in oil prices aroused concerns over the limited fossil-fuel resources that were the main stimuli that drove a lot of government-funded programs and researches towards wind energy alternatives. After the emergence of the three-bladed, stall-regulated rotor and fixed-speed, the simple architectural design that is implemented in today's wind

turbines, the industry flourished in USA, Europe and worldwide (Burton et al., 2001).

Figure 1-1 shows the evolution of wind turbines rotor diameters.

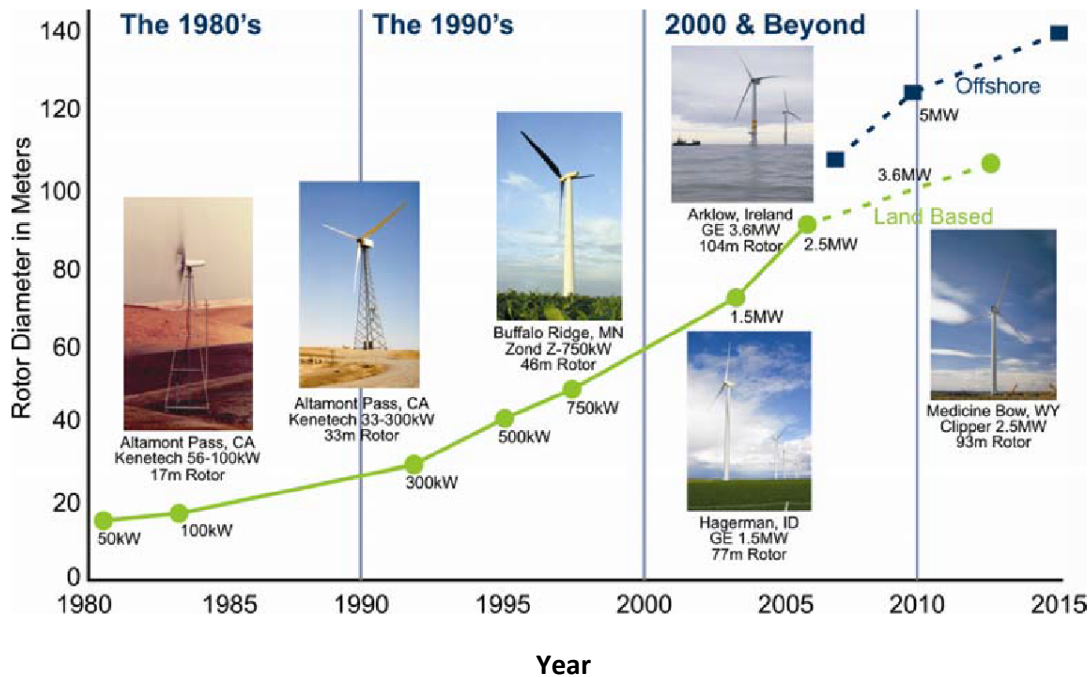


Figure 1-1: Development of wind turbines. (US department of energy, 2008)

1.1.2 Status Quo

In today's world, the fact that harnessing wind power is a green energy makes it even a much more attractive solution in today's society, where the emphasis is on environmental issues, reduction of CO₂ emissions and limiting climate changes. Numerous efforts and accomplishments in engineering design, materials, aerodynamics and production pushed wind energy technologies to the next level and granted it a competitive edge among other energy sources. Now, wind energy is one of the most commercially developed and quickly evolving renewable energy technologies worldwide. Wind turbines have grown

both in size and efficiency; rotor diameters increased to 393.70ft, towers risen over 328.08ft and power output reached 5 megawatts (MW) (The Concrete Center, 2007).

World Wind Energy Association, (2010) confirms that wind power is always growing and it follows the same trend; the installed capacity more than doubles every third year. Furthermore, with the increasing awareness of the economic, social and environmental benefits of wind power, the growth rate is predicted to increase exponentially in the near future and a global capacity of 600,000MW is expected by 2015. Figure 1-2 and Figure 1-3 show the new and total installed world capacity in the last decade and the predicted wind energy growth projection.

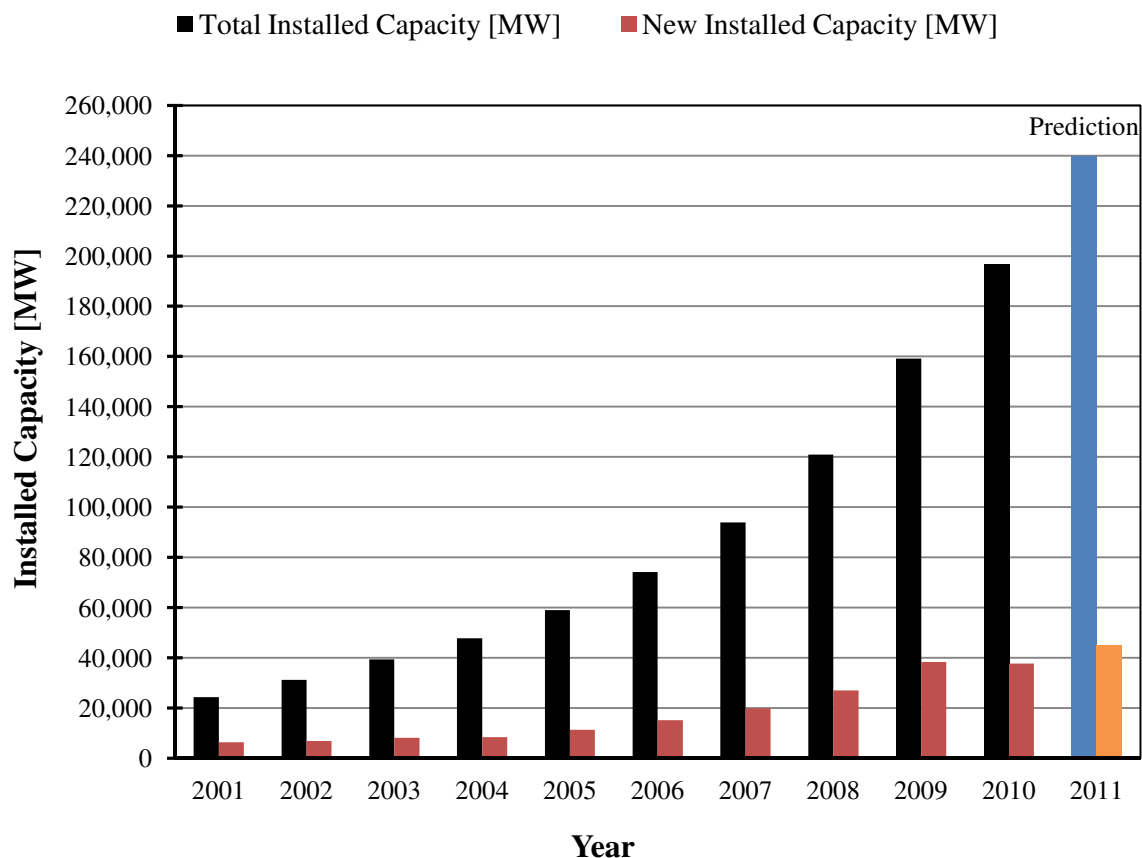


Figure 1-2: World's new and cumulative installed capacity [MW]. (WWEA, 2011)

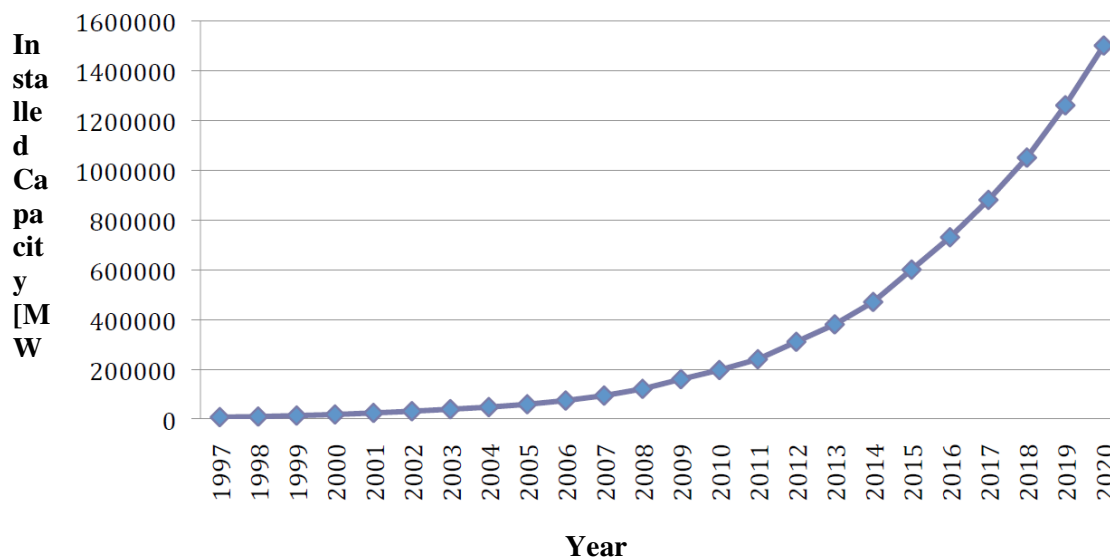


Figure 1-3: Expected growth of the world installed capacity [MW]. (WWEA, 2011)

The United States has established itself as one of the world's largest markets in wind energy. And despite of its market slowdown in 2010, the United States has maintained its status by producing a total of 40,180MW preceded only by China with 44,733MW.

Among the fifty states, Texas is leading the way in total harnessed capacity followed by Iowa. From Figure 1-4 and Figure 1-5, it's obvious that the mid-west has a lot of potential when it comes to wind energy. Most of the mid-west states already have a significant basis of operational wind farms that can be relied on for their energy production, and there is still a lot of room for further developments (American Wind Energy Association, 2011). The state of Nebraska has the fourth greatest wind energy potential among the nation. It had a cumulative wind energy production of 337MW through 2011 year's end.

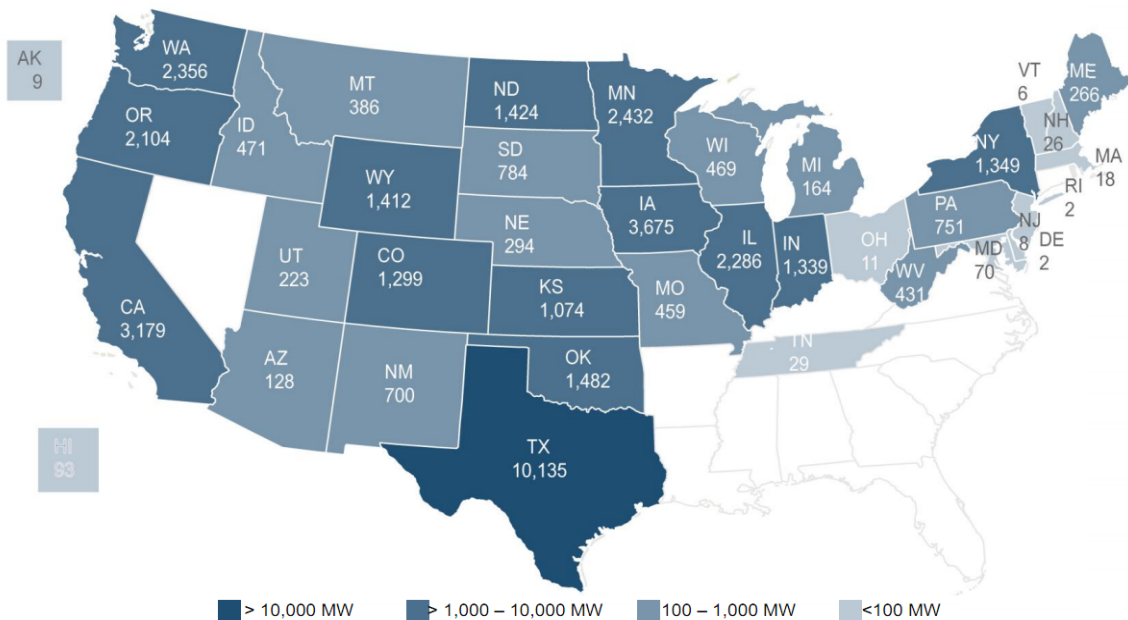


Figure 1-4: United States installed capacities map [MW]. (AWEA, 2011)

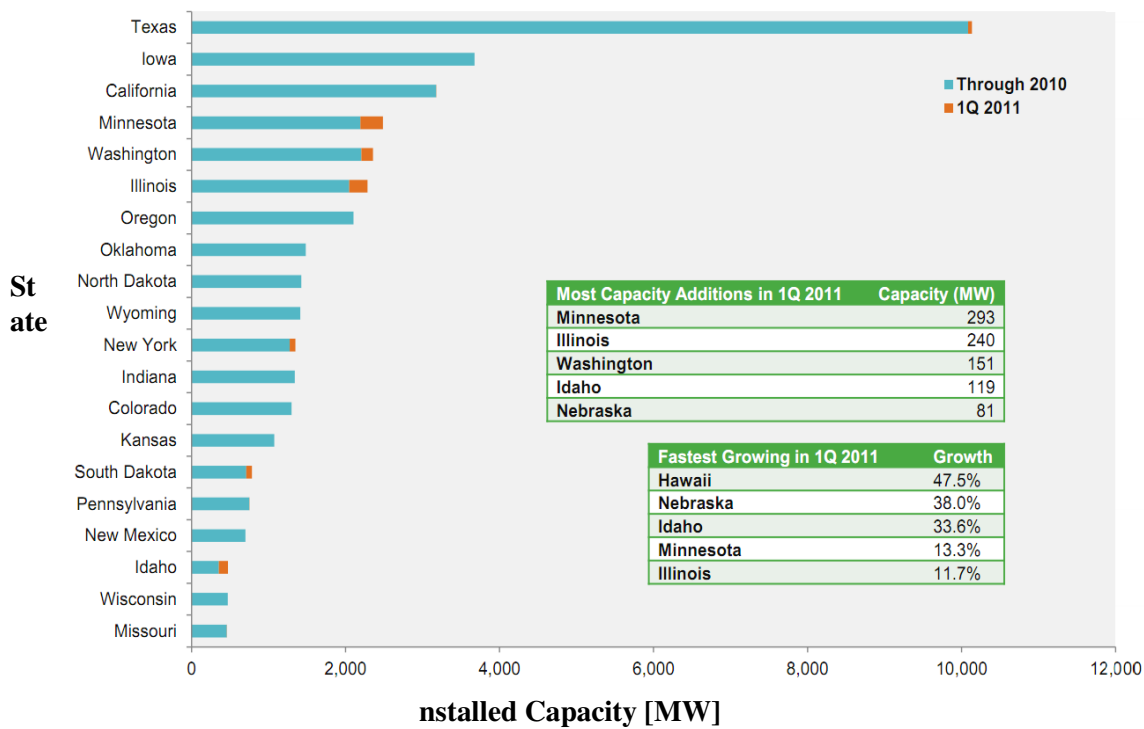


Figure 1-5: Installed capacities by state [MW]. (AWEA, 2011)

1.1.3 Future Development

Between the constant attention that the industry is getting and the continuous development in technology, the future is bound to be even brighter than ever featuring taller, bigger and more efficient wind turbines. It is obvious from Figure 1-3 that the world growth rate is expected to increase exponentially in the future. The same scenario applies for the US growth rate as well. The US Department of Energy, (2008) confirms that the US wind industry is on track to achieve a 16,000MW/year growth approaching 2030 consistent with the expectation of supplying 20% of the US energy from wind energy by 2030 year end.

1.2 Problem Statement

Wind turbine generators are commonly supported on steel structures; either trussed or tubular tower. As the turbines are growing and the towers are elevating, an increase in structural strength and stiffness is required to withstand the applied forces. Recent studies established concrete as a more economic and durable alternative to steel especially when the tower height exceed 240ft. Presently, concrete towers consist of precast rings that are post-tensioned together and assembled at the turbines site. While the tubular shape is compatible with wind variation and behavior, its construction process can be burdensome, demanding and expensive. In this thesis, an effort to reduce the construction cost is proposed by developing a precast prestressed concrete system that consists of vertical columns and horizontal panels. Composed of simple precast concrete elements,

this system is easy to transport, assemble and erect, plus it will reduce if not eliminate the post-tensioning costs.

1.3 Research Objectives

The objective of this research is to develop a concrete precast prestressed wind turbine supporting system solution that is competitive for hub height* exceeding 240ft where construction methodology and logistics are optimized. This objective can be broken down into smaller tasks:

- Simplify concrete forming and casting by reducing the complexity of the precast sections and standardizing them for multiple use.
- Prescribe design procedures compatible with the new shape.
- Optimize the design of the concrete elements in terms of concrete dimensions and steel reinforcement.
- Consider transportation restraints.
- Reduce or eliminate the need for post-tensioning tendons.
- Achieve a fast erection time.
- Maintain the desired aesthetics of the wind turbine tower.

* Hub height is the height measured from the ground level to the center of rotation of the wind turbine blades.

1.4 Scope of this Research

This research is intended for wind turbine structures located in the Mid-West region of the US using wind speeds and seismic acceleration accordingly. This main concern of this research is wind turbines supporting systems and towers; limited literature concerning the turbine mechanisms, aerodynamics or fluid mechanics is included. Concrete applications are the main focus of this research; some steel applications, analysis and design are presented for comparative illustrations.

This thesis presents analysis and design of 240 and 320ft high supporting systems under dead, wind and seismic loading. Comparison between the 240ft proposed system and the current steel solutions with the same hub height, the 320ft proposed system and the current concrete solutions with the same hub height are included.

1.5 Thesis Organization

Chapter 1: This chapter gives a general introduction about wind energy in the US and Worldwide, and it presents the problem statement and the research objectives of this thesis.

Chapter 2: This chapter discusses the available concrete systems that are currently being used by manufacturers and the systems proposed for future use.

Chapter 3: This chapter presents a detailed description of the system proposed in this thesis outlining its advantages and construction sequence. Proposed design procedures are also illustrated.

Chapter 4: This chapter explains the various loads applied on the proposed system along with the standards followed.

Chapter 5: This chapter presents the modeling techniques implemented to accurately represent the structure in a finite element model using SAP 2000 and the design methodology followed when designing the individual tower elements and the corresponding design standards.

Chapter 6: This chapter presents a summary of the system investigated and a comparison between them. It also contains the conclusions drawn from this study.

CHAPTER 2

LITERATURE REVIEW

2.1 Concrete vs. Steel

Concrete has always been the competitive choice for tower like structures including tall chimneys, poles and bridge piers. However that is not the case for wind turbines towers as tubular steel towers have monopolized the market. The reason for steel dominance is due to the fast construction time. Steel towers are light and fast however the global wind market now trends toward higher and larger wind turbines to reduce energy cost and the tubular steel solution cannot keep up with this trend as its erection speed is tied to transportation of complete tube segments to the site which limits the maximum tower diameter to 14.5ft. Almost every wind turbine exceeding 320ft hub height and rated power over 2 to 3MW has employed an alternative tower solution, and turbine manufacturers are investigating new feasible and cost-effective solutions for these turbines. Although precast concrete solutions were initially implemented to reach height where conventional steel tower could not, they proved to be a profitable solution for conventional hub heights. Figure 2-1 through Figure 2-8 shows the construction sequence of steel towers.



Figure 2-1: Transportation of complete steel tube segments. (Sri, S., 2011)



Figure 2-2: Blades transportation. (Sri, S., 2011)



Figure 2-3: Nacelle transportation. (Sri, S., 2011)



Figure 2-4: Lifting of complete steel tube segments. (Sri, S., 2011)



Figure 2-5: Erection of steel towers. (Sri, S., 2011)



Figure 2-6: Nacelle placement. (Sri, S., 2011)

The nacelle of the wind turbine is the heaviest component in the wind turbine structure; therefore the choice of the crane is dependent on its weight. The weight of the 3.6MW wind turbine generator is 350tons. However, the erection of the blades is the most challenging procedure of the construction process as two cranes have to be used to balance and tip the blades and orient them into the vertical direction without dragging them through the ground and potentially damaging them (see Figure 2-7 and Figure 2-8).



Figure 2-7: Blade tipping using two cranes. (Sri, S., 2011)



Figure 2-8: Blade lifting using two cranes. (Sri, S., 2011)

2.2 Current Concrete Applications

Many manufacturers have experimented with new concepts involving precast concrete that can overcome the transportation issues plaguing the tubular steel tower. General Electric, Nordex, WinWinD and Alstom-Ecotecnia have experimented with a hybrid tower setup where the top is a conventional tubular tower supported by in situ concrete.

Vries, (2009) presented a new concrete-steel hybrid wind turbine supporting system developed by Advanced Tower Systems (a joint venture between two Dutch companies, engineering consultancy Mecal BV, large general contractor Hurks BV and a German renewable energy project developer Juwi Holding). Their research efforts aimed to find an optimized tower cross section for the bottom concrete segment suitable for manufacturing. After investigating several shapes they settled on a square cross section with rounded edges. The tower had a hub height of 435ft and supported a 2.3MW Siemens wind turbine. Its cross section consisted of four identical cylindrical-shaped 90 degree corner elements and four flat tapered elements that fit in between them, as shown in Figure 2-9. At its base, the sides of the tower measured 27.23ft. This would allow for a single mold to fabricate all the rounded elements. The upper steel tower was a conventional tubular tower, thus its max diameter was constrained by logistics; max steel tubular steel diameter shouldn't exceed 14.5ft. In consequence, larger wind turbines tower would feature a shorter steel segment so that its max diameter stays in the practical range. To properly connect the steel and concrete segments a square-shaped adaptor was integrated into the top section of the concrete tower. The steel tubular segment was

fastened in the concrete adaptor with the aid of long studs passing through the concrete and fastened from inside. To erect the concrete segment each additional layer is partly assembled on the ground into two halves before hoisting. After placement of the concrete components the structure was post-tensioned.



Figure 2-9: Advanced Tower Systems hybrid tower. (Vries, 2009)

LaNier, M.W., (2005) presents a study done by the National Renewable Energy Laboratory to investigate the feasibility of using wind turbines in low wind speed sites. The wind turbine tower designs were done by BERGER/ABAM Engineers Inc. where different setups and concepts were investigated to determine the most economical approach. The concepts investigated were a tubular steel setup, a steel/concrete hybrid system and an all-concrete tower. The 328ft all-concrete tower, supporting a wind turbine of a rated power of 3.6MW, had a base diameter of 22ft and a top diameter of 12ft. Its base wall thickness was 2.25ft and its top wall thickness was 1.5ft. The designers used a combination of tendons and steel rebar to reinforce the tower and resist the straining actions applied. Figure 2-10 shows the design plans for the all concrete 328ft tower supporting a wind turbine with a rated power of 3.6MW.

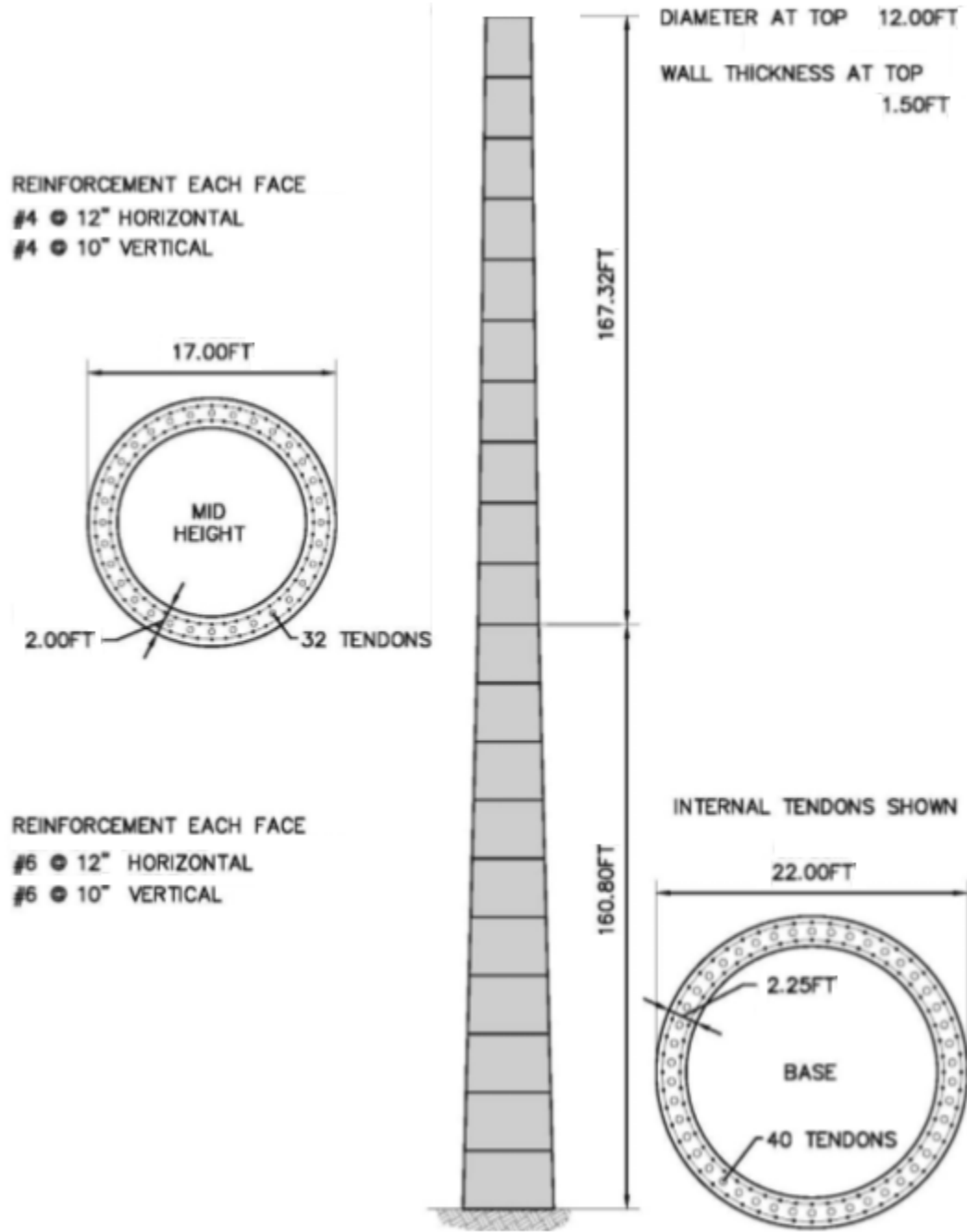


Figure 2-10: 328ft concrete wind turbine with a power of 3.6MW. (LaNier, M.W., 2005)

Acciona Windpower and Enercon have had greater progress with precast concrete towers. Enercon (Enercon GmbH) now is offering precast concrete towers on a commercial scale for wind turbine having a hub height of 246ft and above. The tower consists of precast concrete rings that increase in diameter the closer they are to the tower base with the lower rings split vertically for logistical issues. After placement, the rings are post-tensioned in the vertical direction, Figure 2-11 shows an Enercon wind turbine model E126 and rated power 7.5MW.

The Concrete Center, (2007) offered a similar solution for wind turbine having a hub height of 230ft and 328ft. The towers were supporting wind turbines with a rated power of 2MW featuring 131ft long blades and 4.5MW featuring 197ft long blades respectively. The 230ft tower had a uniform taper while the 328ft tower had a bi-linear one. The tower's diameters at the base are 24.6ft and 39.4ft. A reinforced concrete footing was used to support the structures. Construction process: After the delivery of the ring segments to the construction site, vertical segments of max four rings (39.4ft tall) are assembled on the ground then post-tensioned with minimum prestress force to maintain its stability while hoisting the segment into its place. After placement, the segment would then be post-tensioned with the bottom of the tower with enough force to maintain its stability. After the whole tower is constructed, the main and final post-tensioning is then applied throughout the whole height of the tower. Figure 2-12 shows the elevation of the 328ft tower while Figure 2-13 shows its construction sequence. This study concluded that not only precast concrete solutions can potentially save over 30% compared to its steel counterpart; it can also prolong the service life of the wind turbine to about 40-60 years.



Figure 2-11: Enercon wind turbine with rated power 7.5MW. (Enercon GmbH)

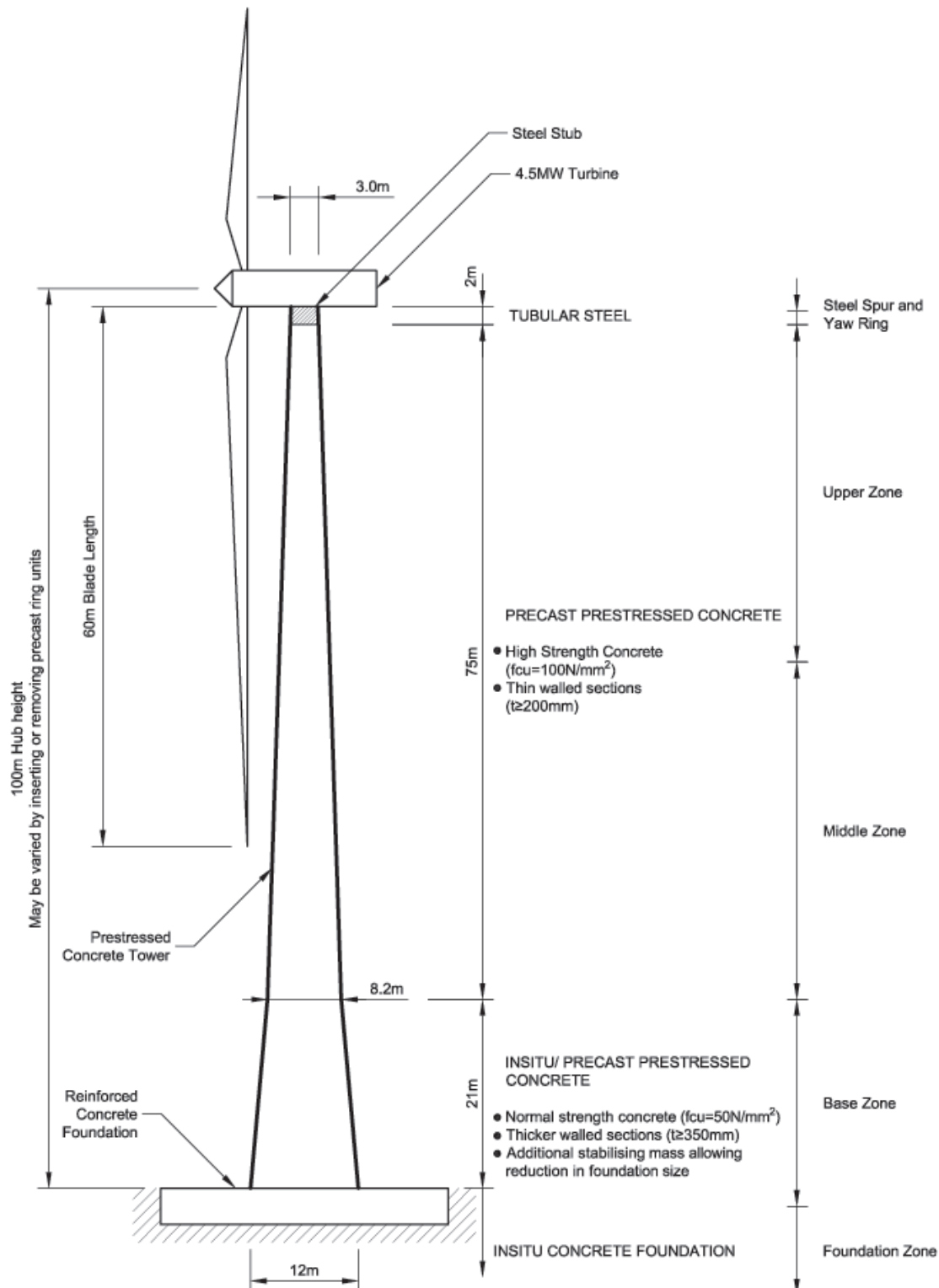


Figure 2-12: The Concrete Center 328ft concrete tower. (The Concrete Center, 2007)

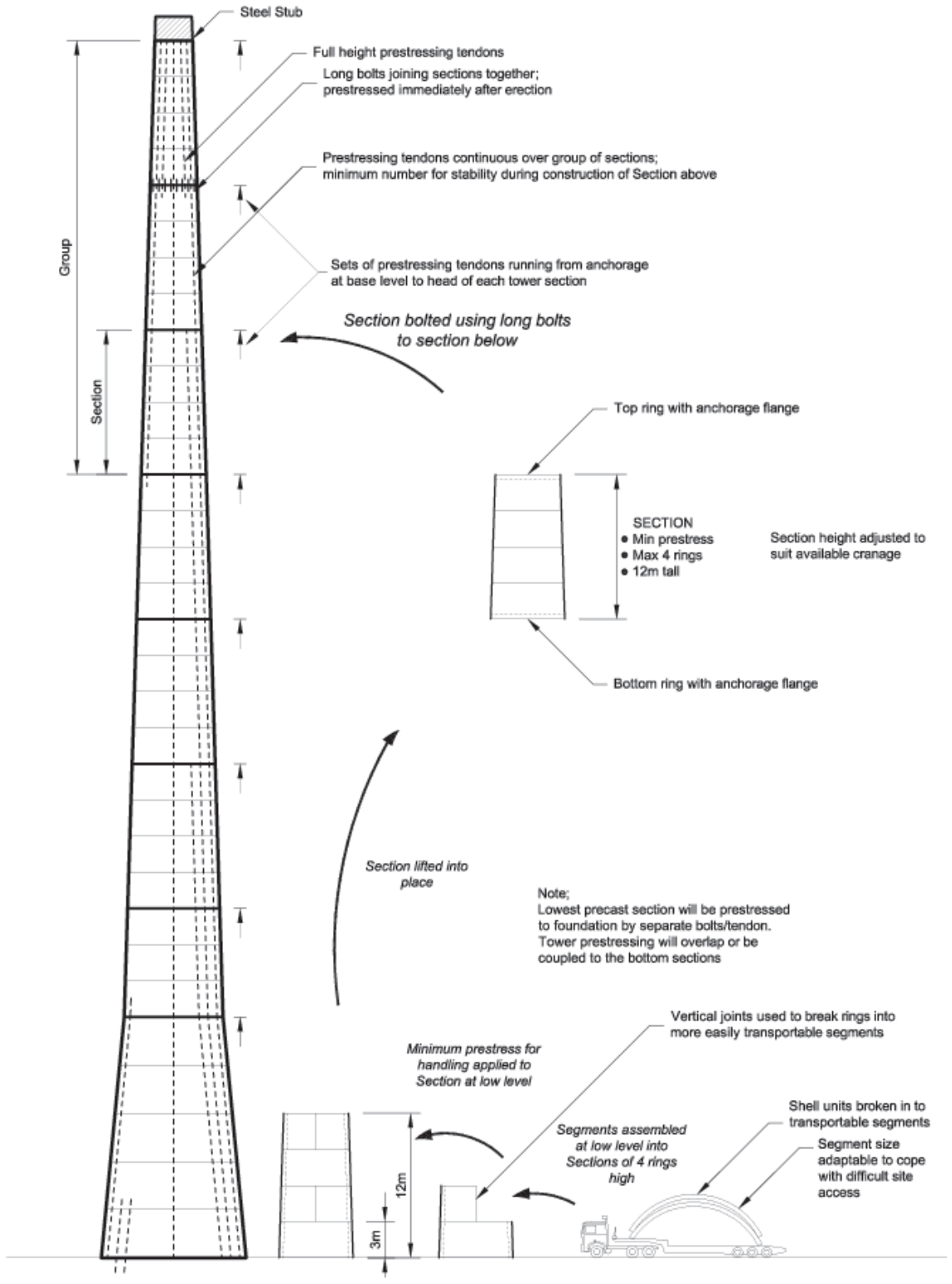


Figure 2-13: The Concrete Center 328ft construction. (The Concrete Center, 2007)

Jimeno, J., (2012) explains another precast concrete tower concept developed by the Spanish company “Inneo Torres” for hub heights of 262ft, 328ft and 393ft and rated power of 1.5MW to 4.5MW. The concept consists of few large precast elements in the form of long narrow panels. The tower is divided into large segments, typically 65ft, and each segment is divided vertically into panel-ring sectors that fit together. During erection, sectors are assembled then hoisted in place. By reducing the number of precast elements, the system managed to achieve a rate of two towers per week, similar to erection rates of its tubular steel counterpart. Figure 2-14 shows the construction of an Inneo Torres tower in Spain.



Figure 2-14: Construction of an Inneo Torres tower in Spain. (Jimeno, J., 2012)

2.3 Concrete's Appeal

As the turbines are growing and the towers are elevating, an increase in structural strength and stiffness is required to withstand the applied forces. This will introduce transportation issues for steel towers, bearing in mind that 14.5ft limit for the diameter of complete ring sections that can be transported along the public highway. While researchers and manufactures are working to develop segmented designs to offset this limitation, costly bolted connections would have to be introduced into the thickest and most heavily loaded sections of the tower. On the other hand, not only do precast concrete towers accommodate these requirements, they offer a variety of associated benefits. The following qualities are the main reasons that grant precast concrete its competitive edge (The Concrete Center, 2007) (Serna, J. & Jimeno, J., 2010).

- **Structural behavior and dynamic performance:**

As oppose to the brittle behavior that the local buckling failure mode and fatigue impose on steel towers, precast concrete towers undergo a ductile behavior that is favorable especially in seismic controlled sites. Prestressed concrete has high tolerance to dynamic loads due to its higher structural damping and fatigue resistance.

- **Weight and foundation:**

The increased weight of the precast concrete gives the tower a much needed stability to resist overturning. It can also be used to control the natural frequency of the tower. Moreover, it reduces the size of the gravity foundation needed and the concrete tower

base has a larger footprint which reduces the foundation's cantilever span and the reinforcement needed.

- **Maintenance and Durability:**

Precast concrete is a very durable material as compared to steel. It has the ability to maintain its properties under harsh weathering conditions. Precast concrete tower require little or no maintenance; i.e. painting the concrete tower is an aesthetic option while Painting the steel tower is a requirement for protection against corrosion.

- **Mix design flexibility:**

Precast concrete is always associated with superior quality control and optimal mechanical properties. In addition, its ability to be fine-tuned to meet unique project requirement is an invaluable quality that comes in handy when dealing harsh conditions and marine applications.

- **Design and construction flexibility:**

Concrete is a very versatile material. It allows all designs and concepts with no limitation on tower cross-section or height.

- **Logistics and transportation:**

Even though concrete towers weight more than its steel counterpart for the same hub height, this won't require a heavier crane to erect the concrete tower as the crane's choice is governed by the nacelle's weight*. Precast concrete technologies allow the possibility of having an on-site temporary manufacturing base that will eliminate

* The nacelle is the box housing all the generating components in a wind turbine, including the generator, gearbox, drive train, and brake assembly.

most of the transportation costs. In case of large wind farms this option is very appealing.

- **Economy:**

Precast concrete can offer an enhanced life cycle value with low initial cost.

Concrete's raw materials are inexpensive. For tall tower, where steel solutions aren't practical, a cost-effective solution with a design life of 40 to 60 year is feasible using precast concrete solutions. In addition, taller wind turbines generate higher levels of power which in turn reduces the payback time.

CHAPTER 3

PROPOSED SYSTEM

The system proposed in this thesis is a precast concrete supporting system that will benefit from all the favorable concrete qualities mentioned in the literature review and improve upon them in several ways. This chapter presents detailed description of the proposed system and its construction procedures. Its expected benefits and design procedures are also included.

3.1 System Description

The proposed wind turbine supporting system is a triangular cross-section precast concrete tower that consists of three columns in each corner of the triangle. The columns are connected together with panels along the height to enclose the interior for the tower shaft and ensure that the columns are resisting the applied actions as one built up section. Along the height the columns are divided into 80ft segments for transportation and erection purposes. In keeping with the current wind turbine supporting systems, the tower has a tapered profile that varies linearly with each vertical segment. This tapered profile will reduce the total weight and the area subjected to wind thus lower the applied moment. It will also enhance the dynamic response of the tower and improve its overall stability. Figure 3-1 shows the tower's cross section.

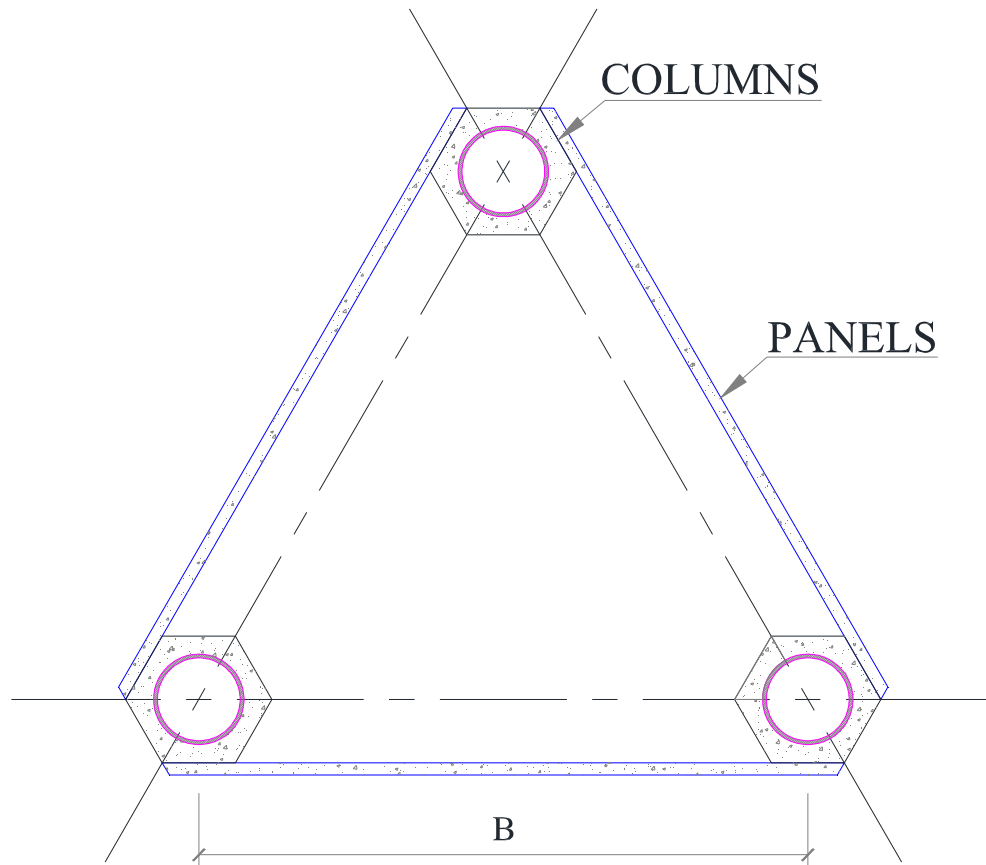


Figure 3-1: Tower's cross section.

The triangular cross section of the tower was chosen as it could accommodate a skeleton type construction composed of vertical columns connected by panels. The triangular section has been implemented in past applications like trussed steel towers. Its shape has an attractive aesthetic view and a good aerodynamic shape that reduces wind pressure and tower vibrations. Contrary to ring sections used in current concrete wind towers, columns and panels are easy to fabricate in the precast plant. Transportation and erection are also simplified. Figure 3-2 shows the cross section of the columns.

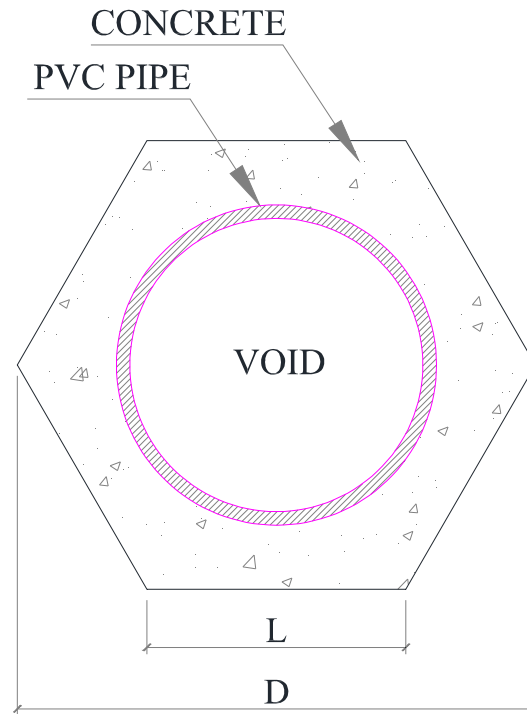


Figure 3-2: Column's cross section.

The columns have a hollow hexagonal cross section to facilitate their connection with the panels. This shape also allows a doubly symmetrical reinforcement pattern that can accommodate the variation in wind direction as explained later in the design chapter. Even though in this system the column segment height is 80ft, it can be modified to fit any tower height or transportation limitation. The column has a hollow circular void at its center to reduce its weight. The hexagon sides measured 3ft each having a diameter of 6ft. The hollow void inside the column is achieved using a 42in. PVC pipe having an inner diameter of 40.73in. and an outer diameter of 44.50in. as per “JM Eagle - Big Blue” pipe manufacturer. However, the inside void could be achieved using any alternative method such as Styrofoam or collapsible forms. Styrofoam is expensive and should be used if PVC pipes aren't available; one the other hand collapsible form could become a

very attractive solution in case of wind farm construction with multiple towers. While the columns were intended to be prestressed and then connected with a splice connection to eliminate post-tensioning costs, an alternative where a portion of the strands are post-tensioned is also included (refer to the design chapter for reinforcement details). For the lower segments of the tower, filling the void inside the columns with plain concrete can help stabilize the tower and resist the overturning moment. It will also add some protection to the post-tensioned duct. However this alternative was not adopted in this study.

The panels' role is to enclose the tower and connect the columns together through shear connections using steel bolts. The panels were design as 6in. thick reinforced concrete having a constant height of 10ft. Their width however varies along the tower's vertical profile shown in Figure 3-3. This tapered profile is suitable for panel's erection as the higher the panel's place in the tower the lighter it will be. The panels' heights also can be adjusted to accommodate transportation, erection or different tower dimensions.

One of the main attractions of the proposed system is its tapered profile. Considering a conventional cantilever column subjected to uniform pressure, its expected bending moment would take a second degree parabolic shape. If the tapered profile of the proposed system was tailored to mimic the bending moment's shape, the columns would only be subjected to axial forces. Moreover, the footprint of the system determines the magnitude of these axial forces. The larger the footprint becomes, the overturning moment would be resisted by a larger lever arm which decreases the loads. However, the increase of the tower's girth will attract more wind pressure which, in turn, increases

the forces. Therefore the tower's profile should be tailored with care to achieve an optimal design. Tweaking the tower's profile add a lot of flexibility to the design of the proposed system. In this profile, every segment, measuring 80ft height, has constant linear slope. Transition between slopes is accommodated in the columns splices. Figure 3-3 shows the tower's profile for both the 240ft and the 320ft towers. Figure 3-4 shows the full elevation of the 240ft concrete tower.

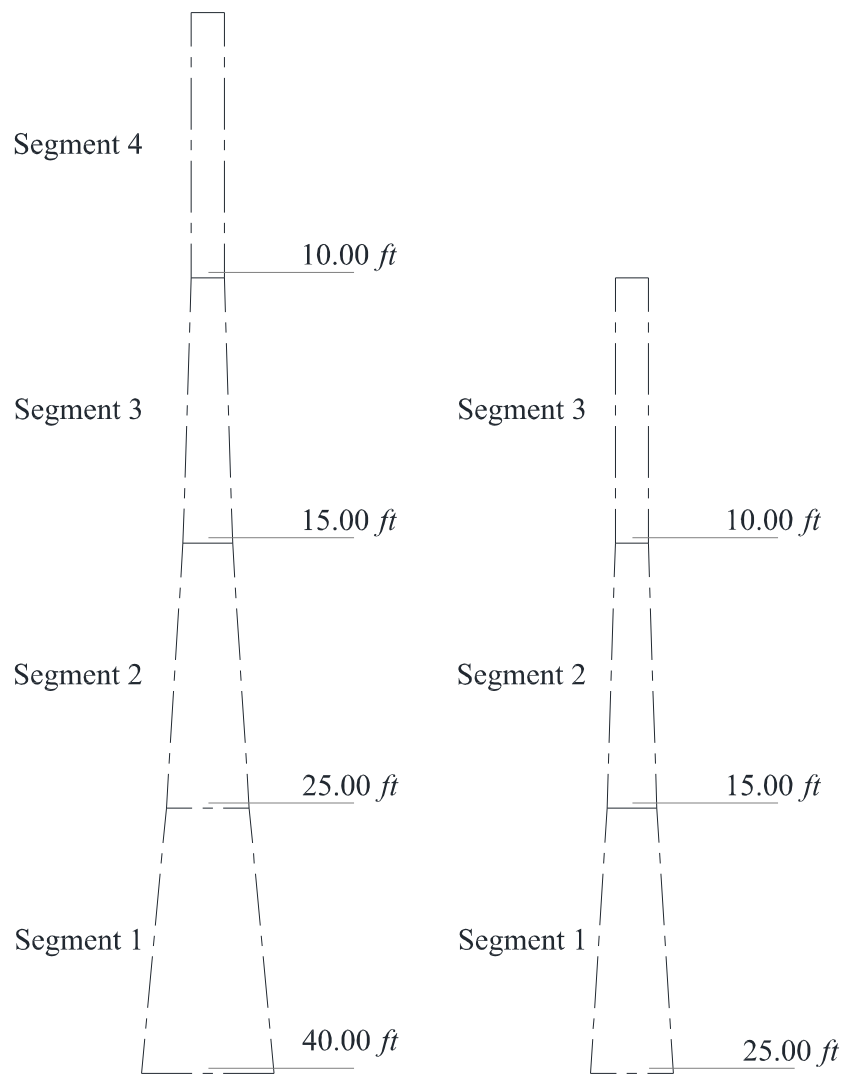


Figure 3-3: Tower's vertical profile for 320ft (left) and 240ft (right) systems.

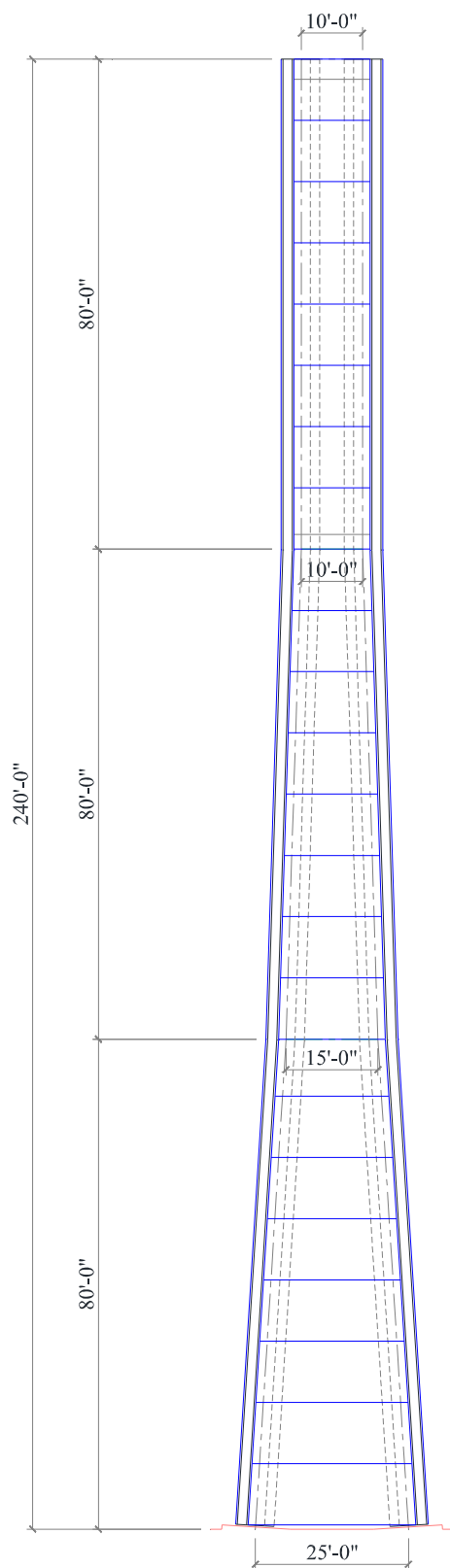


Figure 3-4: 240ft system's elevation.

The 240ft tower is composed of three segments of 80ft each. The center to center widths from the base to the top are 25, 15 and 10ft respectively. The 320ft tower is composed of four segments of 80ft each. The center to center widths from the base to the top are 40, 25, 15 and 10ft respectively.

3.2 Construction Sequence

The construction process of the proposed system is much simpler than that used for current concrete solutions. It is done by simply erecting the columns and then connecting them by the panels. Figure 3-5 through Figure 3-9 illustrate the construction process of 240ft the proposed system. After the construction of the foundation, the columns of the first segment are put into place. Their slope is then controlled by fixing them into the base (Figure 5-16) and using steel temporary beams at the top of the segment (see Figure 3-5). The first segment panels are then installed and fixed in the columns (see Figure 3-6). After the installation of the panels, the temporary beams can then be removed. The same procedure is repeated for segment two and three (see Figure 3-7 and Figure 3-8).

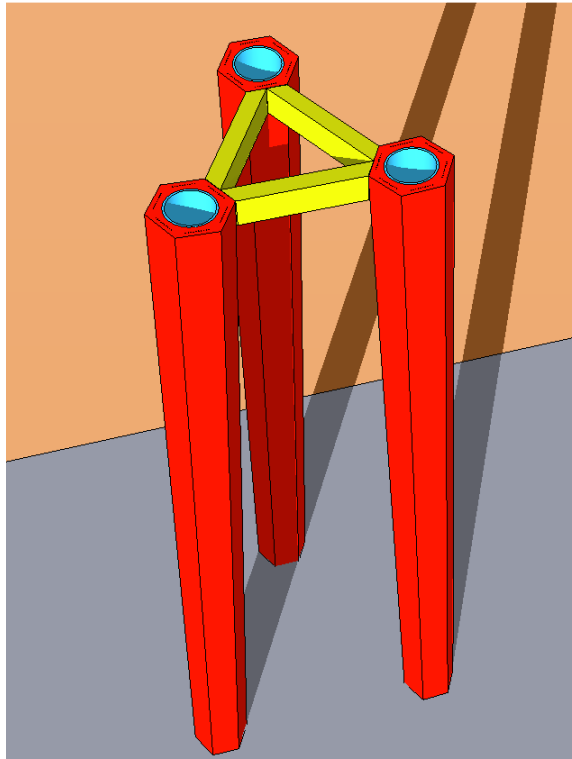


Figure 3-5: Segment 1 columns erection and slope control.

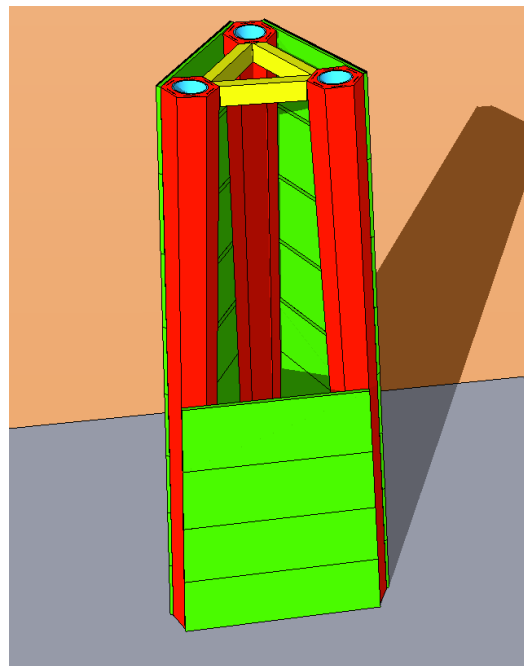


Figure 3-6: Segment 1 panels installation.

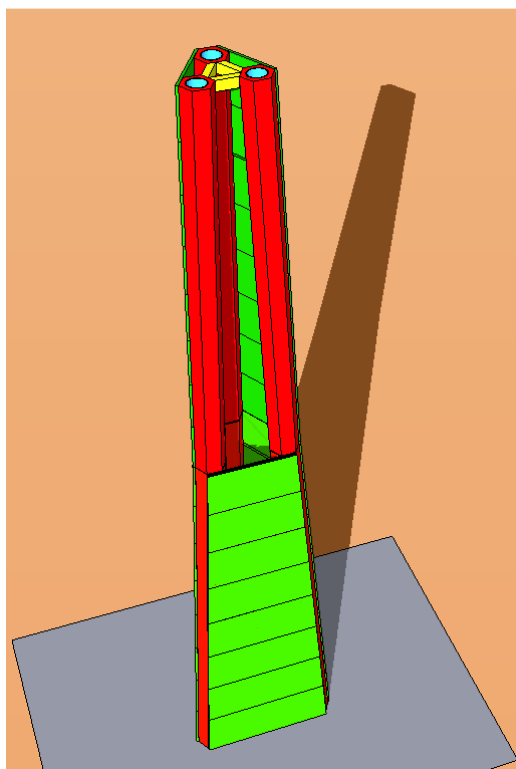


Figure 3-7: Segment 2 erection.

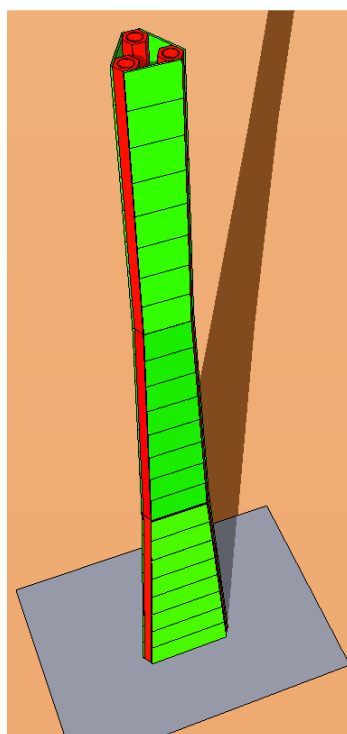


Figure 3-8: Segment 3 erection.

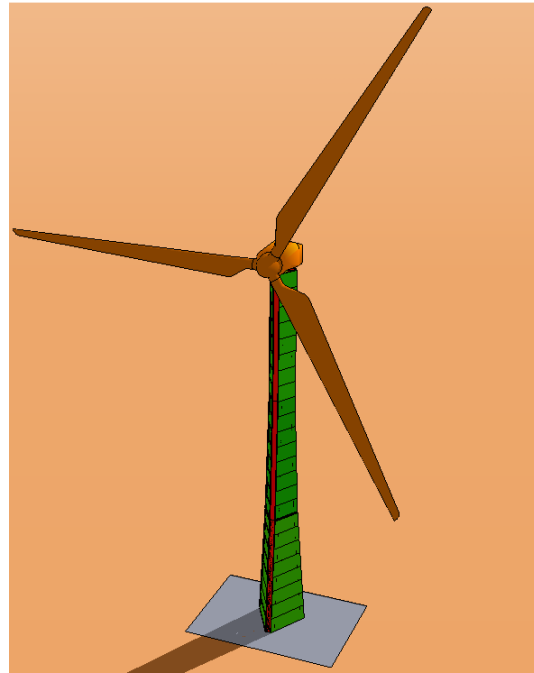


Figure 3-9: Nacelle and blades installation.

3.3 Expected Benefits

While the proposed system benefits from all of the appealing aspects of concrete solutions mentioned in the literature review (refer to section 2.3), it also have some advantages over current concrete solutions including:

- **Flexibility:**

The proposed system can be tailored to accommodate any required dimension, reinforcement or logistics. Several options for the column design and reinforcing patterns are presented in this study including different shear reinforcement option, a prestressed and a post-tensioned option. Filling the lower segments of the columns with plain concrete is also a design alternative that could be adopted to meet specific

design criteria. The tower's vertical profile is a powerful tool that could be employed to reduce columns reinforcement or reducing the tower's footprint. The panels also can accommodate different dimensions, design and connections depending on the required behavior of the system.

- **Fabrication:**

Current concrete towers composed of ring sections also have a tapered profile which makes every ring different in dimensions for its preceding and following rings. This complicates the fabrication procedure as the use of multiple forms or expensive dynamic forms becomes a necessity. However, the proposed system is composed of easier shapes form a fabrication vantage point; the same typical column section and flat panels that don't require special forms to fabricate.

- **Transportation:**

Flat panels can be easily stacked and piled on top of each other using shims, which reduce the number of trips required to transport the towers components. The column segments can be tailored to accommodate transportation. Transportation costs are also reduced. No special care is required during transportation unlike ring section which require fixing and balancing to avoid damage.

- **Erection:**

Once the columns of the proposed system are placed, panels' installation is very quick and easy. Eliminating the need for post-tensioning and connecting the columns using splices will reduce the overall cost of the tower and will simplify the construction process by eliminating the post-tensioning steps.

3.4 Design Procedures and Standards

The wind turbine industry flourished in Europe and its market is monopolized by European wind turbine manufactures. As a result, the European standards are used as a baseline for most wind turbine design. Certification for wind turbines is attained by complying with the International Electrotechnical Commission standards (IEC 61400-1) or European agency-specific standards like GL Rules (GL, 2003). Currently there is no standardized US code for compliance of wind turbine towers. Consequently, a variety of standards, codes and textbooks are integrated together using experience and judgment to design wind turbines in the US. The design has to be rechecked against the European standards before commercial certification (Agbayani, N., 2010).

The process followed in this study to design the wind turbine was based mainly on the following US standards ASCE 7-10, the ACI 318 and the AISC. In instances where the aforementioned codes weren't accurate or didn't prescribe certain specifications for large wind turbine towers, other sources (European standards, textbooks, technical reports and papers) were consulted and followed as outlined in this study. One of the helpful tools in integrating between different design standards and design criteria was the ASCE/AWEA-RP2011 "Recommended Practice for Compliance of Large Land-based Wind Turbine Support Structures". Released in December 2011, it provides guidelines that are compatible with both the IEC (2005) and the US standards and provides recommendations where they differ. Another helpful publication was a technical report done by the National Renewable Energy laboratory (LaNier, M.W., 2005).

Figure 3-10 illustrates the design procedures recommended for the proposed system.

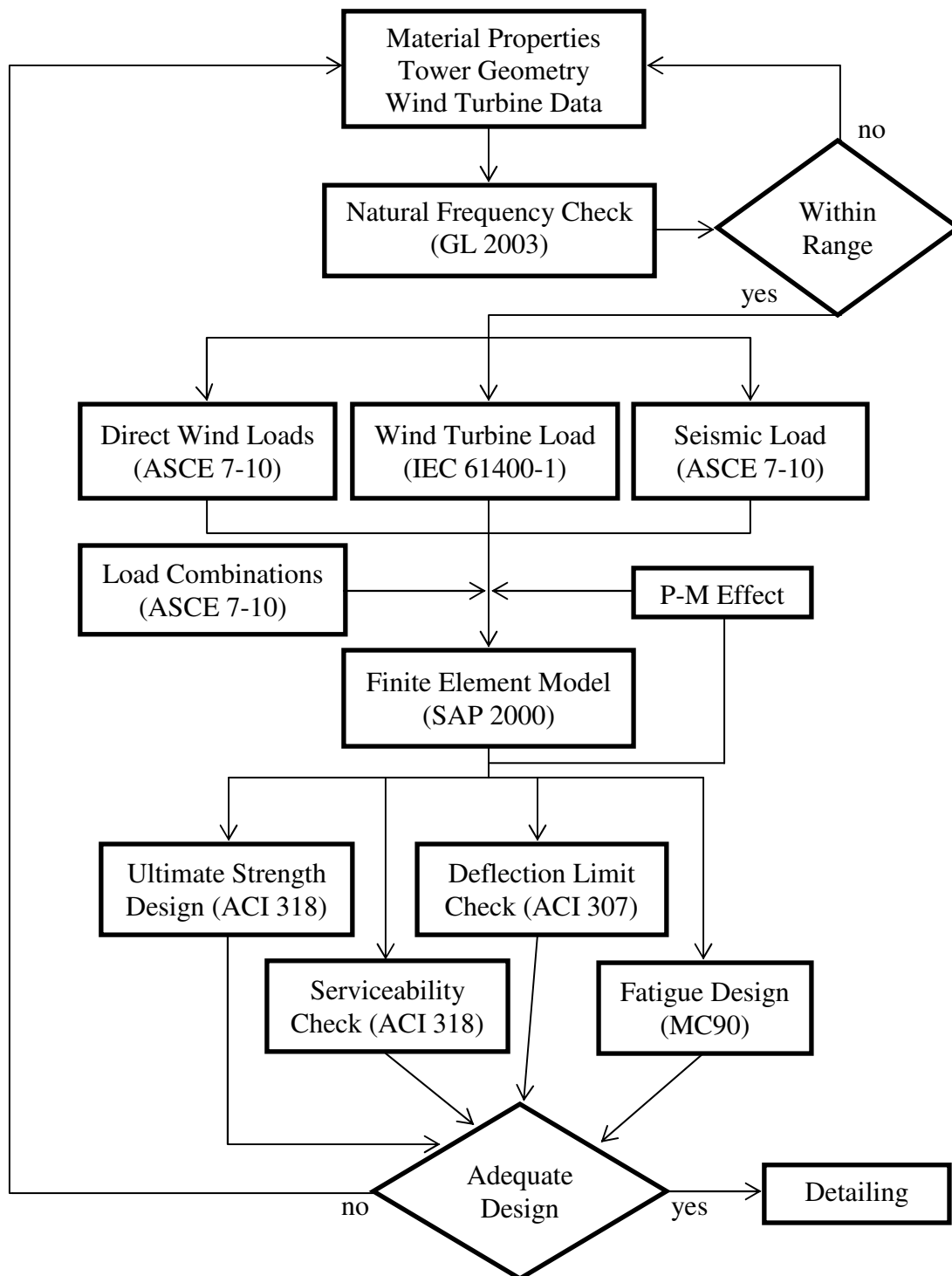


Figure 3-10: Design procedures for proposed system.

3.5 Dynamic Concerns

The wind turbine structure should be designed with sufficient separation between the turbine operational frequencies and the structure natural frequency to avoid any resonance. These turbine operational frequencies results from any harmonic loading including the turbine rotor operational frequency and the blade-pass frequency. Turbine operational frequencies resulting from any transient loading, like start-up conditions, are negligible as there are only applied for a short duration that won't cause resonance. Specifications for the natural frequency separation should comply with Certification Agency Guidelines. The GL Rules (GL, 2003) guidelines were implemented after adjustments recommended by ASCE/AWEA-RP2011.

The natural frequency should have a least a 5% separation from the operational frequencies. A 5% safety margin should be applied to the tower's natural frequency to account for tolerance in design assumptions and calculations. In the practical wind industry, a total of 15% separation is usually required between the natural and operational frequencies. The wind turbine generator used had a rated power of 3.6MW and a rotor speed of 13.2rpm yielding 0.22Hz rotational frequency.

Table 3-1 and Figure 3-11 illustrates the allowable frequency range and the towers natural frequencies.

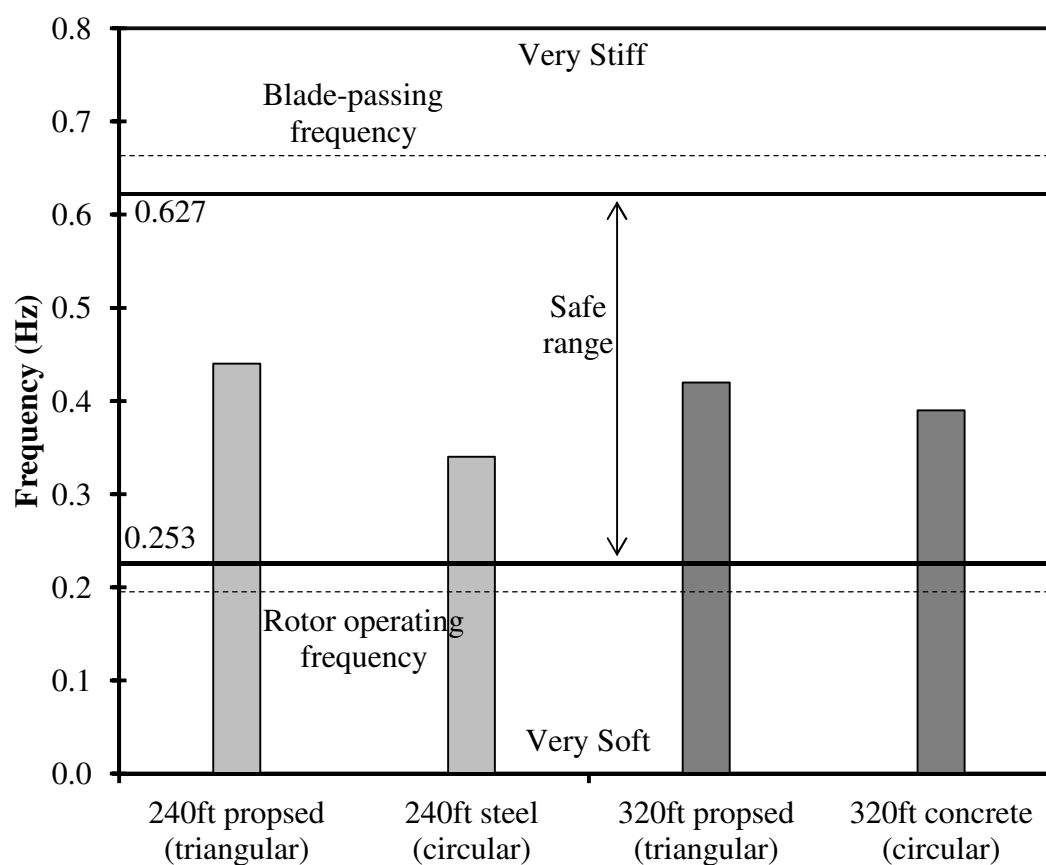


Figure 3-11: Natural frequencies of different towers and operational frequency range.

Table 3-1: Natural frequencies of different towers and operational frequency range.

	Frequency		Period	
	Rotor Speed	13.2	rpm	---
	0.22	Hz	4.55	sec
Safe Frequency Range	0.25	Hz	3.95	sec
	0.63	Hz	1.59	sec
240ft proposed (triangular)	0.44	Hz	2.27	sec
240ft steel (circular)	0.34	Hz	2.94	sec
320ft proposed (triangular)	0.42	Hz	2.38	sec
320ft concrete (circular)	0.39	Hz	2.56	sec

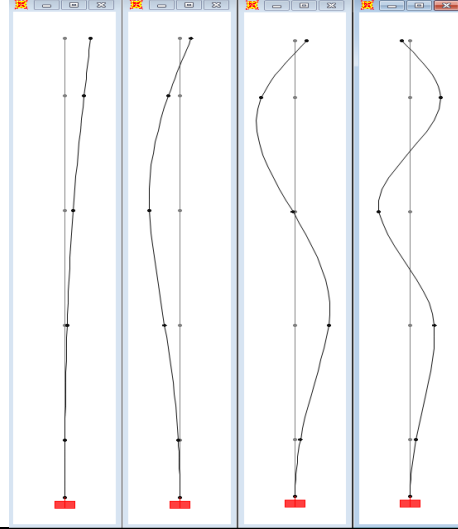
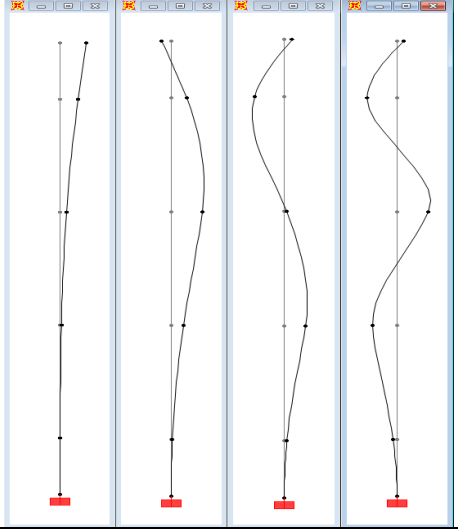
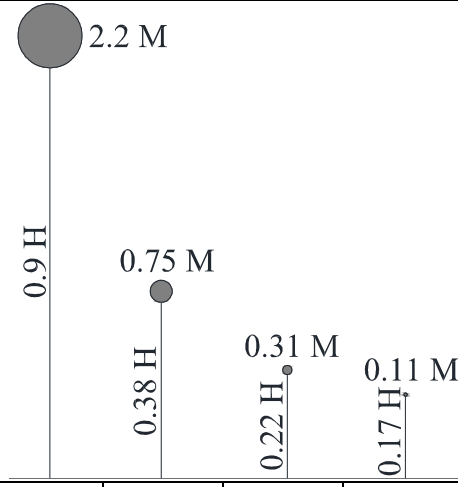
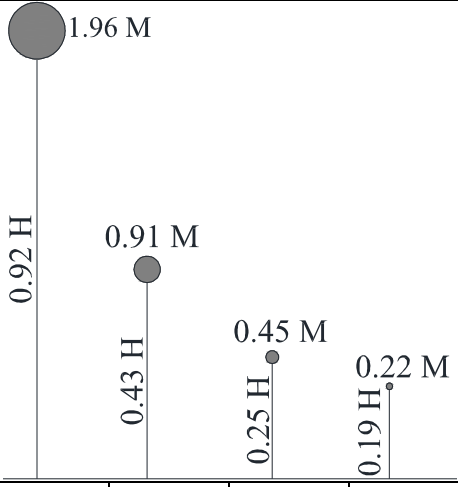
3.5.1 Dynamic Properties Interpretation

The difference between the steel and concrete towers is obvious; the concrete tower is much stiffer than the steel tower having a higher frequency and smaller period. Consequently, the steel tower would undergo larger deflections than the concrete proposed system.

For the 320ft tower, the proposed system is compared against a circular concrete solution currently being used. A complete dynamic analysis was performed for both towers using both, a simplified lumped mass system and finite element analysis, to examine the proposed system's behavior against the current concrete applications. Table 3-2 presents the results of that analysis (refer to appendix D for details). From the results it can be concluded that the two systems have very similar modal properties. The circular system has slightly higher periods than the triangular one which means that it is more flexible. Therefore the circular system will experience greater deformations and vibrations. As for modal contribution, the first mode contribute more to the triangular system's response due to the higher effective modal mass and base straining actions contribution, however the rest of the modes contribute more to the circular system's response.

Figure 3-12 illustrates the mode shapes with their respective natural periods, obtained from finite element model, for the 320ft proposed system.

Table 3-2: Modal properties comparison for 320ft concrete systems.

System	Triangular (proposed)				Circular (current)			
Mode	1	2	3	4	1	2	3	4
Natural period (s)	2.37	0.39	0.14	0.09	2.56	0.43	0.17	0.10
Mode Shapes								
Effective modal masses and heights								
Top deflection contribution	98 %	1.3 %	0.3 %	0 %	98 %	1.7 %	0.08 %	0 %
Base shear contribution	65 %	22.2 %	9.4 %	3.4 %	55.4 %	25.7 %	12.6 %	6.3 %
Base moment contribution	84 %	12.1 %	3.0 %	0.8 %	76.7 %	16.6 %	4.8 %	1.9 %

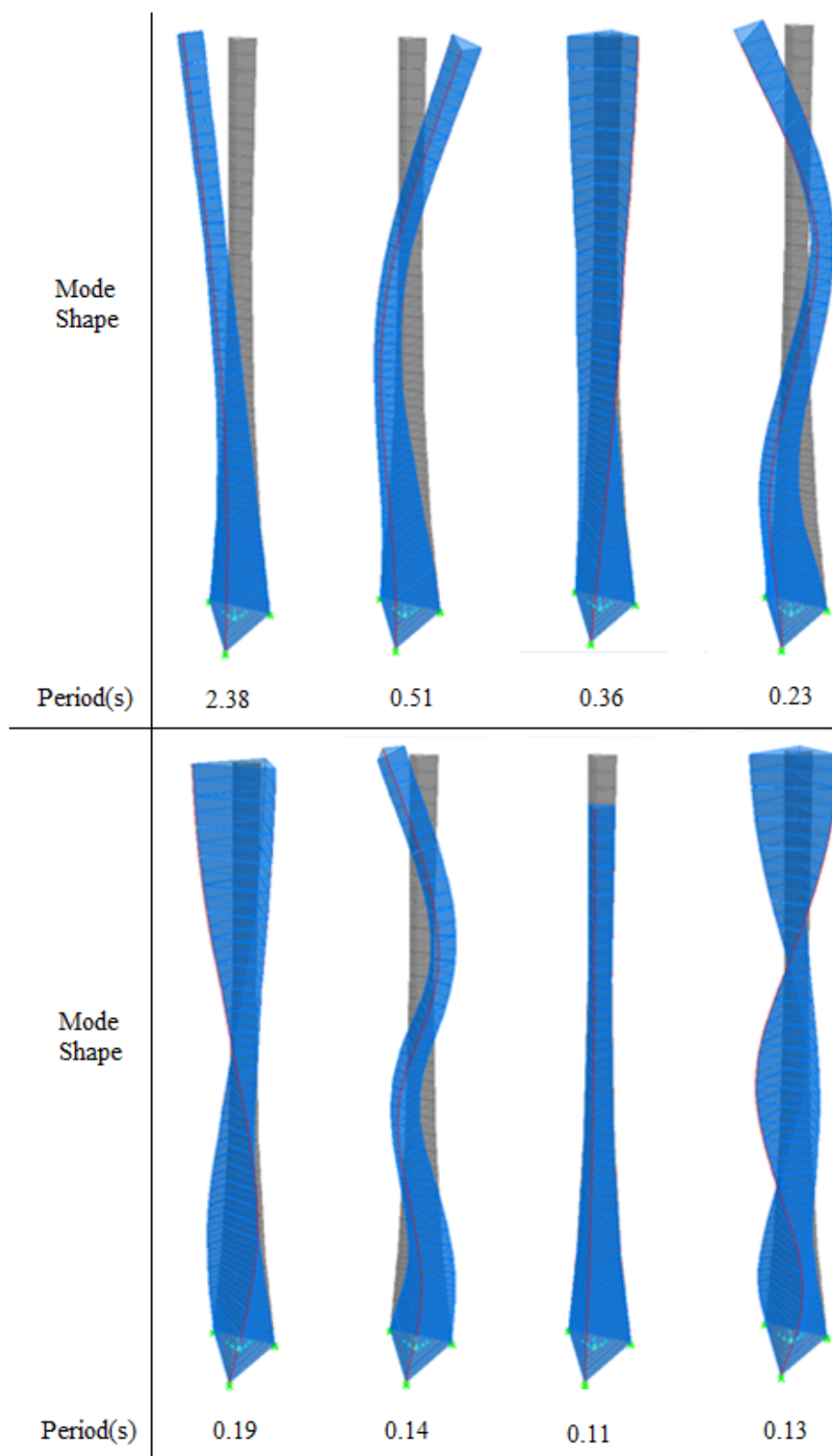


Figure 3-12: Mode shapes and natural periods for the 320ft proposed system.

CHAPTER 4

LOADING

The challenge starts with the wind turbine generator as its prescribed loading patterns and design procedures follow the IEC 61400-1 specifications. To understand the loads induced from wind pressure on the tower, a brief introduction to the design of the wind turbine generator using the IEC 61400-1 is required. The following section highlights the most important aspect relevant to the design of the proposed tower.

4.1 Wind Turbine Generator

Wind turbines are categorized into three classes; I, II and III, according to their respective extreme reference wind speed (V_{ref}^*) and intensity of turbulence. This classification does not accurately represent a specific region and does not differentiate between different seismic conditions. However, a fourth class “S” is included that cover any special conditions. Design values for this class should be specified by the designer.

4.1.1 Wind Models

The IEC 61400-1 prescribes several wind models that should be considered when designing the wind turbine including: *Normal wind speed probability distribution*,

* The reference wind speed is defined as the averaged wind speed at the hub height over 10-minutes.

Normal wind profile model, Normal turbulence model, Extreme wind speed model, Turbulence intensity for extreme conditions, Extreme operating gust, Extreme turbulence model, Extreme direction change, Extreme coherent gust with direction change and Extreme wind shear. The two most important models for the tower are Extreme operating gust (EOG) and Extreme wind speed mode (EWM) respectively.

a) Extreme wind speed model (EWM)

This model represents the extreme conditions applied on the structure whilst the wind turbine non-operational. The conversion from the reference speed (V_{ref}) to the 3-second gust in the IEC 61400-1 is identical to the ASCE 7-10 for open terrains meaning that both standards have identical extreme gust wind profiles (ASCE/AWEA-RP2011). However the IEC 61400-1 requires the consideration of ± 15 degrees of yaw misalignment* .

b) Extreme operating gust (EOG)

This model represents the extreme conditions applied on the structure while the wind turbine operating. This model is considered during several stages of the wind turbine operation; start-up, shut-down, power generation and fault conditions. No equivalent model is provided by the ASCE 7-10.

4.1.2 Safety Factors for Wind Turbine

There are three safety factors in the design of wind turbine according to the IEC 61400-1; component consequence factor, material safety factor and loading safety factor. Depending on the consequence of failure of a certain component the consequence factor

* Yaw misalignment means the direction of the wind is not aligned with the wind turbine axis of rotation.

will be applied accordingly. In most cases it is taken as the same as the importance factor. The material safety factor varies depending on the material of the component in question. In normal situations, the load factor is taken as 1.35 for unfavorable loads and 0.9 for favorable loads.

4.2 Wind Turbine Loads

To analyze the supporting system, the wind turbine reactions have to be determined and then applied on the tower either dynamically or as an amplified static load. In the industry, load documents containing the magnitude and direction of these forces are provided by the wind turbine manufacturers in accordance with the IEC 61400-1 or other certification agency guidelines. In instances where these loads aren't provided, a dynamic simulation is performed to obtain load histograms or equivalent static load. Dynamic simulations are accomplished using software simulators that consider the entire wind turbine mechanisms working in synchronization. These mechanisms include, but not limited to, Main gearbox, Control and Protection functions and Braking, Hydraulic, Yaw and pitch systems. Loading is simulated using dynamic aero-elastic codes considering gravitational, inertial, actuation and aerodynamic loads. Other loads should also be considered like wake and impact effects.

The wind turbine generator used in this study has a rated power of 3.6MW and features 170ft long blades. The turbine static equivalent loads were obtained from technical studies published by the National Renewable Energy Laboratory (Malcolm, D.J. & Hansen, A.C., 2006) & (LaNier, M.W., 2005). The loads were then scaled to match the

reference speed at the hub height for each tower accordingly. Conversions from the ASCE 7-10 basic wind speeds to the IEC reference speeds was achieved using the provided equations in the ASCE/AWEA-RP2011. Appendix A shows the dimensions and specifications of the wind turbine along with the equivalent static loads applied on the turbine after scaling. These loads were used for both the steel and concrete tower.

4.3 Direct Wind Pressure on the Tower

As specified in the ASCE 7-10, a nominal 3-second design wind speed of 115mph at reference height of 33ft above the ground was used to represent the extreme non-operating conditions (EWM). However, for extreme operating condition (EOG), a nominal 3-second design wind speed of 49.7mph at reference height of 33ft above the ground was used after conversion from the IEC 61400-1 reference speed. The wind speed profile along the tower (z) follows (Eq. 4-1) having an exponent “ α_i ” equals 0.11 for the EMW and 0.2 for the EOG.

$$V(z) = \left(\frac{z}{z_{hub}} \right)^{\alpha_i} V_{hub} \quad (\text{Eq. 4-1})$$

The turbine was designed as building category II. The importance factor was assumed as 1.0 following the recommendation of ASCE/AWEA-RP2011. The exposure category of the turbine was assumed as “D” for clear unobstructed flat terrain. The pressure profile along the tower’s height imposed by wind speed can be calculated using (Eq. 4-2). Figure 4-1 shows a graphical representation of the wind pressure in both cases; EWM and EOG for the 240ft concrete tower. For details concerning other tower see its corresponding design appendices B & C.

$$q_z(z) = 0.00256 K_z(z) K_{zt} K_d V^2 \quad (\text{Eq. 4-2})$$

Where,

- V is the basic wind speed
(extreme 3-second gust at 33ft from ground)
- K_{zt} is the topographic factor (=1)
- K_d is the directionality factor (=0.95)
- K_z is the velocity pressure coefficient determined from (Eq. 4-3).

$$K_z = \begin{cases} 2.01 \left(\frac{15ft}{z_g} \right)^{\frac{2}{\alpha}} & \text{for } z < 15ft \\ 2.01 \left(\frac{z}{z_g} \right)^{\frac{2}{\alpha}} & \text{for } z > 15ft \end{cases} \quad (\text{Eq. 4-3})$$

Where,

- z_g is the nominal height of the atmospheric boundary layer (=700ft for expose category "D")
- α = 11.5 for exposure category "D"

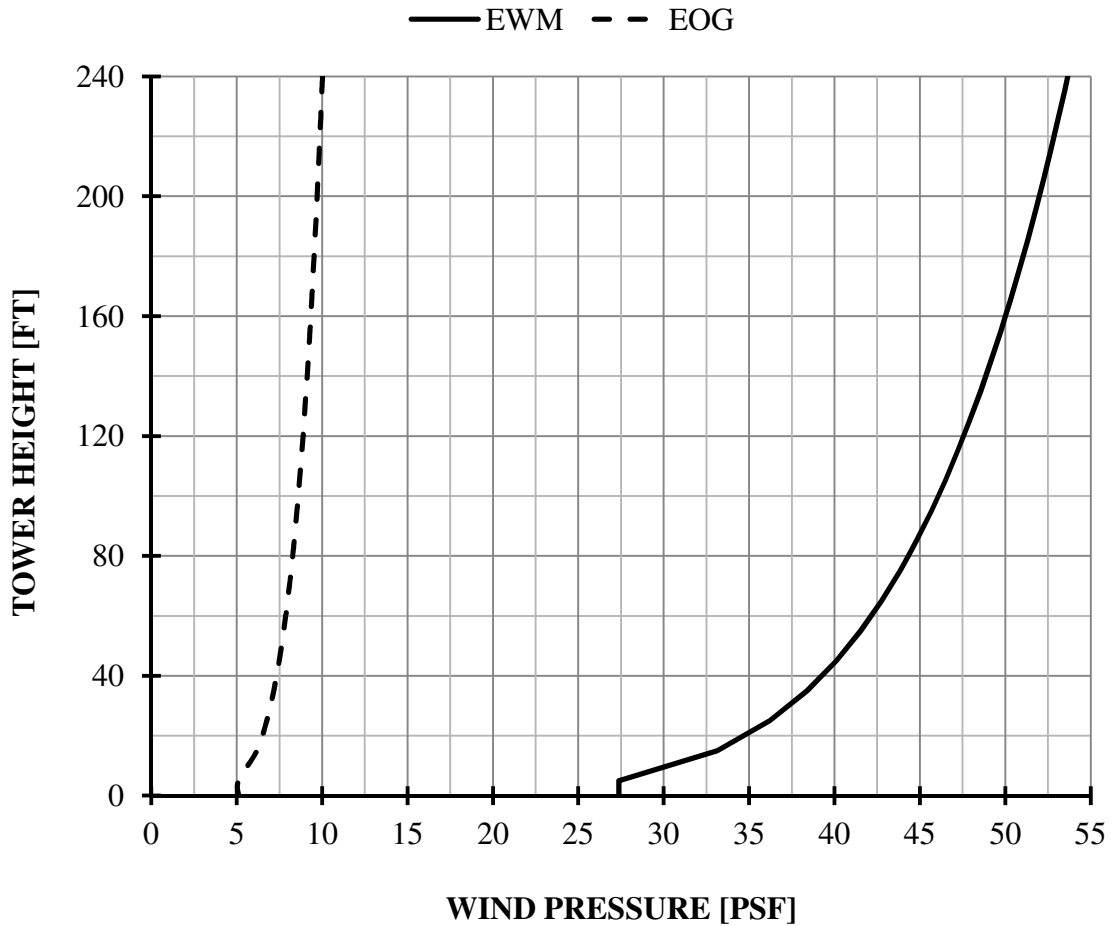


Figure 4-1: Wind pressure profile along the 240ft tower height.

The equivalent lateral static force along the tower's height due to the wind pressure is computed using (Eq. 4-4).

$$F_z(z) = q_z(z) G_f C_f A_f \quad (\text{Eq. 4-4})$$

Where,

A_f is the projected area normal to the wind pressure

C_f is the force coefficient given by Table 4-1 through Table 4-4.

G_f is the gust-effect factor for flexible structures from (Eq. 4-5)

$$G_f = 0.925 \left(\frac{1 + 1.7 I_{\bar{z}} \sqrt{g_Q^2 Q^2 + g_R^2 R^2}}{1 + 1.7 g_v I_{\bar{z}}} \right) \quad (\text{Eq. 4-5})$$

Where,

$I_{\bar{z}}$ is the intensity of turbulence from (Eq. 4-6)

Q is the background response from (Eq. 4-8)

R is the resonant response factor from (Eq. 4-10)

g_R is given by (Eq. 4-7).

g_v & g_Q Are constants taken as 3.4

$$I_{\bar{z}} = c \left(\frac{33}{\bar{z}} \right)^{1/6} \quad (\text{Eq. 4-6})$$

Where \bar{z} is the equivalent height of the structure defined as 60% of the height but not less than z_{min} which equals to 7ft for exposure category “D”.

$$g_R = \sqrt{2 \ln(3,600 n_1)} + \frac{0.577}{\sqrt{2 \ln(3,600 n_1)}} \quad (\text{Eq. 4-7})$$

Where n_1 is the natural frequency of the tower determined from finite element analysis.

$$Q = \sqrt{\frac{1}{1 + 0.63 \left(\frac{B + h}{L_{\bar{z}}} \right)^{0.63}}} \quad (\text{Eq. 4-8})$$

Where,

B is the horizontal dimension of the structure

h is the height of the structure

$L_{\bar{z}}$ is the integral length scale of turbulence at the equivalent height given by (Eq. 4-9)

$$L_{\bar{z}} = l \left(\frac{\bar{z}}{33} \right)^{\bar{\epsilon}} \quad (\text{Eq. 4-9})$$

Where l and $\bar{\epsilon}$ are constants taken as 650ft and 1/8 respectively for exposure category “D”.

$$R = \sqrt{\frac{1}{\beta} R_n R_h R_B (0.53 + 0.47 R_L)} \quad (\text{Eq. 4-10})$$

Where β is the structure damping ratio 2% (refer to section 4.5), R_n is given by (Eq. 4-11), R_L , R_h , and R_B are computed from (Eq. 4-14).

$$R_n = \frac{7.47N_1}{(1 + 10.3N_1)^{5/3}} \quad (\text{Eq. 4-11})$$

$$N_1 = \frac{n_1 L_{\bar{z}}}{\bar{V}_{\bar{z}}} \quad (\text{Eq. 4-12})$$

Where $\bar{V}_{\bar{z}}$ is the mean hourly wind speed at height \bar{z} determined from (Eq. 4-13)

$$\bar{V}_{\bar{z}} = \bar{b} \left(\frac{\bar{z}}{33} \right)^{\bar{\alpha}} \left(\frac{88}{60} \right) V \quad (\text{Eq. 4-13})$$

Where \bar{b} and $\bar{\alpha}$ are constants taken as 0.8 and 1/9 respectively for exposure category “D”.

$$R_x = \begin{cases} \frac{1}{\eta} - \frac{1}{2\eta^2} (1 - e^{-2\eta}) & \text{for } \eta > 0 \\ 1 & \text{for } \eta = 0 \end{cases} \quad (\text{Eq. 4-14})$$

$$R_x = R_h \text{ setting } \eta = 4.6 \frac{n_1 h}{\bar{V}_{\bar{z}}}$$

$$R_x = R_B \text{ setting } \eta = 4.6 \frac{n_1 B}{\bar{V}_{\bar{z}}}$$

$$R_x = R_L \text{ setting } \eta = 15.4 \frac{n_1 L}{\bar{V}_{\bar{z}}}$$

Table 4-1: Force coefficient for towers*.

Cross Section	h/D**		
	1	7	25

Square	wind normal to face	1.3	1.4	2
	wind along diagonal	1	1.1	1.5
Hexagonal or Octagonal		1	1.2	1.4
Round		0.5-0.8	0.6-1.0	0.7-1.2

* Based on ASCE 7-10 Table 29.5-1

** h : Tower Height

** D : Least Base Dimension

Table 4-2: Force coefficient for the 240ft proposed concrete tower cross section.

Wind Direction	Cross Section			Proposed (h/D=8.77)
	Square	Hexagonal	Round	
Normal to Face	1.46	1.22	0.81	1.46
Along Diagonal	1.14			1.14

Table 4-3: Force coefficient for the 320ft proposed concrete tower cross section.

Wind Direction	Cross Section			Proposed (h/D=7.93)
	Square	Hexagonal	Round	
Normal to Face	1.43	1.21	0.81	1.43
Along Diagonal	1.12			1.12

Table 4-4: Force coefficient for the 240ft steel tower (smooth surface).

Cross Section	h/D			h/D=13.33
	1	7	25	
Round	0.5	0.6	0.7	0.64

After calculating the forces along the tower height, the shear forces and bending moments from the direct wind pressure on the supporting system can be readily determined at any point using (Eq. 4-15) and (Eq. 4-16).

$$S(z) = \int_z^h F_z(x) dx \quad (\text{Eq. 4-15})$$

$$M(z) = \int_z^h F_z(z)(x - z)dx \quad (\text{Eq. 4-16})$$

4.4 Fatigue Loads

Fatigue stresses on wind turbine towers are a result of blade rotation and wind fluctuation causing relatively small stress changes but with higher frequencies. Consequently, during the same time span, wind turbine structures endure a higher number fatigue cycles than typical structures. To properly investigate the wind turbine's behavior under fatigue loading, numerous load combinations and complex cases have to be considered in order to account for the unstable wind conditions and the structure's response. The huge number of wind turbine supporting structures along with the fact that fatigue loading is often controlling the design of steel towers makes conservative assumptions regarding fatigue loading not economically feasible. Therefore, no simplified methods, that determine fatigue loading for large wind turbine, have been accepted by the industry.

Most fatigue investigations use published S-N curves to compare against load range spectrum, generated from simulations, for critical components.

4.4.1 S-N Curves

S-N curves are graphs between the nominal stress range on the component in question and the allowable number of cycles it can endure during its design life. The plot uses a log-log plot that transforms the curves into a series of straight lines having different slopes " m ". Figure 4-2 shows a comparison between the S-N curves in the AISC and the EN specifications for structural steel components.

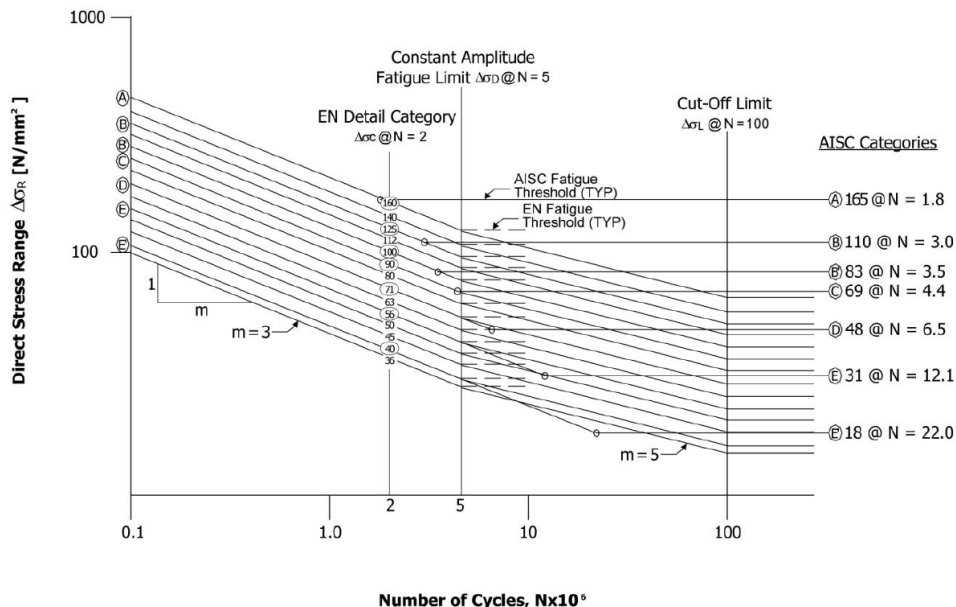


Figure 4-2: EN and AISC fatigue strength curve as shown in ASCE/AWEA RP2011.

At low stresses, structural steel components transition into a cut-off zone where the S-N curve is horizontal on the log-log plot. Stresses lower than the cut-off zone may be repeated for an infinite number of cycles without damaging the components. Even though both the EN and AISC curves were based on identical confidence and probability levels, they have one significant difference in the cut-off stress and number of cycles; the EN cut-off zone starts at 5 million cycles for all categories while the AISC cut-off zone range from 2 to 22 million cycles depending on the component category.

4.4.2 Dynamic Load Simulation

Using complex software simulators wind turbines can be completely modeled, from the flexible blades to the supporting tower, with nonlinear structural and fluid dynamics models. The stress range and number of cycles can be determined from the dynamic

simulation for every component. The adequacy of the design is then determined for critical components using damage summation or stress range assessment. The most commonly used damage summation method is the Palmgren-Miner's summation method. This method assumes that the fatigue damage from each stress range is accumulative and equals to the ratio of the number of cycles of that stress to the total number of cycles. In this study, however, an assessment of stress ranges using a damage equivalent load method was used to determine the adequacy of the design.

4.4.3 Damage Equivalent Load Method

The damage equivalent load (DEL) is the constant load range producing the same damage as calculated using damage summation methods. By assuming a constant slope on the S-N log-log plot, any given load range can be converted to a DEL having the same number of cycles. The accuracy of this method depends on the slope assumed for the S-N curve. This method is only applicable to components having a linear relationship between loading and stress.

4.5 Seismic Loading

Seismic loading is mainly affected by the site location and the tower weight. For the Mid-West regions, seismic loading is not except to control the tower's design; however, zones along the U.S west coast or near fault lines would experience more punishing ground acceleration. Being lighter than concrete towers, steel tower will experience less seismic loading than concrete towers, however, the increasing weight of the wind turbine head (nacelle and blades) makes seismic loading more likely to govern their design. In this

study, the static equivalent earthquake loads and the seismic ground motion values were determined as per the ASCE 7-10 specifications.

A big factor that affects seismic loading is the structural damping of the tower. Wind turbine structural damping lie usually somewhere between 5% and 1%. (Porwell, 2011) showed that using a 1% damping is overly conservative. 2% structural damping is typically used for steel towers; however the proposed concrete system will have a higher damping ratio. Conservatively, a damping ratio of 2% was assumed for both systems. The spectral response values in the ASCE 7-10 were determined and mapped considering 5% structural damping. Following the ASCE/AWEA RP2011, an adjustment factor “B” of 1.23 was used to scale the spectral response values in the ASCE 7-10 to integrate with the 2% damping ratio assumed.

Load combinations in the ASCE 7-10 do not consider wind and seismic events simultaneously, however the ASCE/AWEA RP2011 provides two load combinations that considers seismic loading along with wind operational loading. In this instance where seismic event occurs while the wind turbine is operating, (Prowell, et.al., 2010) shows that an aerodynamic damping effect takes place due to the friction between the turbine blades and the air which increases the structural damping of the tower. Moreover, several relative directions of the wind pressure and seismic acceleration have to be considered.

Therefore, in this study, seismic events were only considered for non-operational conditions as per the ASCE 7-10 load combinations presented in section 4.6.

4.5.1 Design Response Spectrum

The ASCE 7-10 response spectrum is determined using (Eq. 4-17).

$$S_a(T) = \begin{cases} S_{DS} \left(0.4 + 0.6 \frac{T}{T_0} \right) & \text{if } T > T_0 \\ S_{DS} & \text{if } T_0 \leq T \leq T_S \\ \frac{S_{D1}}{T} & \text{if } T_S < T \leq T_L \\ \frac{S_{D1} T_L}{T^w} & \text{if } T_L < T \end{cases} \quad (\text{Eq. 4-17})$$

Where,

T is the fundamental period of the structure.

T_L is the long-period transition period.

S_{DS} & S_{D1} are the design spectral response acceleration parameters at short and 1 second periods calculated from (Eq. 4-18) and (Eq. 4-19). Respectively.

T_S & T_0 are determined using (Eq. 4-22) and (Eq. 4-23) respectively.

$$S_{DS} = \frac{2}{3} S_{MS} \quad (\text{Eq. 4-18})$$

$$S_{D1} = \frac{2}{3} S_{M1} \quad (\text{Eq. 4-19})$$

Where S_{MS} and S_{M1} are the spectral response acceleration for short and 1 second periods respectively. Given by (Eq. 4-20) and (Eq. 4-21).

$$S_{MS} = F_a S_S \quad (\text{Eq. 4-20})$$

$$S_{M1} = F_v S_1 \quad (\text{Eq. 4-21})$$

Where,

S_S & S_1 are the mapped MCE_R spectral response acceleration parameter at short

and 1 second periods respectively multiplied by “ B ” the damping adjustment factor.

F_a & F_v are the site coefficients.

And,

$$T_S = \frac{S_{D1}}{S_{DS}} \quad (\text{Eq. 4-22})$$

$$T_0 = 0.2 \frac{S_{D1}}{S_{DS}} \quad (\text{Eq. 4-23})$$

Figure 4-3 shows a graphical representation of the design response spectrum.

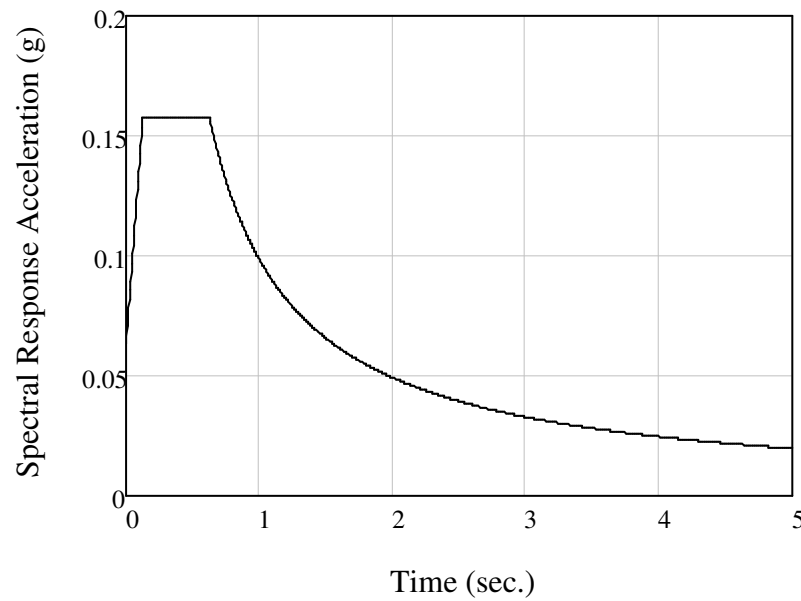


Figure 4-3: Design response spectrum.

4.5.2 Seismic Design load

The equivalent lateral seismic force distribution along the tower’s height follows the same pattern as the tower’s weight. Given by (Eq. 4-24).

$$V = C_s W \quad (\text{Eq. 4-24})$$

Where,

W is the effective seismic weight per section.

C_s is the seismic response coefficient determined from (Eq. 4-25).

$$C_s = \frac{S_{DS}}{\left(\frac{R}{I_e}\right)} \quad (\text{Eq. 4-25})$$

Where,

R is the response modification factor.

I_e is the seismic importance factor.

The ASCE 7-10 does not specify a response modification factor “ R ” for wind turbine, therefore, it was assumed as 1.5 following the recommendations of the ASCE/AWEA RP2011.

The value of C_s computed using (Eq. 4-25) should not exceed (Eq. 4-26) or (Eq. 4-27) and should not be less than (Eq. 4-28).

$$C_s = \frac{S_{D1}}{T \left(\frac{R}{I_e}\right)} \quad \text{for } T \leq T_L \quad (\text{Eq. 4-26})$$

$$C_s = \frac{S_{D1} T_L}{T^2 \left(\frac{R}{I_e}\right)} \quad \text{for } T > T_L \quad (\text{Eq. 4-27})$$

$$C_s = 0.044 S_{DS} I_e \geq 0.01 \quad (\text{Eq. 4-28})$$

Table 4-5 shows the ratio of the seismic force to the wind force in the different system.

Table 4-5: ratio of the seismic force to the wind force.

Supporting system setup	Seismic/Wind Base Shear Ratio
240ft Steel Tower	51.7 %

240ft Proposed concrete system	71.3 %
320ft Proposed concrete system	72.3 %

4.6 Load Combinations

The ASCE 7-10 load combinations were followed in this study. For the wind turbine loads, a load factor of 1.35 was used as per IEC 61400-1 (refer to section 4.1.2). The EWM non-operational conditions were considered for the ultimate load combinations. However, both the EWM non-operational and the EOG operational conditions were considered for service load combinations. Table 4-6 shows all the relevant ASCE 7-10 load combinations used in this study.

Table 4-6: ASCE 7-10 load combinations.

D: dead load, *W*: wind load, *T*: wind turbine load and *E*: seismic load.

Load Combinations	Load Factors	Load Combinations	Load Factors
Ultimate 4	$1.2D+1.0W+1.35T$	Service 5-1	$1.0D+0.6W+1.0T$
Ultimate 5	$1.2D+1.0E$	Service 5-2	$1.0D+0.7E$
Ultimate 6	$0.9D+1.0W+1.35T$	Service 7	$0.6D+0.6W+1.0T$
Ultimate 7	$0.9D+1.0E$	Service 8	$0.6D+0.7E$

CHAPTER 5

ANALYSIS AND DESIGN

This chapter illustrates the different techniques employed to accurately simulate the response of the proposed system when subjected to different loading. Three different modeling techniques are presented and the most accurate method is recommended for future implementation. This chapter also includes the design procedures, methods and standards followed when designing both the concrete and steel towers.

5.1 System Properties and Dimensions

Table 5-1: The 240ft concrete tower properties.

Total Height	240ft
Tower Material	Concrete
No. of Segments	3 segments
Tower Cross Section	Triangular
Segment Height	80ft
Base Dimensions	25ft
1st Segment Dimension	15ft
2nd Segment Dimension	10ft
Top Dimension	10ft
Tower Profile	Tri-linear (Figure 3-13)
Tower Weight	2437 kips
Natural Frequency	0.44 Hz
Expected Controlling Load	Ultimate tension

Table 5-2: The 320ft concrete tower properties.

Total Height	320ft
Tower Material	Concrete
No. of Segments	4 segments
Tower Cross Section	Triangular
Segment Height	80ft
Base Dimensions	40ft
1st Segment Dimension	25ft
2nd Segment Dimension	15ft
3rd Segment Dimension	10ft
Top Dimension	10ft
Tower Profile	Quad-linear (Figure 3-14)
Tower Weight	3579 kips
Natural Frequency	0.42 Hz
Expected Controlling Load	Ultimate tension

Table 5-3: The 240ft steel tower properties.

Total Height	240ft
Tower Material	Steel
Tower Cross Section	Circular
Base Diameter	18ft
Wall Thickness at Base	1.8 in.
Top Diameter	10ft
Wall Thickness at Top	1.0 in.
Tower Profile	linear
Tower Weight	865 kips
Natural Frequency	0.34 Hz
Expected Controlling Load	Fatigue

5.2 Design Approaches

The design concept of current tubular wind turbine towers is relatively simple as the structure can be modeled as one cylindrical cantilever column supporting the wind turbine reactions applied at its summit. Moreover variation in wind directions is rendered unproblematic due to its circular cross section; its symmetrical nature allows the use of vector summation to transform simultaneous loading induced from different directions into one resultant force. Its conventional circular shape coupled with the predictable, fixed-free cantilever column, behavior make for a simple design process. On the other hand, a more challenging design approach should be adopted for the proposed system as its new innovative shape along with its unpredictable behavior result in an interesting and unconventional load path. Instead of considering the whole tower as one column, every element in the proposed system should be analyzed and design separately. Interactions between different elements have to be accounted for depending on their relative stiffness, load direction and connectivity. Special attentions should be granted to connections as they control the interchanging actions between elements.

5.3 Modeling

In this study, the representation of the proposed system in a finite element model was a necessity due to its complex shape. An understanding of the tower's behavior and load path is essential to achieve an accurate replica of the tower when constructing the model.

5.3.1 Elements Role and Load Path

Reinforced with all of the prestressing forces, the columns have the role of resisting the main forces imposed on the system. In order to achieve that, the columns have to work together as a composite section meaning the deflections of the three columns should match in both magnitude and direction. The purpose of the panels is to achieve that composite action between the columns. In this instance, the panels behave as tie beams enduring in plane bending moments and shearing forces. Moreover the panels have to resist direct wind pressure on its exposed surface. In this scenario, out of plane bending moments are the actions governing their design as they mimic the behaviors of one way slabs.

The load path of the loads imposed by the wind turbine generator is obvious as it is distributed equally to the three columns. However, the direct wind pressure on the tower is carried by the panels. After deflecting, the panel's reactions are transmitted to the two columns supporting it. When the two columns start deflecting, a portion of the load is then transmitted into the other two panels attached to the columns. This portion of the load is passed on to the last column achieving the composite action between the three columns. This scenario is identical for the pressure and suction side of the tower (refer to Figure 5-1). Ideally the three columns deflections should be identical. The same concept is applicable for any wind direction.

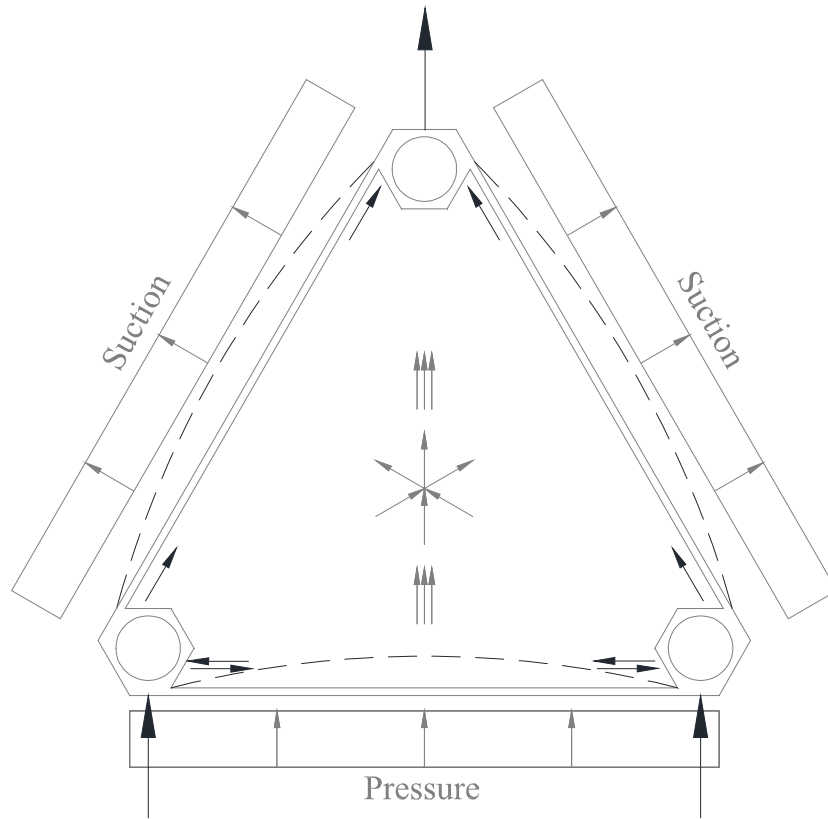


Figure 5-1: Load path for direct wind pressure (S-N direction).

5.3.2 Tower's profile

Another important aspect in understanding the proposed system's behavior is its tapered profile. Considering a conventional cantilever column subjected to uniform lateral pressure, its expected bending moment would take a second degree parabolic shape. If the tapered profile of the proposed system's matched the bending moment's shape, the columns would only be subjected to axial forces. However, the actual wind pressure isn't uniformly distributed along the tower's height; it varies according to Figure 4-1. In addition, the reactions from the wind turbine at the top changes the bending moments shape. Therefore, to optimize the design, several vertical profiles for the tower were

considered in order to mimic the bending moment diagram. The tower's profile chosen at the end, shown in Figure 3-3, was a good approximation yielding small bending moments and large axial forces on individual columns.

5.3.3 Finite Element Models

Three different finite element models using SAP 2000 were constructed to reach a better understanding of the tower's behavior. Each model considers the interaction between the columns and the panels from a different vantage point. After analyzing the tower using each model, an informed decision concerning their accuracy could be reached. In each model the columns were represented as frame elements following the tower's vertical profile. Three different approaches were used to model the panels corresponding to the different models. The wind loads, seismic loads and turbine loads were applied as shown in chapter 4. The base of the tower was considered fixed in the ground. Soil interactions were not considered. Load combinations and wind direction cases were applied accordingly.

The first model used was the shell element model where the panels were modeled as solid shell elements having the same dimensions as their real counterparts. This model is a good representation of the panel's behavior when subjected to out of plane bending from the direct wind pressure. The resulting forces on the columns were as expected; large axial forces and small bending moments. Figure 5-2 shows the axial load in the columns and the max forces in the panels along the tower's height. The top portion of the tower is subjected to axial compression due to the weight of the wind turbine. Moving further to

the bottom, the bending moment starts to take over causing tension on one side and compression on the other.

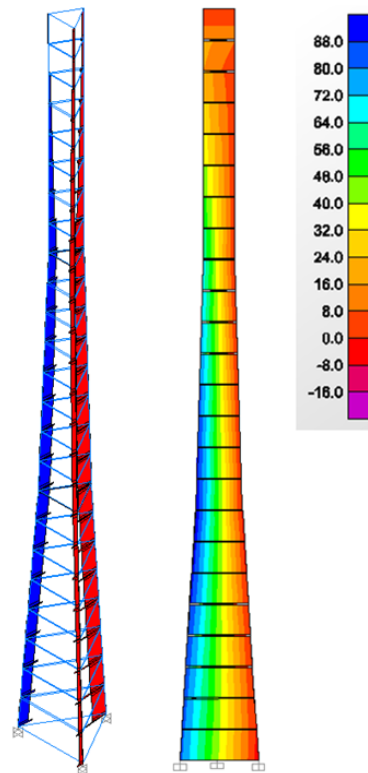


Figure 5-2: Axial forces in columns (left) and panels (right) (240ft tower)

It was apparent from the results that the panels are working as tie beams to transfer the forces between columns. Modeling the panels as shell elements was not the best representation for that purpose. The second model employed was a tie beam model where the panels were represented by flexural elements, having a depth of 10ft, connecting the columns together. In this instance, the panels behave as deep beams carrying shear and moment between the columns (Figure 5-3). The same axial force and bending moment distribution patterns as the shell model emerged yielding very close values. Using the

element forces from this model, the panels can be readily designed as deep beams subjected to in plane shear and bending.

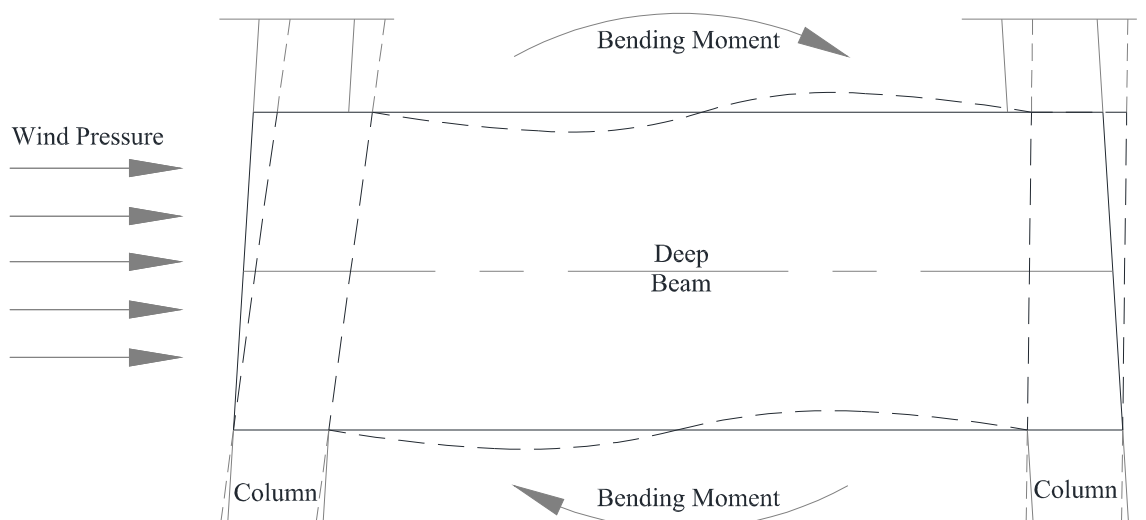


Figure 5-3: Panel represented as tie beams.

The only issue that the tie beam model didn't address is the connection between the column and the panel. The model considers the connection is a fixed connection transferring all the bending moment and shear forces. However, in reality, this connection is achieved using two shear connections at the top and bottom of the panel (refer to Figure 5-13 and Figure 5-14 for details). Even though the lever arm between the top and bottom connections will transfer moment from the column to the panel, representing it as a fixed connection might reduce the accuracy and the level of confidence in the results obtained. The last model addresses this issue, where the panels are represented by X-bracing members connecting the columns forming a space truss (Figure 5-4). The bracing members were fixed in the columns at the connections' center of gravity where moment releases were assigned to simulate hinged boundary conditions.

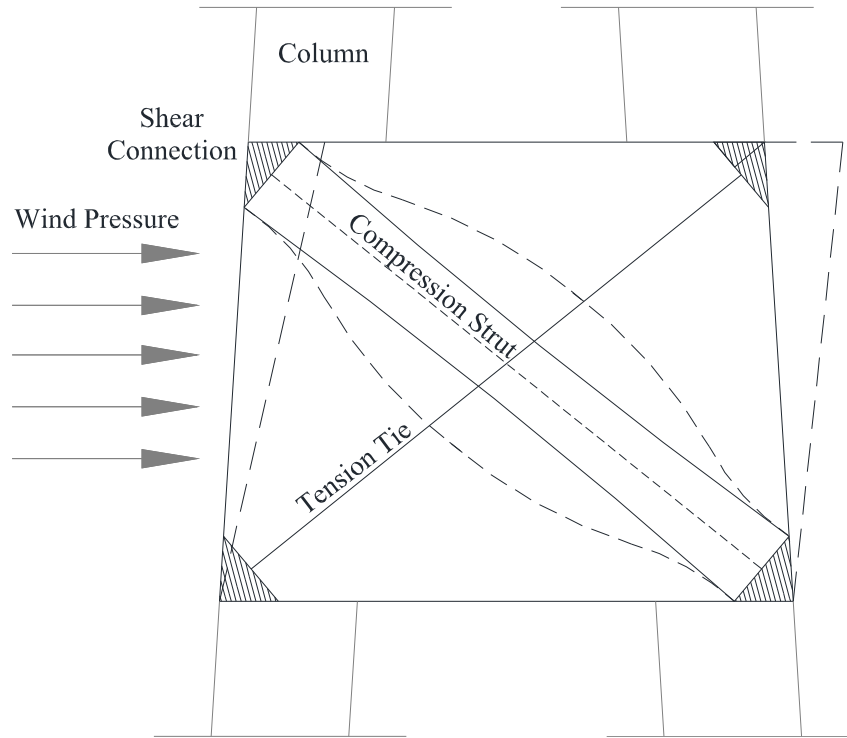


Figure 5-4: Panel represented as X-bracing.

5.3.4 Conclusions

The system actual behavior is independent of the technique used to simulate it. The results obtained from the three models confirmed this fact as the three models yielded very similar behaviors. Figure 5-5 shows the three different SAP models for the 320ft tower.

The columns were mainly subjected to axial forces with low shear and moments (Table 5-4 shows a comparison between the axial loads values obtained at the same critical section in the three models which were within 6% from each other). The panels were subjected to bending from direct wind pressure. The panels also enabled a composite action between the three columns by emulating the behavior of deep beams.

Table 5-4: Axial forces acting on the critical section of the columns.

Load Case	Shell Model	Tie Beam Model	X-bracing Model
Ultimate-4 Tension	2530 (kips)	2590 (kips)	2522 (kips)
Ultimate-4 Compression	-4200 (kips)	-4398 (kips)	-4475 (kips)

After converting the forces in the X-bracing model member forces to get the shear and moment acting on the panel using its free body diagram (refer to Figure 5-6) the same pattern in the in plane forces acting on the panels emerged as their magnitudes from different model lied within 4% from each other.

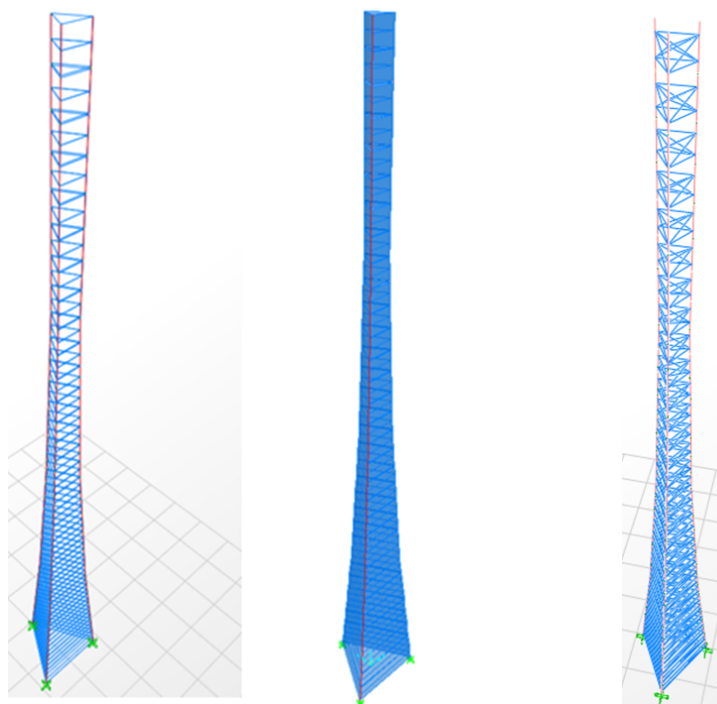


Figure 5-5: SAP models: tie beam (left) shell (middle) X-bracing (right) (320ft tower)

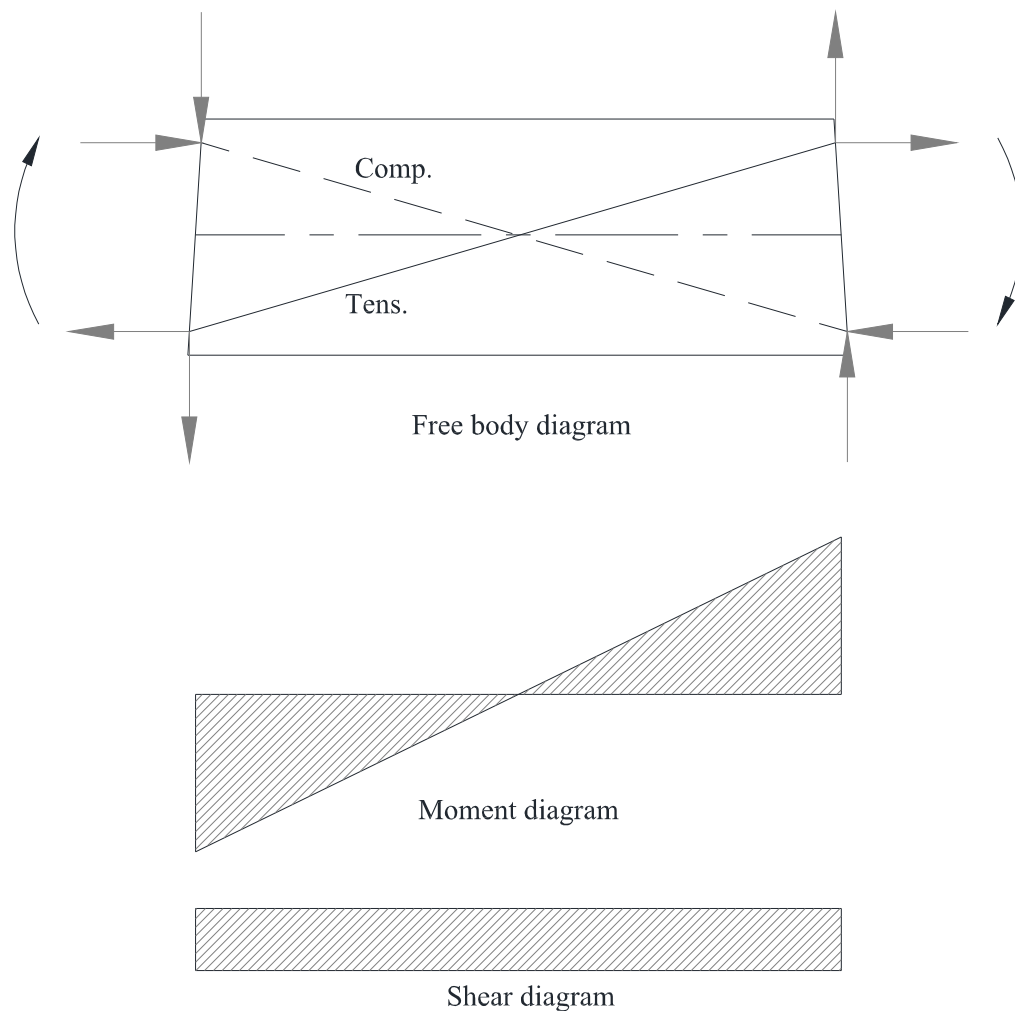


Figure 5-6: Free body, shear and moment diagrams for panels.

The tie beam modeling techniques is the method recommended and followed by this research. It was the most convenient out of the available techniques in terms of model construction and result extraction and interpretation.

5.4 Design

This section prescribes a design procedures for the proposed concrete wind turbine tower outlining the standards followed and methods used. Design of the steel tower is also included. Several limit states were considered for both tower design; ultimate limit state, service limit state and fatigue limit state. Non-operational wind turbine state was assumed for the ultimate limit state and wind speed from the extreme wind model (EWM) was considered. For serviceability check, both wind turbine state; operational and non-operational, were considered with wind speeds from their corresponding state; EOG and EWM respectively. For fatigue check, damage equivalent load method was used to determine the design adequacy. Load and resistance factors were used corresponding to each load, limit state and material. The expected limit state to control the design differs depending on tower material. For steel towers, fatigue almost always controls the tower design as it was the case in this study. For concrete towers, the controlling load is either the tension force in the ultimate state or concrete fatigue. For the proposed system, the ultimate tension governed the design.

5.4.1 Concrete Design

Concrete wind turbine towers currently being used consists of precast load bearing rings that are post-tensioned together to resist the lateral actions from wind and seismic loading. Therefore, design procedures recommended for the proposed system are different than currently implemented concrete schemes. One of the main differences is designing every element constituting the tower separately in the proposed system as

oppose to considering the whole tower as one big cylindrical cantilever column. The 28 day characteristic strength of concrete used was 8ksi and its modulus of elasticity was 5422ksi. The following section presents the different concepts followed when designing each individual element; columns, panels and connections. For detailed calculations refer to Appendix B and C.

a) Columns Design

Reinforced with all of the prestressing forces, columns are the main force resisting elements in the tower. While the design features entirely prestressed columns, an alternative where a fraction of the strands were post-tensioned is available. To endure the loads applied on the tower, the three columns have to work together as one composite section connected by the panels as mentioned earlier in the modeling section. Each column is subjected to biaxial bending moments, shear and axial force, either tension or compression depending on the wind direction. The hexagonal shape of the columns allows easy connection with the panels and evenly distributed reinforcement. Due to the symmetric pattern of the prestressed strands reinforcing the columns, vector summation can be used to simplify the design from biaxial bending to a resultant bending moment. Each column was designed for axial force and a resultant bending moment.

Ultimate design

Ultimate limit state design was performed as per the ACI 318 specifications. The column is reinforced with 10-0.6in. grade 270ksi strands tensioned to $0.75 f_{pu}$ in each side of the hexagonal totaling 60-06in. strands. An alternative where a portion of the strands are post-tensioned is also included. For this case 6-0.6in. strands are pre-tensioned in each

side of the hexagonal totaling 36-06in. strands plus 2 post-tensioned tendons containing 12-0.6in. strands each are use in both sides of the columns. The concrete cover for the prestressing strands was taken as 4in. form the edge of the concrete to the center of the strands. Two alternative shear reinforcements could be implemented depending on the cost efficiency and the practicality of construction; either using grade 75ksi W6 spiral reinforcement with a 12in. pitch or two #6 C-shaped bars grade 60ksi every 24in. Figure 5-7 shows the cross section of the columns once using all prestressed strands and another using prestressed strands and post-tensioned tendons, both shear reinforcement details are also shown.

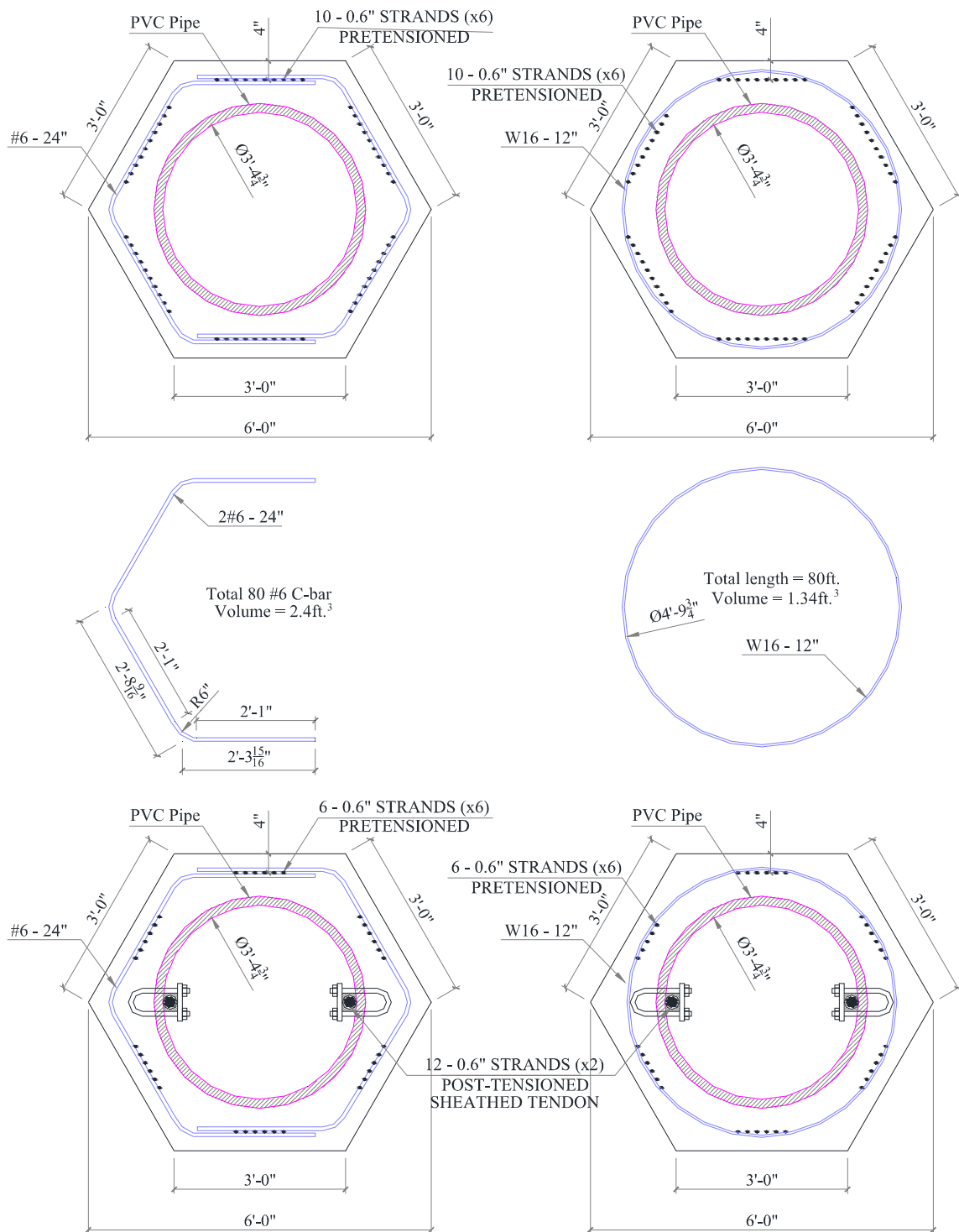


Figure 5-7: Base segment column cross section.

In order to check the adequacy of the design, the column interaction diagram was constructed. Figure 5-8 shows the interaction diagram of the columns in lower segment of the tower.

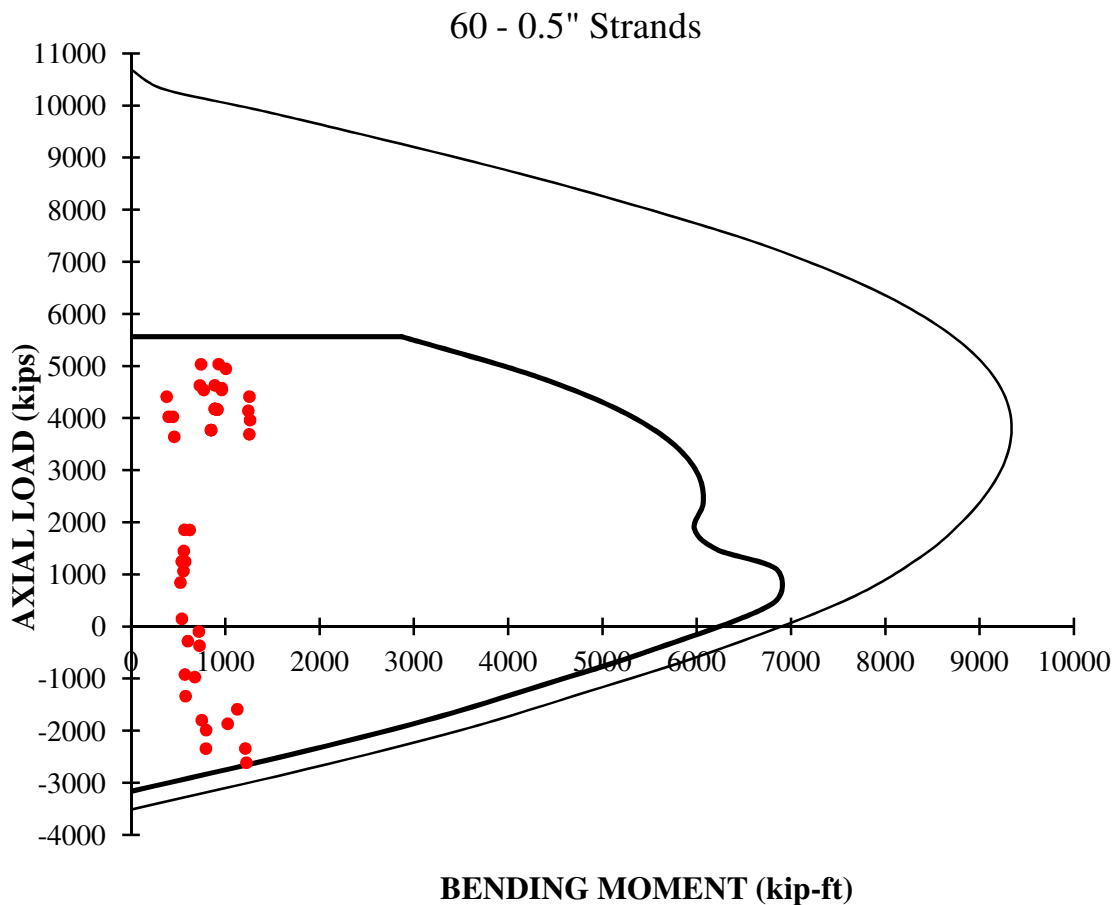


Figure 5-8: Base segment column interaction diagram (240ft tower).

The outer curve in the interaction diagram represents the capacity of the column when subjected to combined axial and bending. The inner curve indicates the column's nominal capacity after applying the resistance factor (ϕ) which fluctuates from 0.9 for pure bending to 0.65 for pure compression. Every point on the interaction diagram represents a loading case with an applied ultimate axial and moment (P_u and M_u). The furthest from

the y-axis the point is, the more bending moment it experiences. Points above the x-axis are subjected to compressive stress while points under it suffer from tensile stress. All the points lie inside the inner line which indicates an adequate design. As expected the controlling load was the tension on the column as can be noticed from the lowest points on the diagram. Shear design was achieved using the simplified method in ACI 318 using a strength reduction factor of 0.75. Minimum shear reinforcement was enough to resist the applied forces.

Service design

Serviceability checks were performed following the allowable stresses set by the ACI 318 in compression ($0.4 f'_c$). No tension on the columns was allowed in any service check whether the wind turbine was stationary or operating. The stresses on the column were calculated using the loads for both speeds (EWM and EOG) after applying the corresponding loads factor.

Deflection

The max deflection of the top of the 240ft and the 320ft towers under service conditions was 8.16in. and 11.11in. respectively. The ACI 318 standards don't specify and limits for deflection of concrete towers or any similar structures. However, since wind turbine structures resemble tall concrete chimneys, the ACI 307 specifications were adopted in this study. As specified in the ACI 307, the max deflection of the top of the tower under service conditions in inches shall not exceed 0.04 of the total height in feet. Meaning the max allowed deflection for the 240ft and the 320ft towers is 9.6in. and 12.8in. respectively.

Fatigue design

Fatigue design consideration for concrete elements is relatively new that started with the increased implementation of high strength concrete. Concrete fatigue is typically considered for bridge applications. These applications typically have applied load cycles less than 10 million cycles, however high stress ranges are imposed on the structure during each cycle. On the other hand, wind turbine tower are subjected to a much higher load cycles, in the magnitude of 10^8 , but these load cycles are associated with small stress range; every blade rotation is a cycles that causes a small stress change. High cycle fatigue is mainly controlled by elastic behavior. Similar structures, subjected to such magnitudes of load cycles, are not fully considered by current design codes. The next section will highlight current code provisions having fatigue specifications for concrete elements.

ACI 215R

The ACI 215R provides limited design recommendations for wind turbines or similar structures.

German Standard (DIN 1045)

Chapter 10.8 addresses both steel (mild and prestressed) and concrete fatigue. The document uses the S-N curves (Figure 4-2) to check mild and prestressed steel fatigue endurance limit. No approach dealing with higher fatigue cycles (more than a million) was included.

CEB- FIB Model Code 1990

The Model Code 1990 (MC90) was published by the International Federation for Prestressing (CEB-FIB) in 1987 and reviewed in 1993. As it stands, MC90 is the most suitable design tool for prestressed concrete towers as it is the only official document having complete design considerations for concrete, mild and prestressed steel subjected to more than 10^8 cycles of loading.

Norwegian Standard (NS 3473)

The NS 3473 also address concrete structures subjected to 10^8 cycles of loading. Chapter 13 of that document offers a simpler approach than MC90 to fatigue design in concrete structures. However, specifications for prestressed steel are not addressed in the standard.

Conclusion

Fatigue design for structure subjected to more than 10^8 load cycles is not fully covered in DIN 1045 and the ACI 215R. Prestressed strands and tendons fatigue design is not addressed in NS 3473. Therefore MC90 is the only document that offers specifications covering all the details of fatigue design of prestressed concrete wind turbine structures.

Fatigue Design According to MC90

The MC90 offer three different methods for fatigue design; the simplified procedure, Single and spectrum of load levels procedures. In cases where the load histogram of the fatigue cycles is available, rigorous spectrum of load levels procedures are required. However, in the absence of such data, a more simplified procedure using damage equivalent load is acceptable to check the integrity of the tower. The simplified procedure

was enough to check the fatigue limit for the proposed system; if the simplified check was unsafe, a more detailed calculation would have been required using single load level. The following section presents a summary of the simplified procedure (MC90 section 6.7.1 to 6.7.3).

Concrete Fatigue design procedures:

Sections subjected to compressive stress:

$$(\gamma_{sd})(\sigma_{c,max})(\eta_c) \leq 0.45(f_{cd,fat}) \quad (\text{Eq. 5-1})$$

Section subjected to tensile stress:

$$(\gamma_{sd})(\sigma_{t,max}) \leq 0.33(f_{ctd,fat}) \quad (\text{Eq. 5-2})$$

Where,

$\sigma_{c,max}$ is the max applied compressive stress

$\sigma_{t,max}$ is the max applied tensile stress

γ_{sd} is the partial load factor

η_c is the fatigue parameter from (Eq. 5-3)

$$\eta_c = \frac{1}{1.5 - 0.5 |\sigma_{c1}|/|\sigma_{c2}|} \quad (\text{Eq. 5-3})$$

Where,

$|\sigma_{c1}|$ is the lower value of the compressive stress within a distance no more than 11.8in. from the surface.

$|\sigma_{c2}|$ is the larger value of the compressive stress within a distance no more than 11.8in. from the surface

$f_{cd,fat}$ is the fatigue reference strength from (Eq. 5-4)

$$f_{cd,fat} = \frac{0.85(\beta_{cc}(t))}{\gamma_c} \left[f_{ck} \left(1 - \frac{f_{ck}}{f_{cko}} \right) \right] \quad (\text{Eq. 5-4})$$

Where,

- f_{cko} is the concrete reference strength
 f_{ck} is the characteristic concrete cylinder strength
 γ_c is the partial concrete material factor
 $\beta_{cc}(t)$ is the concrete age factor from (Eq. 5-5)

$$\beta_{cc}(t) = e^{0.2 \left(1 - \sqrt{28/t} \right)} \quad (\text{Eq. 5-5})$$

Where,

- t is the concrete age at loading start
 $f_{ctd,fat}$ is the fatigue reference tensile strength from (Eq. 5-6)

$$f_{ctd,fat} = \frac{f_{ctd,min}}{\gamma_c} \quad (\text{Eq. 5-6})$$

Where,

- $f_{ctd,min}$ is the lower bound of the characteristic tensile strength from (Eq. 5-7)

$$f_{ctd,min} = f_{ctko,min} \left(\frac{f_{ck}}{f_{cko}} \right)^{2/3} \quad (\text{Eq. 5-7})$$

Where,

$$f_{ctko,min} = 0.138 \text{ ksi}$$

Steel Strands Fatigue:

$$(\gamma_{sd})(\max\Delta\sigma_{ss}) \leq \frac{\Delta\sigma_{Rsk}}{\gamma_{s,fat}} \quad (\text{Eq. 5-8})$$

Where,

$\max\Delta\sigma_{ss}$ is the maximum applied stress range

$\Delta\sigma_{Rsk}$ is the characteristic fatigue strength at 10^8 cycles.

$\gamma_{s,fat}$ is the partial steel material factor

b) Panels Design

As explained in the modeling section, the panels serve a dual purpose; resisting the wind pressure subjected directly on their surface and connecting the columns together to enable composite action. In the former case, the panels behave as deep beams enduring in plane bending moments and shearing forces, however, in the latter case, out of plane bending moments are the actions governing their design as they mimic the behaviors of one way slabs. It can be inferred that their slab action will dictate their behavior and control their reinforcement as the panels stiffness resisting these actions is very small compared to their strong axis stiffness resisting in plane bending stresses. It should be noted that the panels won't be subjected to the maximum in plane and out of plane actions in the same time. Depending on the wind direction, the panels might experience maximum out of plane bending with no in plane actions or maximum in plane bracing action with a corresponding lower direct wind bending. Figure 5-9 shows the most critical cases that the panels are expected to go through depending on the wind direction.

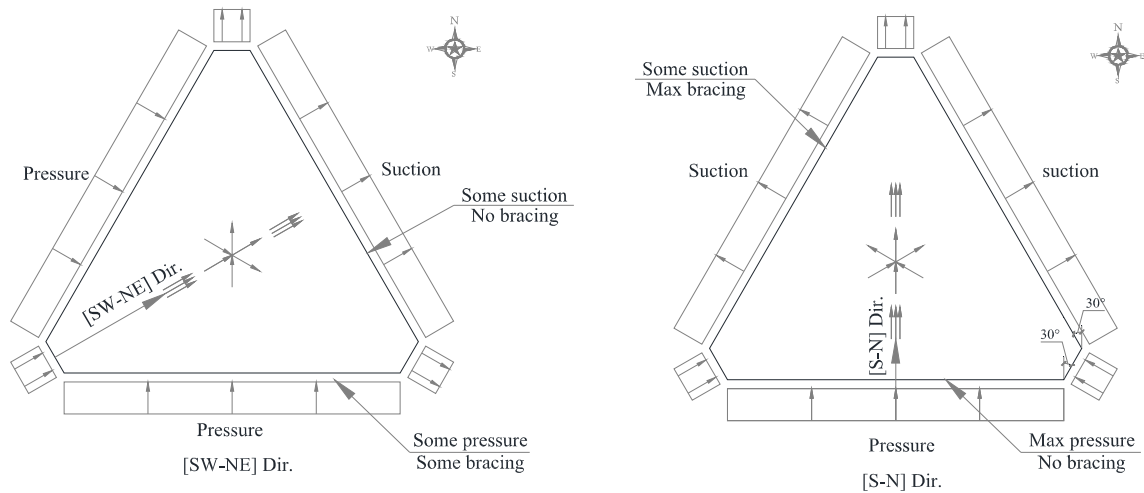


Figure 5-9: Straining actions on panels according to wind direction.

Design of panels as slabs

Due to the relatively small out of plane stiffness of the panels, out of plane bending is expected to be the controlling design case. From Figure 5-9 the panels are subjected to maximum wind pressure when the wind direction is perpendicular to any face. In these cases the bracing action forces are almost non-existing. To analyze the bending moments and design the panels the wind pressure and the panels span are required. Due to the tapered profile of the tower, the panel span varies with height having the maximum at the base and the minimum at the top. The wind pressure also varies with the height following the profile calculated in the loading chapter also shown in Figure 4-1. Table B-16 in the design appendix calculates the bending moments applied on the panel at each panels taking into consideration the pressure applied, wind direction, speed and the panel clear span. Despite the fact that the panel width decrease with the tower height; top panel is 10ft by 10 ft while the bottom panel is 25ft by 10ft, its behavior will not deviate from one way bending to two ways bending as it is only supported by the columns from two

opposite sides. The nominal resisting moment capacity was calculated as per to the ACI 318 specifications. Using a W20-12" welded wire mesh in each face (to satisfy shear reinforcement) the nominal capacity is 5.4 (kip-ft) per linear foot of the panel.

Design of panels as deep beams

Due to its geometry, deep beams do not experience the same one dimensional linear stress that regular beams do. However they experience a two dimensional state of stress where Bernoulli's theory, of plane sections remain plane after bending, does not apply. Therefore, the resulting strain distribution becomes nonlinear taking into account shear deformations normally neglected in regular beams. Figure 5-10 and Figure 5-11 show the strain distribution in normal and deep beams. The ACI 318 requires rigorous nonlinear strain procedures or strut and tie modeling for deep beams design. However, the CEB code offers a simplified procedure for designing deep beams taking into account the nonlinear strain distribution. In this study, the CEB's simplified method was used to check the design of the panels as deep. The design of deep beams is governed by shear deformations therefore it is required to provide shear reinforcement in both the horizontal and vertical direction. The welded wire reinforcement was chosen as the most suitable form of reinforcement as it is serving the dual purpose of resisting the out of plane bending moments and the in plane shearing forces since their peaks do not occur simultaneously. Additional flexural reinforcements were provided at a distance "y" from the top and bottom of the deep beam to resist in plane bending moments. The following section presents a brief summary of the procedures and Figure 5-12 shows the panel reinforcement details from the elevation, plan and side view perspective.

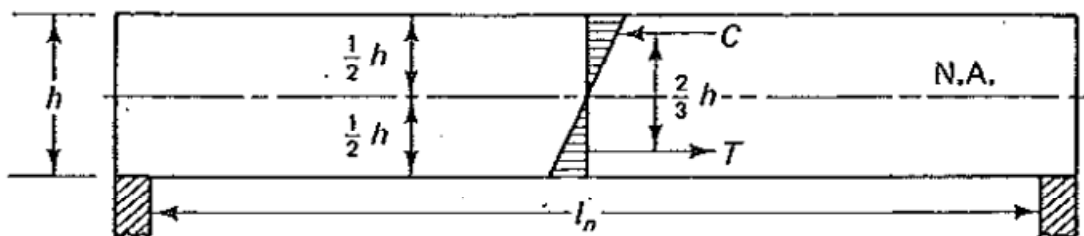


Figure 5-10: Linear strain distribution in normal beams. (Nawy, E., 2008)

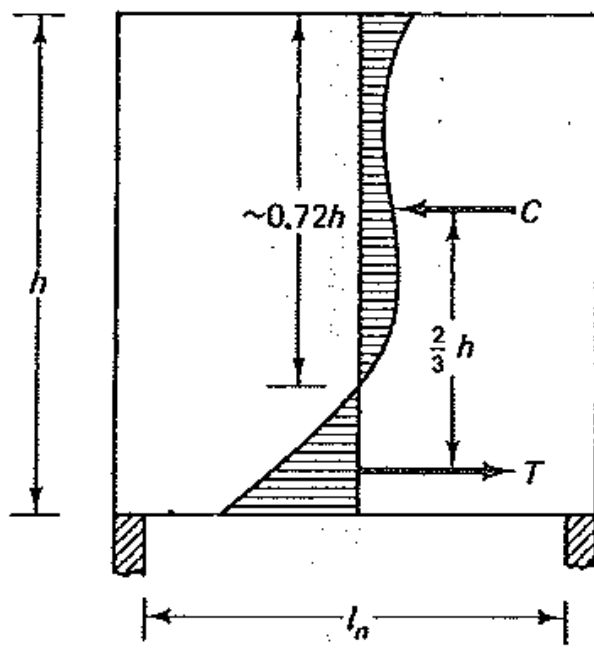


Figure 5-11: Nonlinear strain distribution in deep beams. (Nawy, E., 2008)

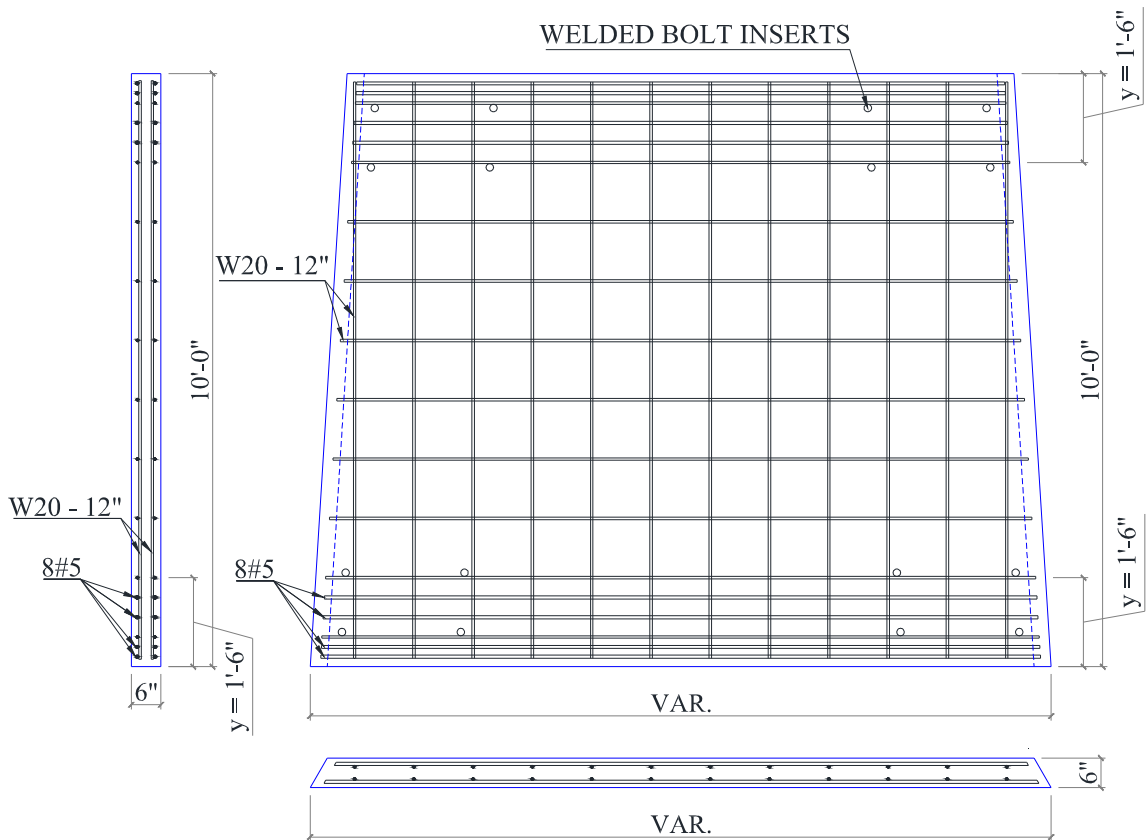


Figure 5-12: Panel reinforcement details.

The factored shear force has to satisfy the following condition (Eq. 5-9)

$$V_u \leq \phi [10\sqrt{f'_c} b_w d] \quad (\text{Eq. 5-9})$$

Where,

- V_u is the factored shear force
- ϕ is the strength reduction factor (= 0.75)
- f'_c is the characteristic strength of concrete (=8 ksi)
- b_w is the width of the panel (=6 in)
- d is the panel depth (= (0.9)(h) = 108 in) where “ h ” is panel height

The nominal shear resisting force of the plain concrete is calculated using (Eq. 5-10):

$$V_c = \left(3.5 - 2.5 \frac{M_u}{V_u d}\right) \left(1.9\sqrt{f'_c} + 2500\rho_w \frac{V_u d}{M_u}\right) b_w d \leq 6\sqrt{f'_c} b_w d \quad (\text{Eq. 5-10})$$

Where,

$$1.0 < \left(3.5 - 2.5 \frac{M_u}{V_u d}\right) \leq 2.5 \quad (\text{Eq. 5-11})$$

This factor is a multiplier of the basic equation of V_c in normal beams to account for the higher resisting capacity of deep beams.

M_u is the factored bending moment

ρ_w is the flexural reinforcement ratio

The nominal shear resisting force of the reinforcement is calculated using (Eq. 5-12):

$$V_s = \left[\frac{A_v}{S_v} \left(\frac{1.0 + \frac{L_n}{d}}{12} \right) + \frac{A_{vh}}{S_h} \left(\frac{11 - \frac{L_n}{d}}{12} \right) \right] f_y d \quad (\text{Eq. 5-12})$$

Where,

L_n is the clear span of the panel

A_v is the total area of vertical reinforcement spaced at S_v in the horizontal direction at both faces of the beam

A_{vh} is the total area of horizontal reinforcement spaced at S_h in the vertical direction at both faces of the beam

Maximum $s_v \leq \frac{d}{5}$ or 12 in. and maximum $s_h \leq \frac{d}{5}$ or 12 in.

Minimum $A_{vh} = (0.0015)bs_h$ and minimum $A_v = (0.0025)bs_v$

The nominal moment capacity is calculated using (Eq. 5-13):

$$M_n = A_s f_y j d \quad (\text{Eq. 5-13})$$

Where,

A_s is the flexural reinforcement

f_y is the yielding stress of the flexural reinforcement

j_d is the moment arm from (Eq. 5-14)

$$j_d = 0.2(l + 2h) \quad \text{for } 1 \leq \frac{l}{h} < 2 \quad (\text{Eq. 5-14})$$

$$j_d = 0.6l \quad \text{for } \frac{l}{h} < 1$$

Where,

l is the effective span (center to center)

The minimum flexural reinforcement is calculated using (Eq. 5-15):

$$A_s \geq \frac{3\sqrt{f'_c}}{f_y} bd \geq \frac{200bd}{f_y} \quad (\text{Eq. 5-15})$$

The tension reinforcement has to be placed in the lower (tension side) segment of the beam such that the segment height is “y” calculated by (Eq. 5-16):

$$y = 0.25h - 0.05l < 0.20h \quad (\text{Eq. 5-16})$$

c) Connections and splices

For this proposed system, three types of connections and splices are used to connect the tower together. The first is panel connections that connects the panels to the columns, second are the columns splices that links individual column segments to form one element and last are the base connections connecting the columns to the foundation. Compressible filler is used under the panels so that they can bear on each other.

Panel Connections

The panels are connected to the columns at its four corners using shear connections to simulate a hinged connection; therefore each individual connection won't transfer any

bending moment. However using two connections each side of the panel transferring shear forces will produce a bending moment, equal to these forces multiplied by the lever arm, which in turn is transfer to the panels as in plane bending moment. In short, each panel side is supported by two connections resisting shear forces and torsional moment as shown in Figure 5-14. Four 1½in. A490-N grade 60ksi bolts ($\phi V_n=79.5$ kips) are used in each corner of the panel, Figure 5-13 and Figure 5-14 show the elevation and cross section of the connection. See appendix B for design details.

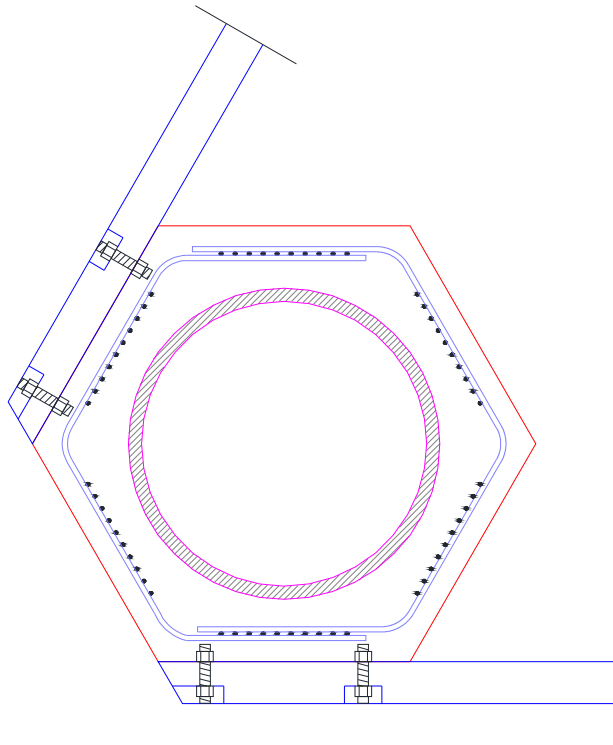


Figure 5-13: Panel connection cross section details.

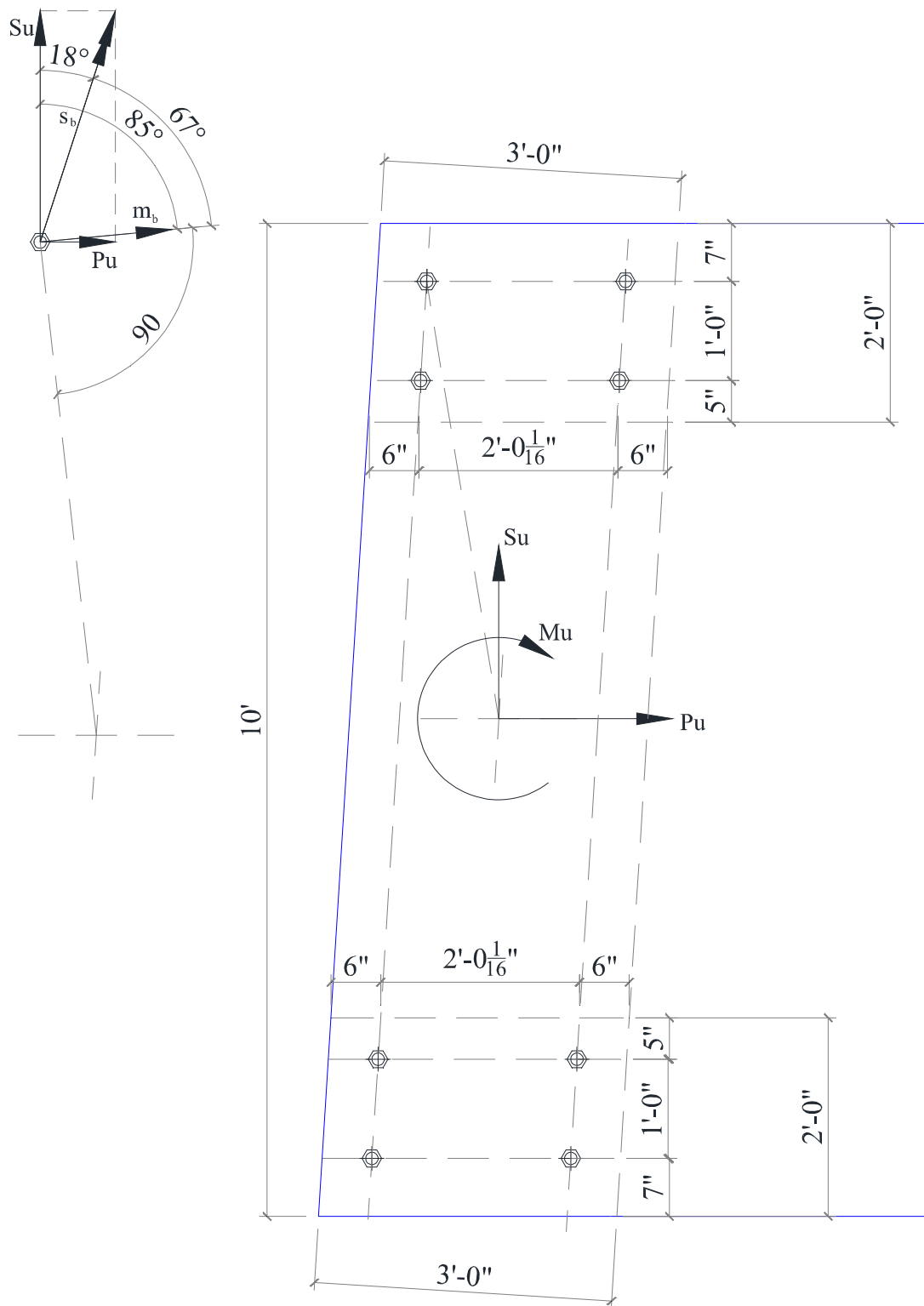
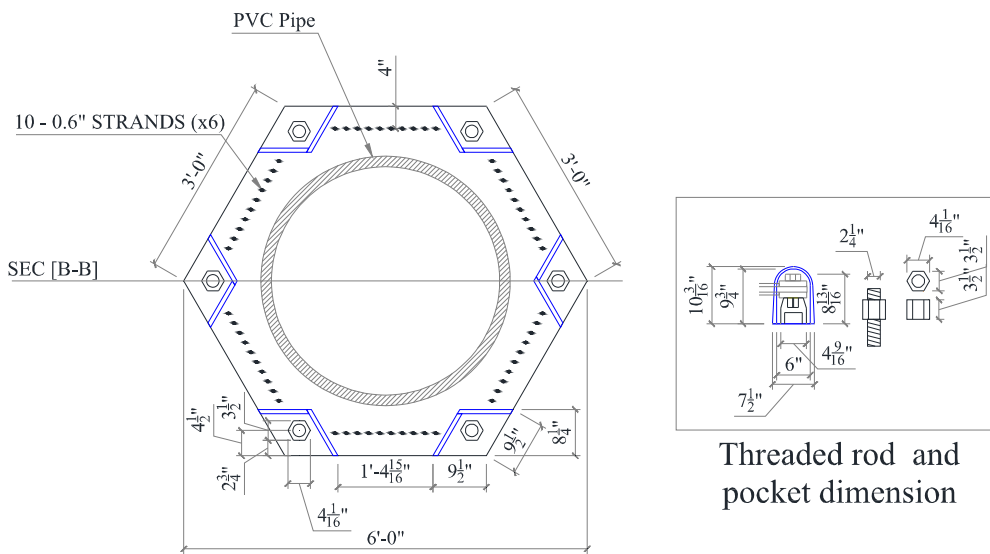


Figure 5-14: Panel connection elevation details.

Columns Splices

Columns splices are used to connect two column segments together. In the 240ft height tower, there is a total of two column splices per column connecting its three segments together, in the 320ft tower, three splices are required. The splices weren't design to withstand their corresponding applied loads but rather the nominal capacity of the columns they are connecting. This approach will eliminate any weak or potential failure points along the columns and will make the splice connection as strong, if not stronger, as the column itself. Six 2¼ in. grade 150ksi threaded rods ($\phi F_u = 613$ kips) are used for the splice, one in each corner of the column. Figure 5-15 shows the columns splice connection details along with the threaded rod dimensions. The threaded rods have to extend 2½ft. in the columns to overcome the transfer length of the strands so that the force throughout the connection doesn't drop. However, due to the tapered profile of the tower, the two segments of the columns, connected by the splice, are not perfectly aligned which might cause problems during construction. Shims are used between the two segments to adjust the tapering angle (maximum slope = 16 to 1). Another alternative to the extension of the threaded rods 2½ft. in the columns, to transfer the full force, is to use a base plate at the end of the segments and fix the strands in it using chucks. That way the threaded bars don't have to extend in the columns as the transfer length will be drastically reduced. After the threaded bars are tightened, the pockets can be grounded or covered with plastic caps to maintain the aesthetic view.



Column Splice Cross Section

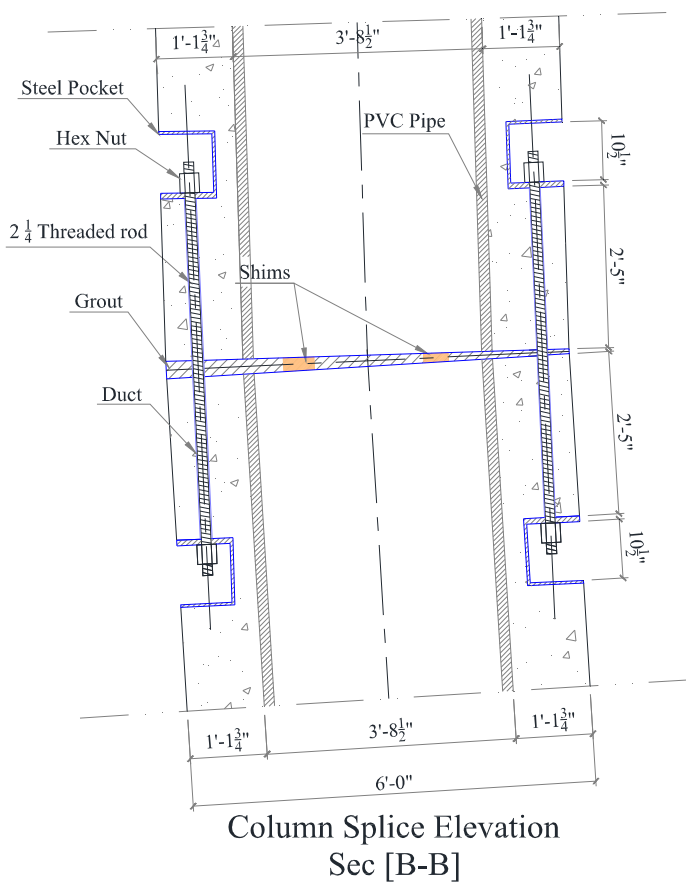


Figure 5-15: Column splice details.

Base Connection

Base connections are used to connect the columns to the foundation. They are designed to withstand the base reactions from the columns. Like the columns splice, six 2¼ in. grade 150ksi threaded rods ($\phi F_u = 613$ kips) are used for the base connection, one in each corner of the column. Figure 5-16 shows the connection details. The angle of inclination of the columns is formed in the concrete foundation to simplify column fabrication and erection procedures.

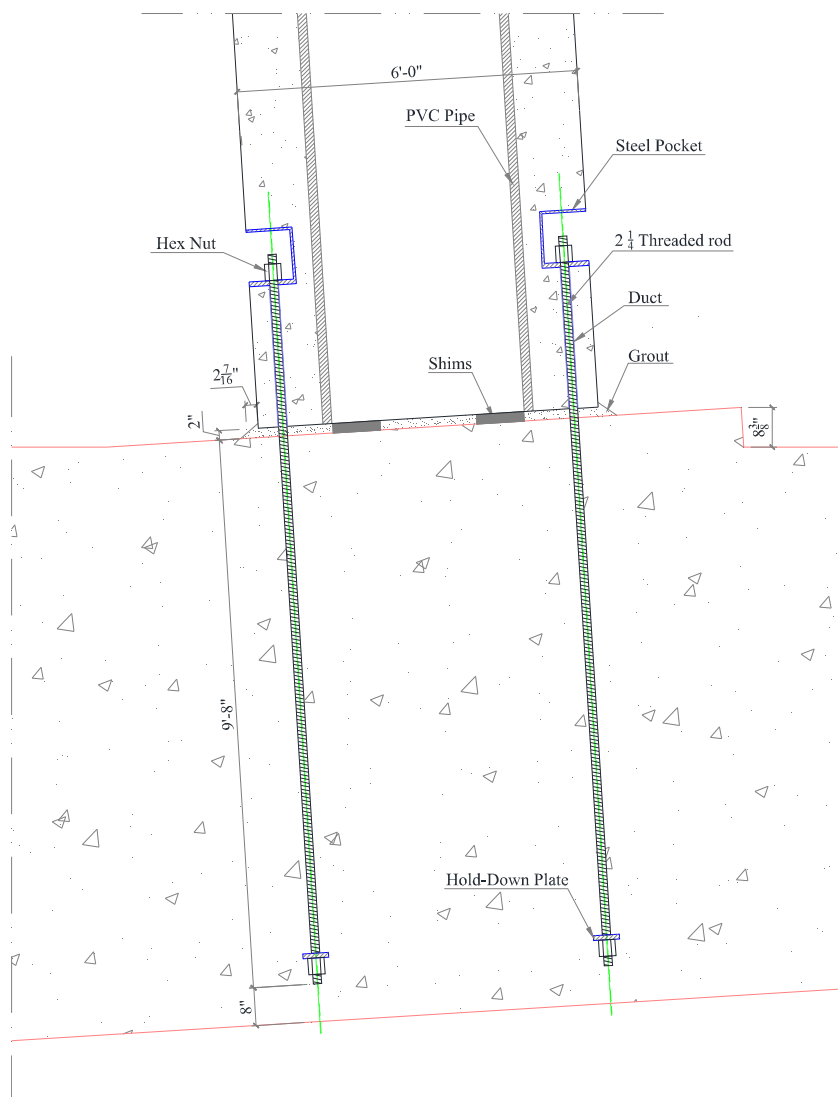


Figure 5-16: Base connection details.

5.4.2 Steel Design

Steel towers are typically composed of tapered prefabricated conical tubes with decreasing diameter and thickness along the height. Its dimensions are tailored to meet stiffness, buckling and fatigue requirements. This section explains the procedures followed in order to design the steel tower.

a) Allowable Stress Design

In this study, the steel tower was designed using the allowable stress design method as per the AISC-89 Specifications. Structural steel having a yielding stress of 50ksi was used. The allowable compression stress is given by (Eq. 5-17).

$$F_a = \frac{\left[1 - \frac{(KL/r)^2}{2C_c^2}\right] F_y}{\frac{5}{3} + \frac{3(KL/r)}{8C_c} - \frac{(KL/r)^3}{8C_c^3}} \quad (\text{Eq. 5-17})$$

Where,

K is the effective length factor (= 2 for cantilever structures).

L is the height of the tower.

r is the radius of the tower.

C_c is the material coefficient calculated according to (Eq. 5-18).

$$C_c = \sqrt{\frac{12\pi^2 E}{F_y}} \quad (\text{Eq. 5-18})$$

Where,

E is the steel's elastic modulus.

When the slenderness ration (KL/r) is greater than the material coefficient(C_c), the allowable compression stress is recalculated using (Eq. 5-19).

$$F_a = \frac{12\pi^2 E}{23(KL/r)^2} \quad (\text{Eq. 5-19})$$

The allowable bending stress is given by (Eq. 5-20).

$$F_b = 0.6F_y \quad (\text{Eq. 5-20})$$

And the allowable shear stress is determined by (Eq. 5-21).

$$F_v = 0.4F_y \quad (\text{Eq. 5-21})$$

The combined stress for the applied compression and bending stresses should satisfy the interaction equation given by (Eq. 5-22).

$$\frac{f_a}{F_a} + \frac{f_b}{F_b} \leq 1.0 \quad (\text{Eq. 5-22})$$

By the same token, the combined stress for the applied shear and torsion should be less than the allowable shear stress.

b) Local Buckling Stress

Due to the large diameter of the tube compared to its wall thickness, local buckling check is preformed to assess whether it is a controlling parameter. The compressive strength of the tower is the lesser of the yielding strength and the elastic buckling stress given by (Eq. 5-23).

$$\sigma_{cr} = 0.605E t/r \quad (\text{Eq. 5-23})$$

Where,

t is the tower's wall thickness

Due to imperfection the axial strength of the tower will be reduced according to (Burton, et al., 2001) by a reduction factor given by (Eq. 5-24).

$$\alpha_0 = \begin{cases} \frac{0.83}{\sqrt{1 + 0.01 r/t}} & \text{if } r/t < 212 \\ \frac{0.7}{\sqrt{1 + 0.01 r/t}} & \text{if } r/t > 212 \end{cases} \quad (\text{Eq. 5-24})$$

(Eq. 5-25) gives the reduction factor for bending.

$$\alpha_B = 0.1887 + 0.8113\alpha_0 \quad (\text{Eq. 5-25})$$

(Eq. 5-26) computes the buckling stress.

$$\sigma_u = \begin{cases} F_y \left[1 - 0.4123 \left(\frac{F_y}{\alpha_B \sigma_{cr}} \right)^{0.6} \right] & \text{if } \alpha_B \sigma_{cr} > F_y/2 \\ 0.75 \alpha_B \sigma_{cr} & \text{if } \alpha_B \sigma_{cr} < F_y/2 \end{cases} \quad (\text{Eq. 5-26})$$

The maximum applied stress from normal and shear is determined using (Eq. 5-27).

$$\sigma_a = \sqrt{(f_a + f_b)^2 + 3f_v^2} \quad (\text{Eq. 5-27})$$

c) Fatigue Design

Steel tower are more often than not governed by fatigue stresses. The IEC specifications prescribe a combined partial safety factor of 1.265. Damage equivalent load method was used with the S-N curves to determine the adequacy of the design. See appendix C for design details.

5.4.3 Recommended design Procedures for the proposed system

a) Column design

Controlling load case: ultimate tension (initial dimensions and prestressing).

Ultimate limit state: design for axial and moment using interaction diagram (ACI 318).

Service limit state: check stresses on the columns allowing no tensile stresses (ACI 318).

Deflection: check the actual service deflection against the allowable values (ACI 307).

Fatigue: check the adequacy of the design using the appropriate method corresponding to the available loading data (MC 90).

b) Panel design

Ultimate out of plane bending: determine initial dimensions and reinforcements using one way slab design theory (ACI 318).

Ultimate in plane bending and shear: Check the adequacy of the design using deep beam design theory (CEB).

c) Connections design

Panel connection: design the connection on one side of the panel for shear and moment.

Column splice: Design the column splice to transfer the max nominal capacity of the segments it is connecting.

Base connection: design the connection to withstand the max base reactions of the three columns.

CHAPTER 6

SUMMARY AND CONCLUSIONS

In this chapter the results obtained from the study are summarized and conclusions are drawn. The 240ft proposed concrete system was compared against the 240ft steel tubular tower while the 320ft proposed concrete system was compared against a current 320ft circular concrete tower published by LaNier, M.W., (2005) (Figure 6-4).

6.1 Design Summary

Table 6-1 and Table 6-2 and Figure 6-1 through Figure 6-4 summarize each tower's final specifications, dimensions and reinforcement.

Table 6-1: The 240ft systems design summary.

Criteria		Proposed System	Tubular Steel Tower
Total Height		240ft	240ft
Tower Material		Concrete	Steel
Wind Turbine		3.6MW	3.6MW
No. of Segments		3 segments	4 segments
Tower Cross Section		Triangular	Circular
Segment Height		80ft	60ft
Tower Profile		Tri-linear (Figure 6-1)	linear
Dimension/ Diameter	Base	25ft	18ft
	Top of 1st Segment	15ft	16ft
	Top of 2nd Segment	10ft	14ft
	Top of 3rd Segment	---	12ft
	Top of Tower	10ft	10ft
Panel/Wall thickness	Base	6in.	1.8in.
	Top of 1st Segment		1.6in.
	Top of 2nd Segment		1.4in.
	Top of 3rd Segment		1.2in.
	Top of Tower		1.0in.
Tower Weight		2437 kips (1218 ton)	865 kips (433 ton)
Natural Frequency		0.44 Hz	0.34 Hz
Controlling Load		Ultimate tension	Fatigue
Column Reinforcement	Segment 1	60-0.6" Strands	
	Segment 2	60-0.6" Strands	
	Segment 3	42-0.6" Strands	
	Shear	W16-12" Spiral	
Panel Reinforcement	Shear	W20-12" WWR each side	
	Bending	8#5 top and bottom	

Table 6-2: The 320ft systems design summary.

Criteria		Proposed System	Circular Concrete Tower
Total Height		320ft	320ft
Tower Material		Concrete	Concrete
Wind Turbine		3.6MW	3.6MW
No. of Segments		4 segments	2 segments
Tower Cross Section		Triangular	Circular
Segment Height		80ft	160-167ft
Tower Profile		Quad-linear (Figure 6-3)	Bi-linear
Dimensions/ Diameter	Base	40ft	22ft
	Top of 1st Segment	25ft	17ft
	Top of 2nd Segment	15ft	12ft
	Top of 3rd Segment	10ft	---
	Top of Tower	10ft	12ft
Panel/Wall thickness	Base	6in.	2.25ft
	Top of 1st Segment		2.00ft
	Top of Tower		1.5ft
Tower Weight		3579 kips (1790 ton)	2475 kips (1238 ton)
Natural Frequency		0.42 Hz	0.39 Hz
Controlling Load		Ultimate tension	Ultimate tension
Column Reinforcement	Segment 1	60-0.6" Strands	---
	Segment 2	60-0.6" Strands	---
	Segment 3	42-0.6" Strands	---
	Segment 4	30-0.6" Strands	---
	Shear Reinforcement	W16-12" Spiral	---
Panel Reinforcement	Shear Reinforcement	W20-12" WWR each side	---
	Bending Reinforcement	8#5 top and bottom	---
Tower Reinforcement	Segment 1	---	240-0.6" Strands
	Segment 2	---	192-0.6" Strands
Horizontal Skin Reinforcement	Segment 1	---	#6-12"
	Segment 2	---	#4-12"
Vertical Skin Reinforcement	Segment 1	---	#6-10"
	Segment 2	---	#4-10"

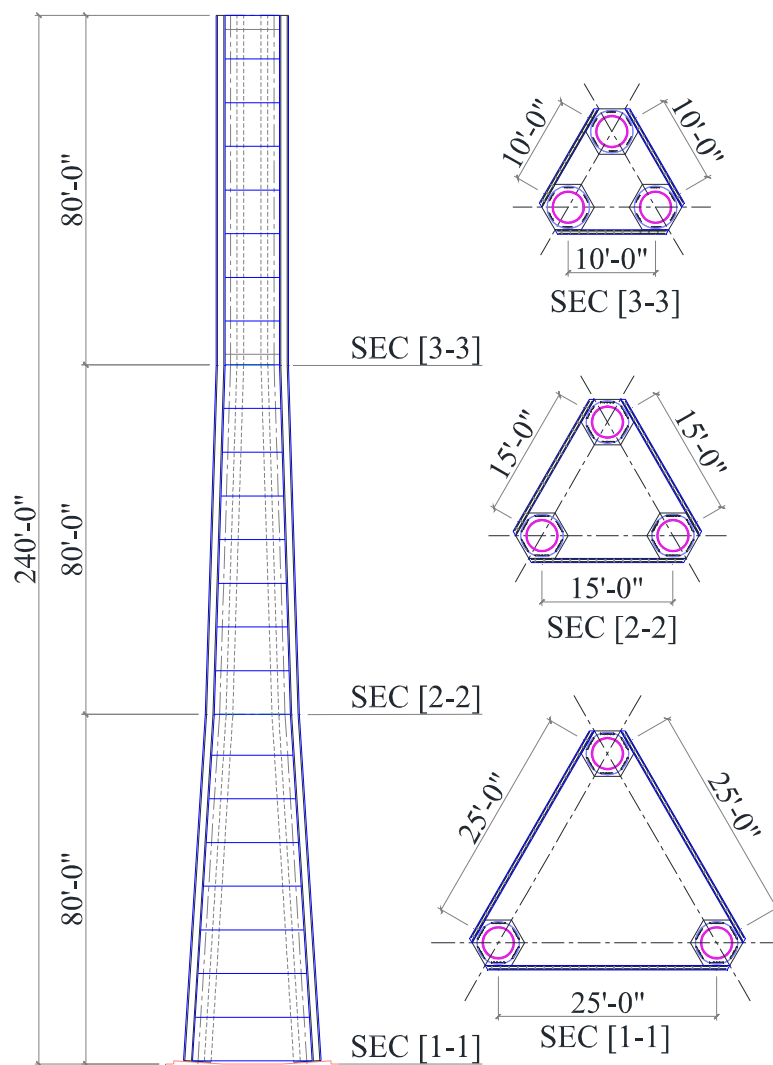


Figure 6-1: The 240ft proposed concrete system's design plan.

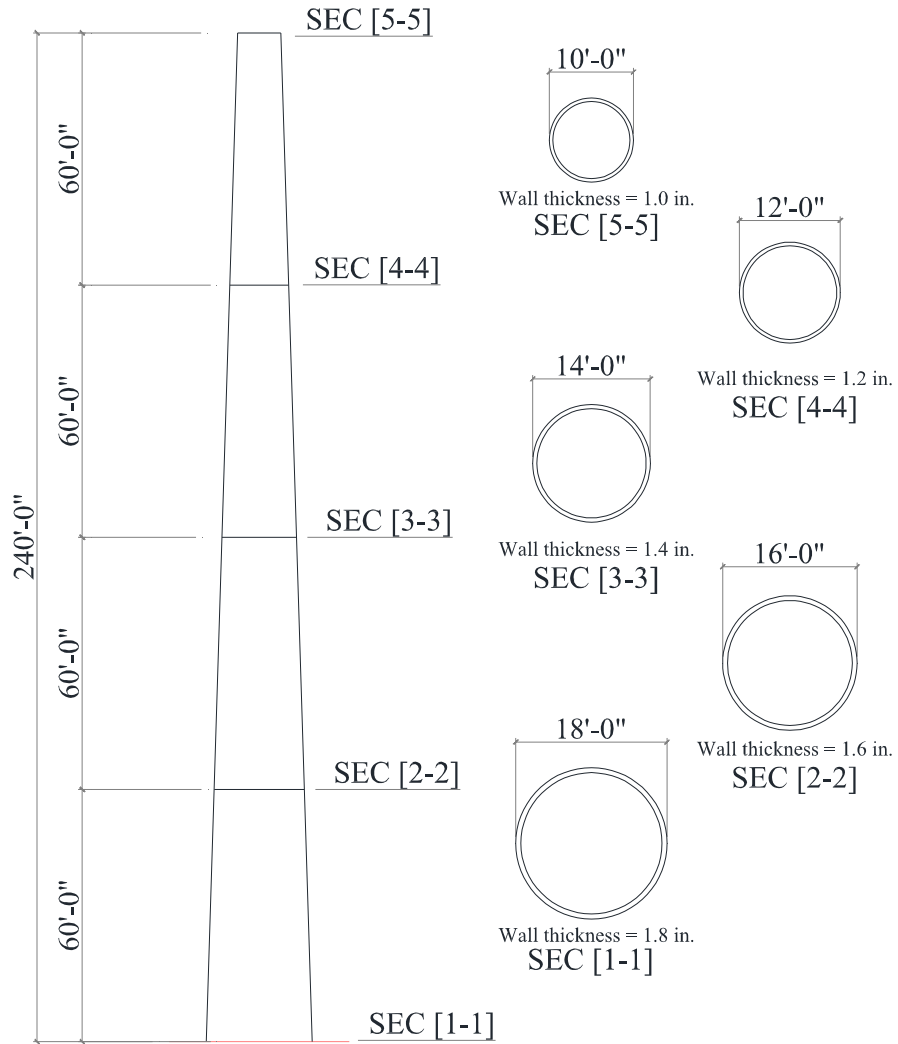


Figure 6-2: The 240ft Steel tower's design plan.

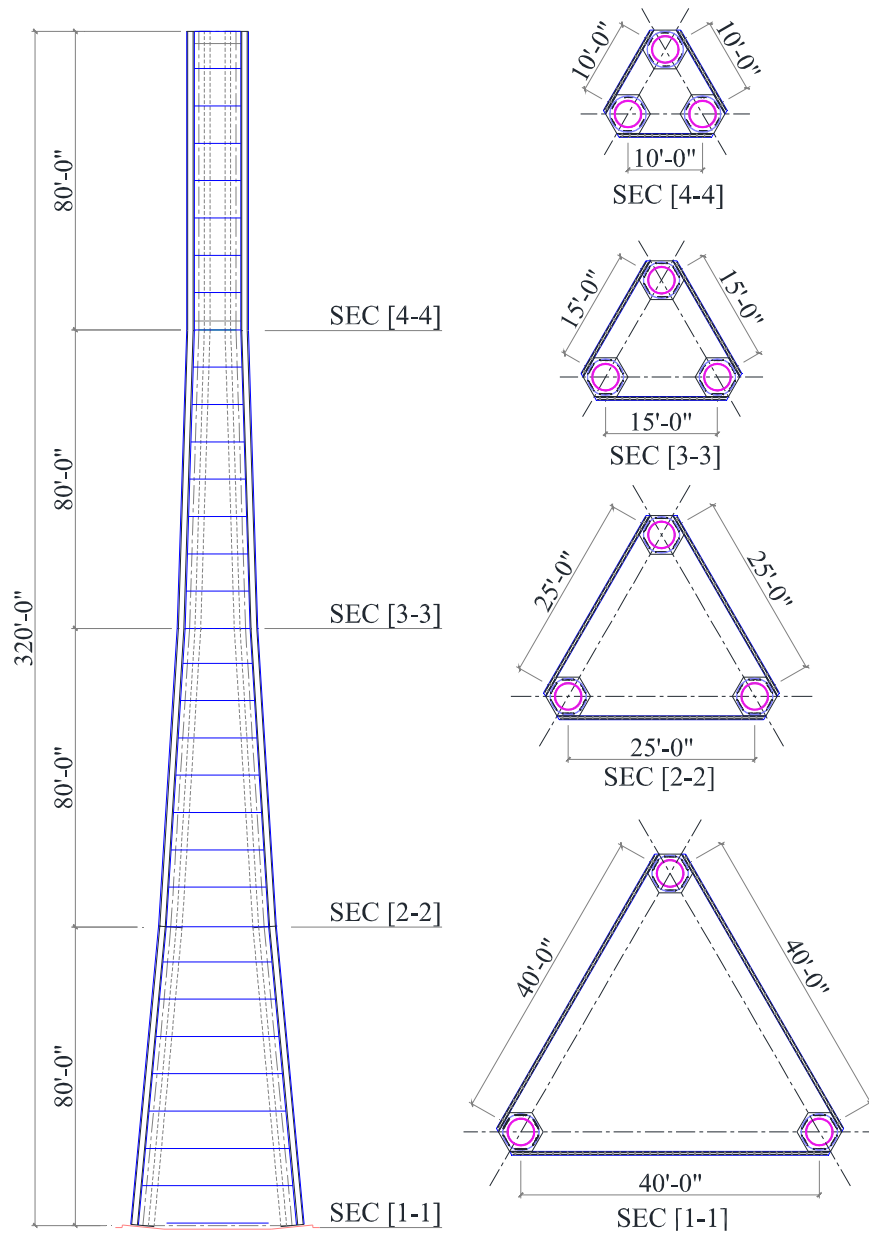


Figure 6-3: The 320ft proposed concrete system's design plan.

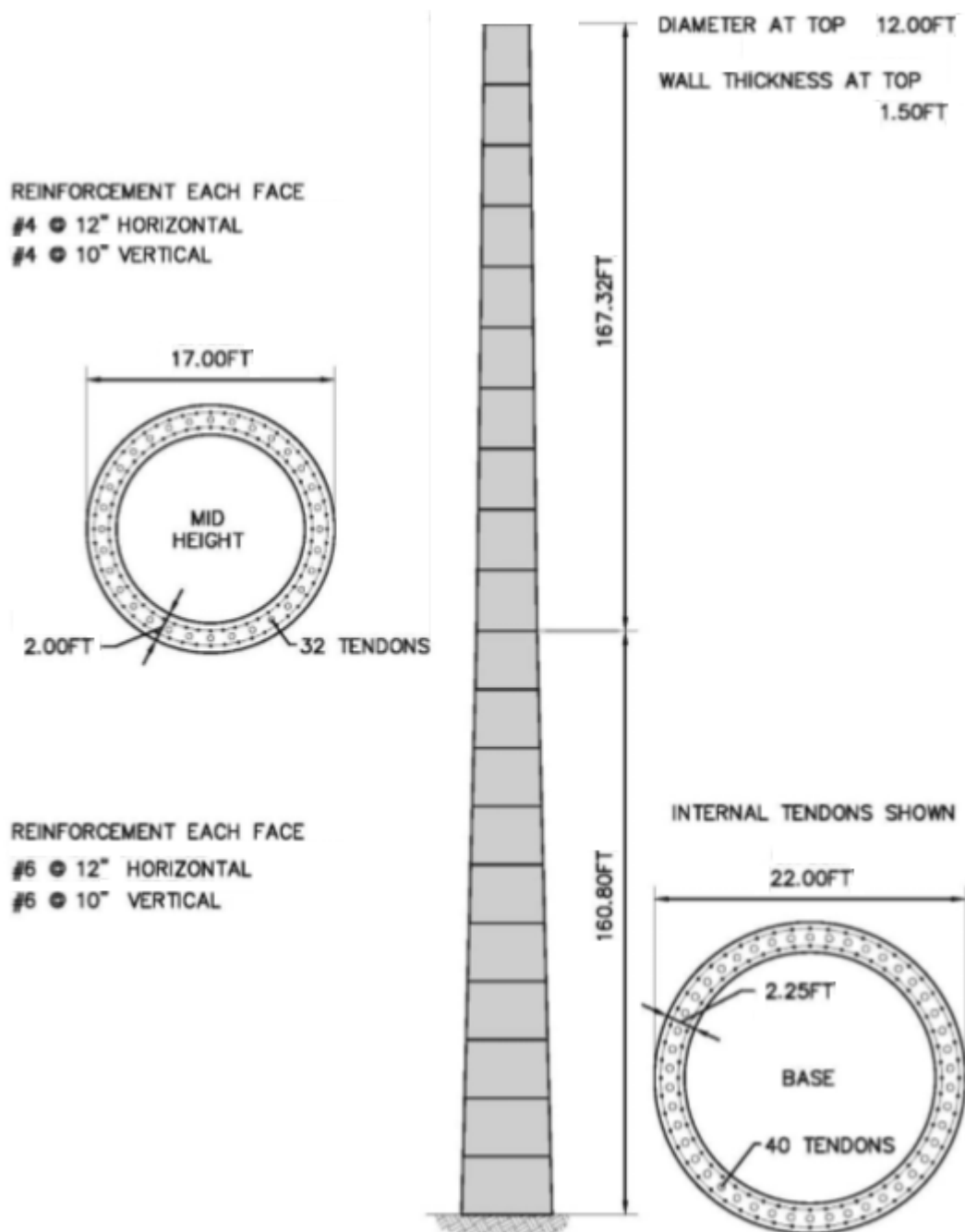


Figure 6-4: The 320ft concrete circular tower's design plan. (LaNier, M.W., 2005)

6.2 Quantities

Table 6-3 presents the material quantities used for each tower along with approximate cost estimation. Material unit cost were estimated based on experience, and are used for comparative illustrations.

Table 6-3 Material quantities and cost.

System Material	Proposed (240ft)	Tubular steel (240ft)	Proposed (320ft)	Unit Cost
Concrete (yd ³)	600	---	880	\$ 400
Prestressing strands (lb)	28,500	---	34,000	\$ 1.50
Post-tensioning tendons (lb)	---	---	---	\$ 2.30
Threaded Bars (ft)	300	---	400	\$ 22.5
Reinforcement bars (lb)	50,800	---	73,500	\$ 1.00
Structural Steel (lb)	---	614,700	---	\$ 1.50
Material Cost	\$ 340,000	\$ 922,000	\$ 486,000	

6.3 Systems Comparison

6.3.1 Comparing the 240ft systems

The most noticeable difference between the proposed system and the steel tower is the weight and dimension increase from the steel tower to the proposed system. The following points are the main characteristics that favor the proposed system over the steel tower.

Structural behavior: As oppose to the brittle behavior that the local buckling and fatigue failure modes impose on the steel tower, the proposed system experienced a more favorable ductile behavior.

Weight distribution and foundation: The increased weight coupled with the tapered profile of the proposed system gives the tower a much needed stability yielding better resistance to overturning and improved dynamic behavior. Moreover, it reduces the size of the gravity foundation needed. And the proposed system's base has a larger footprint which reduces the foundation's cantilever span and the reinforcement needed.

Dynamic performance: The proposed system has higher tolerance to dynamic loads; it benefits from a greater structural stiffness, than the steel tower, having higher frequencies and lower periods. Consequently, the steel tower would undergo greater deflections and vibrations than the proposed system.

Transportation and Erection: The limit for the diameter of complete steel ring sections that can be transported along the public highway is 14.5ft. This will introduce transportation issues for two lower segments in the steel tower, therefore costly bolted connections would have to be introduced into the thickest and most heavily loaded sections of the tower. While steel towers are characterized by fast erection, the introduction of vertical bolted connections would slow down the process. On the other hand, the proposed system can easily accommodate these logistical issues, while maintaining short erection times. Moreover, precast concrete technologies allow the possibility of having an on-site temporary manufacturing base that will eliminate most of the transportation costs and further shorten the construction time. In case of large wind farms with several wind turbine towers this option becomes very appealing.

Maintenance and Durability: Precast concrete is a very durable material as compared to steel. It has the ability to maintain its properties under harsh weathering conditions. The proposed system requires little or no maintenance and painting it is and aesthetic option not a requirement for protection against corrosion.

Flexibility: The proposed system can be tailored to accommodate any required dimension, reinforcement or logistics. Several options for column design and reinforcing patterns are presented in this study including different shear reinforcement option, a prestressed and a post-tensioned option. Filling the lower segments of the columns with plain concrete is also a design alternative that could be adopted to meet specific design criteria. The tower's vertical profile is a powerful tool that could be employed to reduce columns reinforcement or reducing the tower's footprint. Moreover, precast concrete is

always associated with superior quality control and optimal mechanical properties. In addition, its ability to be fine-tuned to meet unique project requirement is an invaluable quality that comes in handy when dealing harsh weathering conditions.

Enhanced Design Lifetime: The steel tower has limited design life as it is controlled by fatigue load cycles. Increasing its expected lifetime would result in an increase in fatigue cycles and consequently increase in dimensions and cost. However, the proposed system's has a better tolerance to fatigue loads yielding longer design lifetime with little maintenance.

Cost Efficiency: The proposed system offers an enhanced life cycle value with low initial cost. Concrete's raw materials are inexpensive, and for tall tower a cost-effective solution with an extend design life is feasible using the proposed system.

6.3.2 Comparing the 320ft systems

Unlike the 240ft systems, both of these systems are concrete systems which make them similar to each other. The most noticeable differences between the two systems are the tower profiles and the dimensions to reinforcement ratio. The proposed system has a vertical profile that varies linearly every segment making it a quad-linear profile, however the one employed in the circular system is a bi-linear profile. The other noticeable difference is the tower footprints; 40ft for the proposed system vs. 22ft for the circular tower. These different footprints have different reinforcement; the proposed system was reinforced with 60-0.6" strands in each column totaling a 180-0.6" strands at

the base, while the circular tower was reinforced with 40 post-tensioning tendons having 6-0.6”strands each, totaling 240-0.6” strands at the base. The following characteristics favor the proposed system over the circular system:

Tapered profile: The proposed system’s vertical profile was tailored to the expected bending moment diagram yielding an optimal weight distribution along the tower’s height and smaller applied forces compared to the circular system.

Dimensions and reinforcement: The dimensions of the system determine the magnitude of the applied forces; the larger the dimensions, the smaller the forces. Wind turbine tower are usually built in remote places to benefit from unobstructed wind speeds, therefore, the increase in dimensions is unproblematic. For the proposed system, the columns cross-section dimensions are constant and the panels are only 6in. thick, which allows an increase in dimensions without a significant increase in weight and materials. In turn, these dimensions allow a reduction in the reinforcement required which reduces the overall cost. On the other hand, the base wall thickness of the circular tower measures 2.25ft causing a significant increase in weight and materials with the increase of the tower’s footprint.

The proposed system’s weight, which is larger than the circular system, coupled with the tapered profile grants the proposed system a better stability to resist overturning moments and improved dynamic behavior. Cost savings can also be expected in the gravity foundation due to the increased weight and footprint.

Dynamic performance: The circular system has a slightly higher natural period than the triangular one making it more flexible and more susceptible to vibration. Consequently, it would undergo larger deflections than the proposed system.

Flexibility: Tweaking the tower's vertical profile add a lot of flexibility to the design of the proposed system allowing it to accommodate any dimensions and reinforcement required. Several options for column design and reinforcing patterns are presented in this study including different shear reinforcement option, a prestressed and a post-tensioned option.

Fabrication: The circular concrete tower has a bi-linear tapered profile which makes every ring section in the tower unique in dimensions and different for its preceding and following ring sections. This complicates the fabrication procedure as the use of multiple forms or expensive dynamic forms becomes a necessity. However, the proposed system is composed of non-complicated sections that could be easily standardized; hollow hexagonal column section and flat panels with sloped edges. As mentioned earlier, the column's inside void was achieved using a PVC pipe, Styrofoam or collapsible forms. Styrofoam could be expensive and should be used if PVC pipes aren't available, on the other hand collapsible form could become a very attractive solution in case of wind farm construction with multiple towers. The sloped edges in the flat panels are easily achieved without any complicated equipment.

Transportation: Cost savings can be expected as flat panels can be easily stacked and piled on top of each other using shims, which reduce the number of trips required to transport the towers components to the construction site. The column segments can be

tailored to accommodate transportation limitations. No special care should be exerted during shipping and handling unlike ring section which require some finesse.

Erection: The construction procedures for the circular tower are challenging and time consuming. Extra care must be exerted when erecting this tower as every ring has its unique place that it fits and mixing and matching isn't an option. Moreover, the multiples post-tensioning operations required, during erection to maintain stability and after completion to resist the applied load, complicate the construction process even further. On the other hand, once the columns of the proposed system are placed, panels' installation is very quick and easy. Eliminating the need for post-tensioning by connecting the columns using splices will reduce the overall cost of the tower and will simplify the construction process by eliminating the post-tensioning steps.

6.4 Conclusions

The proposed concrete system did achieve a competitive and cost-effective solution, for wind turbine tower having a hub height of up to 320ft. Further studies may prove cost effectiveness for taller towers, which are likely to be proposed in future years. The proposed system was optimized to include the following features:

- An enhanced life cycle value with low initial cost.
- An optimized concrete design in terms of concrete dimensions, steel reinforcement, weight distribution and dynamic performance.
- A flexible design concept that can accommodate any logistical issues, desired dimensions or site specific conditions.

- Simple concrete fabrication procedures featuring non-complex precast sections for standardization purposes.
- A fast erection time and simple construction sequence
- A design where shipping and handling limitations were rendered unproblematic resulting in cost savings.
- Attractive aesthetics.

As a result, it can be shown that the proposed system has the potential to have low initial cost, little maintenance cost, fast un-complicated erection and excellent aesthetics in comparison with the dominantly used steel shaft system and the recently introduced precast concrete segmented system. In addition, the system is highly adjustable to accept different geometries. Above all, there is no need for expensive factory initial capital as most US plants have been making similar panels and can easily make a concentrically prestressed column.

BIBLIOGRAPHY

- ACI 215, “Considerations for Design of Concrete Structures Subject to Fatigue Loading”, American Concrete Institute, Farmington Hills, MI.
- ACI 307-98, “Design and Construction of Reinforced Concrete Chimneys”, American Concrete Institute, Farmington Hills, MI.
- ACI 318-08, “Building Code Requirements for Structural Concrete”, American Concrete Institute, Farmington Hills, MI.
- AISC 89, “Manual of Steel Construction”, Ninth edition, American Institute for Steel Construction, Chicago, IL 60611.
- American Wind Energy Association, 2011, “US Wind Industry First Quarter Market Report”, Washington, DC.
- ASCE 7-10, “Minimum Design Loads for Buildings and Other Structures”, American Society of Civil Engineers, Reston, VA.
- Burton, Tony, Sharpe, David, Jenkins, Nick, Bossanyi, Ervin, 2001, “Wind Energy Handbook”, John Wiley & sons, Ltd. New York, NY.
- CEB-FIP, 1993, “Model Code 1990 – Design Code”, Comité Euro-International du Béton and International Federation for Prestressing, Thomas Telford Services Ltd.

- DIN 1045-1, 2001, “Concrete, Reinforced and Prestressed Concrete Structures – Part 1: Design”, Deutsches Institut für Normung.
- Enercon GmbH, 2011, Tower Versions available at: www1.enercon.de
- Nawy, E., 2008, “Reinforced Concrete: A Fundamental Approach”, Prentice Hall, Upper Saddle River, NJ.
- GL, 2003, “Rules and Guidelines, IV–Industrial Services, Part 1–Wind Energy, Guidelines for the Certification of Wind Turbines”, Germanischer Lloyd Wind Energie GmbH, Hamburg, Germany.
- IEC 61400-1, 2005, “Wind Turbine Generator Systems–Part 1: Safety Requirements”, Third Edition, International Electrotechnical Commission, Geneva, Switzerland, Edition 3.
- IBC, “International Building Code”, International Code Council (ICC), Country Club Hills, Illinois.
- Jimeno, J., 2012, “Concrete Towers for Multi-Megawatt Turbines”, windsystemsmag.com, February, pp.40-45
- LaNier, M.W., 2005, “Evaluation of Design and Construction Approaches for Economical Hybrid Steel/Concrete Wind Turbine Towers”, Technical Report NREL/SR-500-36777, National Renewable Energy Laboratory, Golden, Colorado.
- Malcolm, D.J. & Hansen, A.C., 2006, “WindPACT Turbine Rotor Design Study” Technical Report, NREL/SR-500-32495, National Renewable Energy Laboratory, Golden, Colorado.

- Prowell, I., Elgamal, A., Romanowitz, H., Duggan, J.E., and Jonkman, J., 2010, "Earthquake Response Modeling for a Parked and Operating Megawatt-Scale Wind Turbine", NREL/TP-5000-48242, National Renewable Energy Laboratory, Golden, Colorado, USA..
- Prowell, I., 2011, "An Experimental and Numerical Study of Wind Turbine Seismic Behavior", Dissertation, presented to University of California, San Diego, CA, in partial fulfillment of the requirements for the degree of Doctor of Philosophy.
- Serna, J. & Jimeno, J., 2010, "Precast Concrete Wind Towers – The Rise to the Next Level in Hub Height and Support Capacity for Large Turbines". Modern Energy Review, Volume 2, Issue 2, pp. 54-59.
- Sri, S., 2011, "Wind Turbine Systems – Soils, Foundation and Tower", <http://home.eng.iastate.edu/~JDM/wind/REU_Course_-_Tower_and__Foundation_-_June_2011.pdf> (Apr. 16, 2012).
- The Concrete Center, 2007, "Concrete Towers for Onshore and Offshore Wind Farms". Technical Report, Camberley, Surrey.
- US department of energy, 2008, "20% Wind Energy by 2030 Increasing Wind Energy's Contribution to U.S. Electricity Supply", Report, DOE/GO-102008-2567, Oak Ridge, TN.
- Vries, E., 2009, "Concrete-Steel Hybrid Tower from ATS", Renewable Energy World, September – October 2009, pp. 109-111.
- World Wind Energy Association, 2011, "World Wind Energy Report 2010", 10th World Wind Energy Conference & Renewable Energy Exhibition, Cairo, Egypt.

APPENDIX A

A. WIND TURBINE SPECIFICATIONS AND LOADS

Table A-1: Wind turbine specifications.

Rotor Type	3-bladed, horizontal axis
Rotor Position	Upwind
Rotor Diameter	355.6 ft
Swept area	99,315 ft ²
Rotor speed	13.2 rpm
Power regulation	Pitch regulation with variable speed
Rotor tilt	6 degrees
Blade length	170.6 ft
Tip chord	3.3 ft
Root chord	13.8 ft
Aerodynamic profile	NACA 63.xxx, FFAxxx
Blade Tip Speed	168 mph
Generator Nominal power	3,600 kW
Working Frequency Range (1.15P to 2.85P)	0.253 Hz to 0.627 Hz
Head Weight (incl. nacelle, hub and blades)	694.26 kips (347.13 tons)

Coordinate system:

x: down-wind

y: across-wind

z: vertical.

Table A-2: Wind turbine loads.

Forces at hub height	EWM	EOG	Units
Extreme 3-second velocity gust at hub height)	115	78.3	mph
F_x	107.25	268.87	Kips
F_y	-148.5	-18.2	Kips
F_z	-694.26	-694.26	Kips
M_x	7843	3143.49	Kip-in
M_y	4950.5	-6601.2	Kip-in
M_z	1900.7	1177.88	Kip-in

Table A-3: Wind turbine fatigue loads.

Damage equivalent load for fatigue		
F_x	32.15	Kips
M_x	318.63	Kip-in
M_y	1600.51	Kip-in
M_z	1637.39	Kip-in

APPENDIX B

B. 240 FT PROPOSED CONCRETE SYSTEM DESIGN

Loading

Geometry and Dimensions

Tower Height:	$H_t := 240\text{ft}$
Segment Height:	$H_{\text{seg}} := 80\text{ft}$
Number of Segments:	$N_{\text{seg}} := 3$
1st Segment Base Dimensions: (Sec.2 - See Figure 1)	Center Lines: $B_{\text{seg.1.cl}} := 300.000\text{in} = 25\text{ ft}$
	$L_{\text{seg.1.cl}} := 259.808\text{in} = 21.651\text{ ft}$
	Concrete Edges: $B_{\text{seg.1.ce}} := 378.928\text{in} = 31.577\text{ ft}$
	$L_{\text{seg.1.ce}} := 328.162\text{in} = 27.347\text{ ft}$
	Center Lines: $B_{\text{seg.2.cl}} := 180.000\text{in} = 15\text{ ft}$
	$L_{\text{seg.2.cl}} := 155.885\text{in} = 12.99\text{ ft}$
2nd Segment Base Dimensions: (Sec.3 - See Figure 1)	Concrete Edges: $B_{\text{seg.2.ce}} := 258.928\text{in} = 21.577\text{ ft}$
	$L_{\text{seg.2.ce}} := 224.238\text{in} = 18.686\text{ ft}$
	Center Lines: $B_{\text{seg.3.cl}} := 120.000\text{in} = 10\text{ ft}$
	$L_{\text{seg.3.cl}} := 103.923\text{in} = 8.66\text{ ft}$
3rd Segment Dimensions: (Sec.4 - See Figure 1)	Concrete Edges: $B_{\text{seg.3.ce}} := 198.928\text{in} = 16.577\text{ ft}$
	$L_{\text{seg.3.ce}} := 172.277\text{in} = 14.356\text{ ft}$

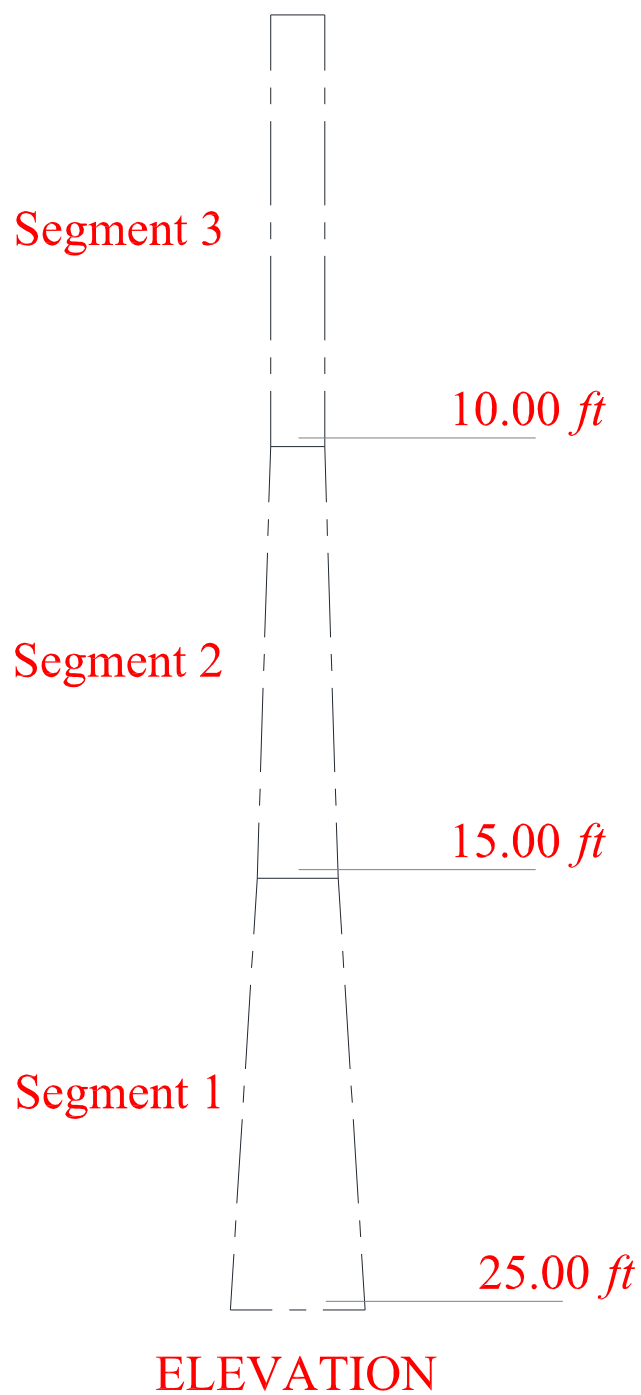


Figure B-1: Tower profile.

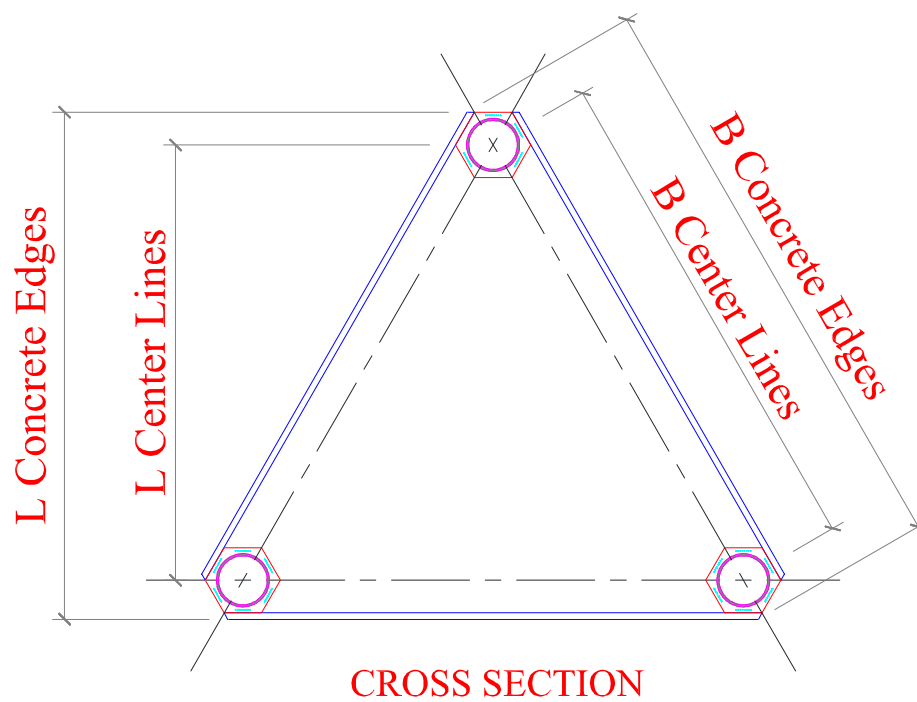


Figure B-2: Tower cross section.

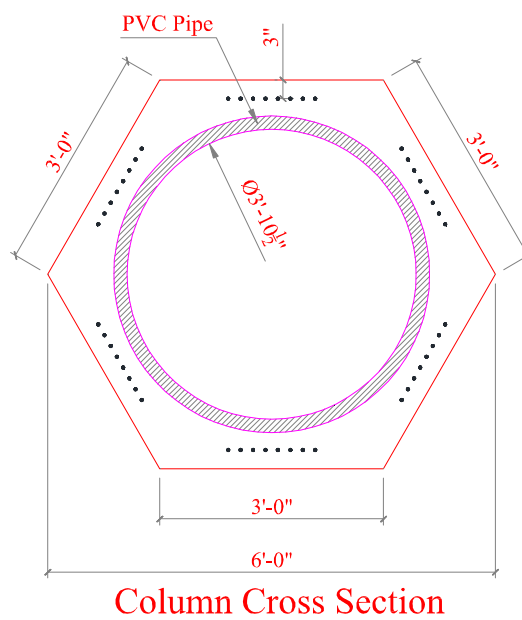


Figure B-3: Column cross section.

Concrete Properties

Concrete Compressive Strength:

$$f_c' := 8 \cdot \text{ksi}$$

Concrete Density:

$$\rho_c := 150 \text{pcf}$$

Concrete Elastic Modulus:
(AASHTO LRFD - Eq. 5.4.2.4-1)

$$E_c := 33000 \left(\frac{\rho_c}{1000 \text{pcf}} \right)^{1.5} \cdot \sqrt{\frac{f_c'}{\text{ksi}}} \text{ksi}$$

$$E_c = 5.422 \times 10^3 \cdot \text{ksi}$$

3.6 MW Wind Turbine

Turbine Head Weight:
(WindPACT Report, 2005)

$$W_{\text{turbine}} := 694.26 \cdot \text{kip}$$

Columns Properties

Columns Area:

$$A_{\text{col}} := 1811.8222 \text{in}^2$$

Number of Columns in Cross-Section:

$$N_{\text{col}} := 3$$

PVC Pipe Own Weight:

$$Ow_{\text{pvc}} := 231.22 \frac{\text{lbf}}{\text{ft}}$$

Column Own Weight:

$$Ow_{\text{col}} := Ow_{\text{pvc}} + A_{\text{col}} \cdot \rho_c$$

$$Ow_{\text{col}} = 2.119 \times 10^3 \cdot \frac{\text{lbf}}{\text{ft}}$$

Weight of One column:

$$Ow_{\text{col}} \cdot H_{\text{seg}} = 84.741 \cdot \text{tonf}$$

Total Weight of columns:

$$W_{\text{cols}} := Ow_{\text{col}} \cdot H_{\text{seg}} \cdot N_{\text{col}} \cdot N_{\text{seg}}$$

$$W_{\text{cols}} = 1.525 \times 10^3 \cdot \text{kip}$$

Panels Properties

Panel Thickness:

$$th_{\text{panel}} := 6 \text{in}$$

Number of Panels in Cross-Section

$$N_{\text{panel}} := 3$$

Panel Height:

$$h_{\text{panel}} := 10 \text{ft}$$

Total Number of Panels:

$$N_p := \frac{H_t}{h_{\text{panel}}} \cdot N_{\text{panel}} = 72$$

Panel Widths:

$$\text{Sec. 1: } w_{p,1} := 332.536 \text{in} = 27.711 \text{ft}$$

$$\text{Sec. 2: } w_{p,2} := 212.536 \text{in} = 17.711 \text{ft}$$

$$\text{Sec. 3: } w_{p,3} := 152.536 \text{in} = 12.711 \text{ft}$$

First Panel Weight (Heaviest):

$$w_{ave} := \left(\frac{332.536in + 317.54in}{2} \right)$$

$$Ow_{p1} := w_{ave} \cdot th_{panel} \cdot h_{panel} \cdot \rho_c$$

$$Ow_{p1} = 10.157 \cdot tonf$$

Last Panel Weight (Lightest):

$$Ow_{p2} := w_{p.3} \cdot th_{panel} \cdot h_{panel} \cdot \rho_c$$

$$Ow_{p2} = 4.767 \cdot tonf$$

Total Panel Volume:

$$Vol := \left[\left(\frac{w_{p.1} + w_{p.2}}{2} \right) + \left(\frac{w_{p.2} + w_{p.3}}{2} \right) + (w_{p.3}) \right] \cdot H_{seg} \cdot th_{panel} \cdot N_{panel}$$

Total Panel Weight:

$$W_{Panels} := Vol \cdot \rho_c$$

$$W_{Panels} = 911.412 \cdot kip$$

Tower Weights

Miscellaneous Additional Weights:

(Connections, bolts and steel plates)

$$W_{misc} := 250kip \quad (\text{Assumed})$$

Total Tower Weight:

$$W_{tot} := W_{turbine} + W_{cols} + W_{Panels} + W_{misc}$$

$$W_{tot} = 3.381 \times 10^3 \cdot kip$$

$$W_{tot} = 1.691 \times 10^3 \cdot tonf$$

Variations along the Height:

$$B(z) := \begin{cases} \left[\left(\frac{H_{\text{seg}} - z}{H_{\text{seg}}} \right) \cdot (B_{\text{seg}.1.\text{ce}} - B_{\text{seg}.2.\text{ce}}) + B_{\text{seg}.2.\text{ce}} \right] & \text{if } z \leq H_{\text{seg}} \\ \left[\left(\frac{H_{\text{seg}} - (z - H_{\text{seg}})}{H_{\text{seg}}} \right) \cdot (B_{\text{seg}.2.\text{ce}} - B_{\text{seg}.3.\text{ce}}) + B_{\text{seg}.3.\text{ce}} \right] & \text{if } H_{\text{seg}} < z \leq 2H_{\text{seg}} \\ B_{\text{seg}.3.\text{ce}} & \text{if } 2H_{\text{seg}} < z \leq 3H_{\text{seg}} \end{cases}$$

$$L(z) := \begin{cases} \left[\left(\frac{H_{\text{seg}} - z}{H_{\text{seg}}} \right) \cdot (L_{\text{seg}.1.\text{ce}} - L_{\text{seg}.2.\text{ce}}) + L_{\text{seg}.2.\text{ce}} \right] & \text{if } z \leq H_{\text{seg}} \\ \left[\left(\frac{H_{\text{seg}} - (z - H_{\text{seg}})}{H_{\text{seg}}} \right) \cdot (L_{\text{seg}.2.\text{ce}} - L_{\text{seg}.3.\text{ce}}) + L_{\text{seg}.3.\text{ce}} \right] & \text{if } H_{\text{seg}} < z \leq 2H_{\text{seg}} \\ L_{\text{seg}.3.\text{ce}} & \text{if } 2H_{\text{seg}} < z \leq 3H_{\text{seg}} \end{cases}$$

Wind Loading (Mid-West)

Direct Wind on the Tower:

Building Category: II
(ASCE 7-10 - Tbl. 1.5-1)

Wind Importance Factor: $I := 1.0$
(ASCE 7-10 - Tbl. 1.5-2)

Basic Wind Speed: $V_w := 115 \text{mph} = 51.41 \cdot \frac{\text{m}}{\text{s}}$
(ASCE 7-10 - Fig. 26.5-1A)

Design Wind Speeds:

Extreme 3-sec gust at reference height (33-ft from ground):

Non Operational Load Case (EWM): $V_1 := 115 \text{mph}$ Extreme wind speed model

Operational Load Case (EOG): $V_2 := 49.7 \text{mph}$ Extreme operational gust

At Hub Level:

Non Operational Load Case (EWM): $V_{1_EWM} := \left[V_1 \cdot \left(\frac{33 \text{ft}}{H_t} \right)^{-0.1} \right] = 140.239 \cdot \text{mph}$

Operational Load Case: $V_{2_EOG} := \left[V_2 \cdot \left(\frac{33 \text{ft}}{H_t} \right)^{-0.2} \right] = 73.909 \cdot \text{mph}$

Directional Factor: $K_d := 0.95$
(ASCE 7-10 - Tbl. 26.6-1)
(Triangular shape)

Terrain Exposure Constants: Exposure Category: " D "
(ASCE 7-10 - Art. 26.7.3)
(ASCE 7-10 - Tbl. 26.9-1)

$$\alpha_{\text{ex}} := 11.5$$

$$c_{\text{ex}} := 0.15$$

$$b_{\text{ex}} := 0.8$$

$$z_{\text{g.ex}} := 700 \text{ft}$$

$$z_{\text{min.ex}} := 7 \text{ft}$$

$$l_{\text{ex}} := 650 \text{ft}$$

$$\varepsilon_{\text{ex}} := \frac{1}{8.0}$$

$$\alpha'_{\text{ex}} := \frac{1}{9.0}$$

Topographic Factor:

(ASCE 7-10 - Art. 26.8)

(No hills)

$$K_{zt} := 1.0$$

Gust-Effects:

Flexible Structure:

(ASCE 7-10 - Art. 26.2)

$$n < 1.0\text{Hz}$$

Equivalent Height of Structure:

(ASCE 7-10 - Eq. 26.9-7)

$$z_{eq} := 0.6 \cdot H_t = 144 \text{ ft} \quad z > z_{\min.ex} \quad \text{ok}$$

Intensity of Turbulence:

(ASCE 7-10 - Eq. 26.9-7)

$$I_z(z) := c_{ex} \left(\frac{33\text{ft}}{z} \right)^{\frac{1}{6}}$$

Integral Length scale of turbulence:

(ASCE 7-10 - Eq. 26.9-9)

$$L_z(z) := l_{ex} \cdot \left(\frac{z}{33\text{ft}} \right)^{\epsilon_{ex}}$$

Background Response:

(ASCE 7-10 - Eq. 26.9-8)

$$Q(z) := \sqrt{\frac{1}{1 + 0.63 \cdot \left(\frac{B(z) + H_t}{L_z(z)} \right)^{0.63}}}$$

Peak Factor for Background Response:

(ASCE 7-10 - Eq. 26.9-10)

$$g_Q := 3.4$$

Peak Factor for Wind Response:

(ASCE 7-10 - Eq. 26.9-10)

$$g_v := 3.4$$

Natural Frequency of the Tower:

(ASCE 7-10 - Eq. 26.9-4)

$$n_a := \frac{75\text{ft}}{H_t} = 0.313 \quad \text{from SAP} \quad n_1 := 0.44\text{Hz}$$

Peak Factor for Resonant Response:

(ASCE 7-10 - Eq. 26.9-11)

$$g_R := \sqrt{2 \cdot \ln \left(3600 \cdot \frac{n_1}{\text{Hz}} \right)} + \frac{0.577}{\sqrt{2 \cdot \ln \left(3600 \cdot \frac{n_1}{\text{Hz}} \right)}}$$

$$g_R = 3.989$$

Mean Hourly Velocity:

(ASCE 7-10 - Eq. 26.9-16)

$$V_z(z, v) := b_{ex} \cdot \left(\frac{z}{33\text{ft}} \right)^{\alpha'_{ex}} \cdot \left(\frac{88}{60} \right) \cdot v$$

$$V_z(z_{eq}, V_1) = 158.933 \cdot \text{mph} \quad (\text{EWM})$$

$$V_z(z_{eq}, V_2) = 68.687 \cdot \text{mph} \quad (\text{EOG})$$

Reduced Frequency:

(ASCE 7-10 - Eq. 26.9-14)

$$N_1(z, v) := \frac{n_1 \cdot L_z(z)}{V_z(z, v)}$$

$$N_1(z_{eq}, V_1) = 1.475 \quad (\text{EWM})$$

$$N_1(z_{eq}, V_2) = 3.413 \quad (\text{EOG})$$

Damping Factor: $\beta := 2\%$ (ASCE-AWEA - Art. 5.4.4)

Resonant Response Factor: (ASCE 7-10 - Eq. 26.9-12)

$$\eta_{Rh}(z, v) := 4.6 \cdot n_1 \cdot \frac{H_t}{V_z(z, v)} \quad (\text{ASCE 7-10 - Eq. 26.9-15a})$$

$$\eta_{RB}(z, v) := 4.6 \cdot n_1 \cdot \frac{B(z)}{V_z(z, v)} \quad (\text{ASCE 7-10 - Eq. 26.9-15a})$$

$$\eta_{RL}(z, v) := 4.6 \cdot n_1 \cdot \frac{L(z)}{V_z(z, v)} \quad (\text{ASCE 7-10 - Eq. 26.9-15a})$$

$$R_h(z, v) := \frac{1}{\eta_{Rh}(z, v)} - \frac{\left[1 - e^{(-2 \cdot \eta_{Rh}(z, v))}\right]}{2(\eta_{Rh}(z, v))^2} \quad R_h(z_{eq}, V_1) = 0.367$$

$$R_h(z_{eq}, V_2) = 0.186$$

$$R_B(z, v) := \frac{1}{\eta_{RB}(z, v)} - \frac{\left[1 - e^{(-2 \cdot \eta_{RB}(z, v))}\right]}{2(\eta_{RB}(z, v))^2} \quad R_B(z_{eq}, V_1) = 0.906$$

$$R_B(z_{eq}, V_2) = 0.801$$

$$R_L(z, v) := \frac{1}{\eta_{RL}(z, v)} - \frac{\left[1 - e^{(-2 \cdot \eta_{RL}(z, v))}\right]}{2(\eta_{RL}(z, v))^2} \quad R_L(z_{eq}, V_1) = 0.917$$

$$R_L(z_{eq}, V_2) = 0.824$$

$$R_n(z, v) := \frac{7.47 \cdot N_1(z, v)}{(1 + 10.3 \cdot N_1(z, v))^{\frac{5}{3}}} \quad (\text{ASCE 7-10 - Eq. 26.9-13})$$

$$R_n(z_{eq}, V_1) = 0.106$$

$$R_n(z_{eq}, V_2) = 0.064$$

$$R(z, v) := \sqrt{\frac{1}{\beta} \cdot R_n(z, v) \cdot R_h(z, v) \cdot R_B(z, v) \cdot (0.53 + 0.47 \cdot R_L(z, v))} \quad (\text{ASCE 7-10 - Eq. 26.9-12})$$

$$R(z_{eq}, V_1) = 1.302$$

$$R(z_{eq}, V_2) = 0.664$$

Gust - Effect Factor:

(ASCE 7-10 - Eq. 26.9-10)

$$G_F(z, v) := 0.925 \cdot \left(\frac{1 + 1.7 \cdot I_z(z) \cdot \sqrt{g_Q^2 \cdot Q(z)^2 + g_R^2 \cdot R(z, v)^2}}{1 + 1.7 \cdot g_V \cdot I_z(z)} \right)$$

Enclosure Classification:

(ASCE 7-10 - Art. 26.10)

Enclosed Building (Openings less than 10 %)

Velocity Pressure Coefficient:

(ASCE 7-10 - Tbl. 29.3-1)

$$K_Z(z) := \begin{cases} 2.01 \cdot \left(\frac{15\text{ft}}{z_{g,ex}} \right)^{\alpha_{ex}} & \text{if } z < 15\text{ft} \\ 2.01 \cdot \left(\frac{z}{z_{g,ex}} \right)^{\alpha_{ex}} & \text{if } 15\text{ft} \leq z \leq z_{g,ex} \end{cases}$$

(ASCE 7-10 - Eq. 29.3-1)

$$q_z(z, v) := K_Z(z) \cdot K_{zt} \cdot K_d \cdot \left(\frac{v}{\text{mph}} \right)^2 \cdot 0.00256 \cdot (\text{psf})$$

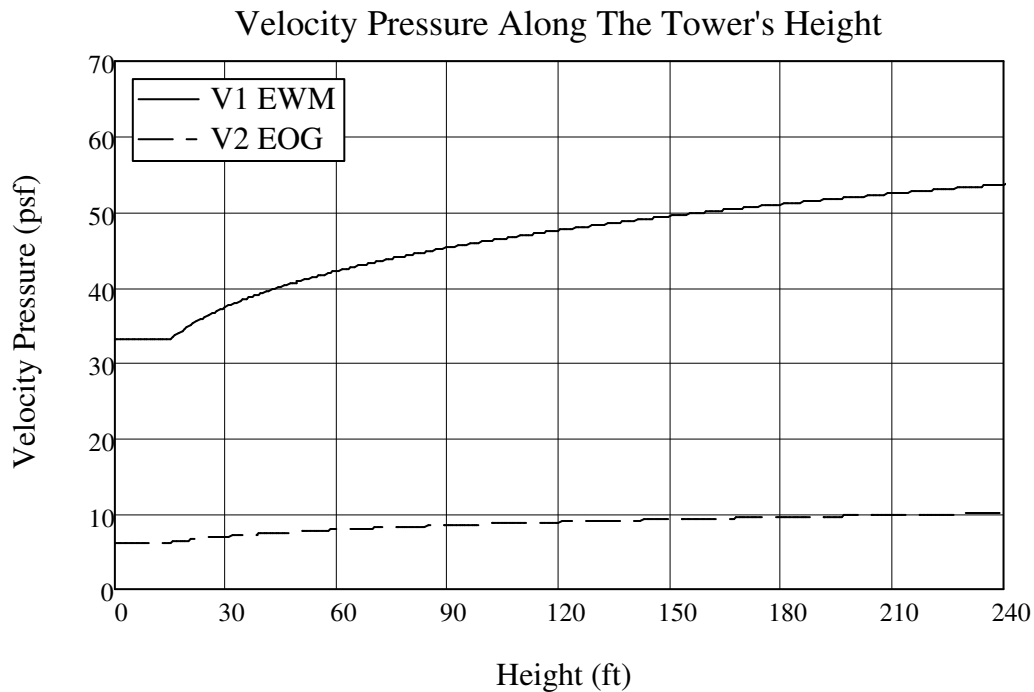


Figure B-4: Velocity pressure along the tower height.

Force Coefficient:
(ASCE 7-10 - Tbl. 29.5-1)

$$\frac{H_t}{\min(B(0), L(0))} = 8.776$$

Table B-1: Force coefficient for towers*

Cross Section		h/D**			h/D=8.776
		1	7	25	
Square	wind normal to face	1.3	1.4	2	1.46
	wind along diagonal	1	1.1	1.5	1.14
Hexagonal or Octagonal		1	1.2	1.4	1.22
Round		0.5-0.8	0.6-1.0	0.7-1.2	0.81

* Based on ASCE-07 Table 29.5-1

** h : Tower Height

** D : Least Structure Dimension

Table B-2: Force coefficient for proposed cross section (h/D=8.776)

Wind Direction	Cross Section			Proposed
	Square	Hexagonal	Round	
Normal to Face	1.46	1.22	0.81	1.46
Along Diagonal	1.14	1.22	0.81	1.14

Force along the Tower:
(ASCE 7-10 - Eq. 29.5-1)

$$C_{f1} := 1.46 \quad C_{f2} := 1.14$$

$$F := q_z \cdot G_f \cdot C_f \cdot A_f$$

$$F_{w1}(z, v) := q_z(z, v) \cdot G_f(z, v) \cdot C_{f1} \cdot B(z) \, dz$$

$$F_{w2}(z, v) := q_z(z, v) \cdot G_f(z, v) \cdot C_{f2} \cdot B(z) \, dz$$

Shearing Force along the Tower:

$$S_{w1}(z, v) := \int_z^{H_t} F_{w1}(x, v) \, dx$$

$$S_{w2}(z, v) := \int_z^{H_t} F_{w2}(x, v) \, dx$$

Base Shear (EWM):

$$S_{w1}(0, V_1) = 389.946 \cdot \text{kip}$$

$$S_{w2}(0, V_1) = 304.478 \cdot \text{kip}$$

Base Shear (EOG):

$$S_{w1}(0, V_2) = 59.243 \cdot \text{kip}$$

$$S_{w2}(0, V_2) = 46.258 \cdot \text{kip}$$

Bending Moment Along the Tower:

$$M_{w1}(z, v) := \int_z^{H_t} F_{w1}(x, v) \cdot (x - z) \, dx$$

$$M_{w2}(z, v) := \int_z^{H_t} F_{w2}(x, v) \cdot (x - z) \, dx$$

Base Moment (EWM):

$$M_{w1}(0, V_1) = 4.517 \times 10^4 \cdot \text{kip} \cdot \text{ft}$$

$$M_{w2}(0, V_1) = 3.527 \times 10^4 \cdot \text{kip} \cdot \text{ft}$$

Base Moment (EOG):

$$M_{w1}(0, V_2) = 6.898 \times 10^3 \cdot \text{kip} \cdot \text{ft}$$

$$M_{w2}(0, V_2) = 5.386 \times 10^3 \cdot \text{kip} \cdot \text{ft}$$

Wind Turbine Load: (WindPact Report)

Coordinate System: x: Downwind, y : Lateral, and z : Gravity.

Turbine Offset: offset := 0ft

Straining Actions on Top of the Tower:

$$F_{x.T.V1} := 143\text{kip}$$

$$F_{x.T.V2} := 269\text{kip}$$

$$F_{y.T.V1} := 198\text{kip}$$

$$F_{y.T.V2} := 18\text{kip}$$

$$F_{z.T.V1} := 709\text{kip}$$

$$F_{z.T.V2} := 703\text{kip}$$

$$M_{x.T.V1} := 10458\text{kip}\cdot\text{ft}$$

$$M_{x.T.V2} := 3143\text{kip}\cdot\text{ft}$$

$$M_{y.T.V1} := 6601\text{kip}\cdot\text{ft}$$

$$M_{y.T.V2} := 6601\text{kip}\cdot\text{ft}$$

$$M_{z.T.V1} := 2534\text{kip}\cdot\text{ft}$$

$$M_{z.T.V2} := 1178\text{kip}\cdot\text{ft}$$

Fatigue Range:

$$\Delta F_{x.T} := 32\text{kip}$$

$$\Delta M_{z.T} := 1637\text{kip}\cdot\text{ft}$$

$$\Delta M_{x.T} := 319\text{kip}\cdot\text{ft}$$

$$\Delta M_{y.T} := 1600\text{kip}\cdot\text{ft}$$

Extreme 3-sec gust at reference height (33-ft from ground):

(ASCE 7-05 - Fig. 6-1)

$$V_{mw} := 40 \frac{\text{m}}{\text{s}}$$

Reference wind speed over 10 min at hub height:

(ASCE/AWEA-RP 2011 - Eq. C5-6)

$$V_{\text{ref}} := V_{mw} \cdot \left(\frac{H_t}{z_{g,\text{ex}}} \right)^{\alpha_{\text{ex}}} = 36.445 \cdot \frac{\text{m}}{\text{s}}$$

Extreme 3-sec gust at hub height:

(ASCE/AWEA-RP 2011 - Eq. C5-4)

$$V_{e50}(z) := 1.4 \cdot V_{\text{ref}} \cdot \left(\frac{z}{H_t} \right)^{0.11}$$

$$V_{e50}(240\text{ft}) = 51.023 \cdot \frac{\text{m}}{\text{s}}$$

Class II wind Turbine:

(ASCE/AWEA-RP 2011 - Eq. C5-4)

$$V_t := 59.5 \frac{\text{m}}{\text{s}}$$

Speed Modification Factor:

$$c_{\text{sc}} := \left(\frac{V_{e50}(240\text{ft})}{V_t} \right)^2 = 0.735$$

$$\text{Take } c_{\text{sc}} := 0.75$$

Wind Turbine Load Distribution along the Tower:

$$F_{x.V1} := F_{x.T.V1} \cdot c \qquad F_{x.V2} := F_{x.T.V2}$$

$$F_{y.V1} := F_{y.T.V1} \cdot c \qquad F_{y.V2} := F_{y.T.V2}$$

$$F_{z.V1} := F_{z.T.V1} \cdot c \qquad F_{z.V2} := F_{z.T.V2}$$

$$M_{x.V1}(z) := M_{x.T.V1} \cdot c + F_{y.V1} \cdot (H_t - z)$$

$$M_{x.V2}(z) := M_{x.T.V2} + F_{y.V2} \cdot (H_t - z)$$

$$M_{y.V1}(z) := M_{y.T.V1} \cdot c + F_{x.V1} \cdot (H_t - z)$$

$$M_{y.V2}(z) := M_{y.T.V2} + F_{x.V2} \cdot (H_t - z)$$

$$M_{z.V1}(z) := M_{z.T.V1} \cdot c$$

$$M_{z.V2}(z) := M_{z.T.V2}$$

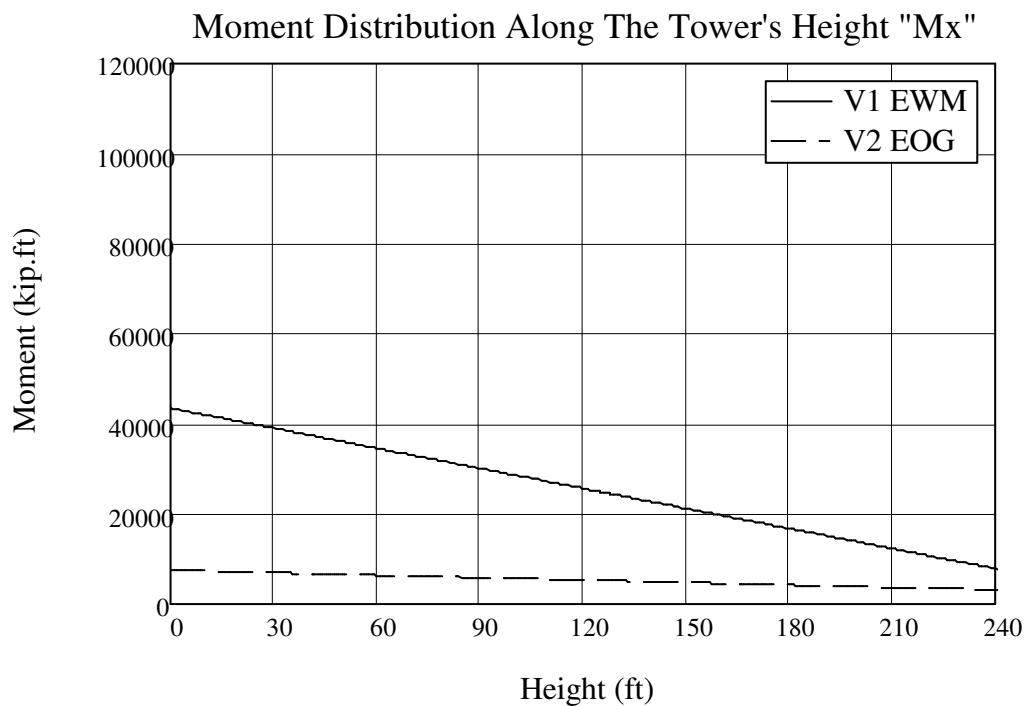


Figure B-5: Moment distribution in the X-direction.

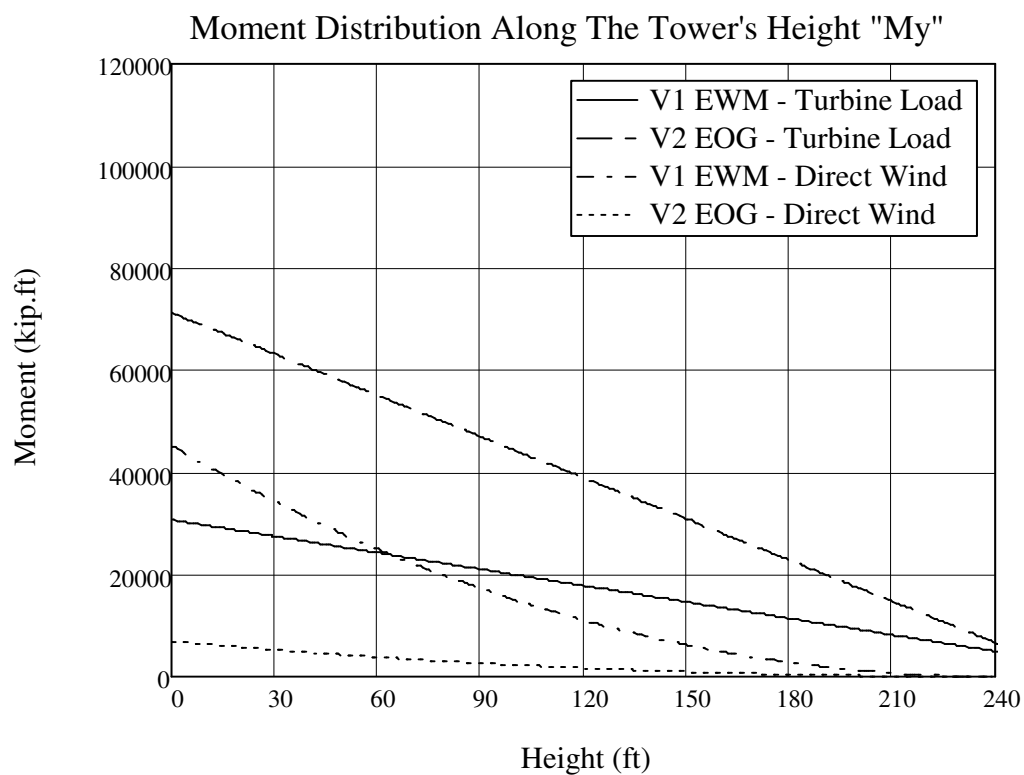


Figure B-6: Moment distribution in the Y-direction.

Seismic Loading (Mid-West)

Seismic Importance Factor:
(ASCE 7-10 - Tbl. 1.5-2)

$$I = 1$$

Site Class:
(ASCE 7-10 - Art. 11.4.2)

Soil Class "D"

Damping Adjustment Factor:
(ASCE-AWEA - Tbl. 5-6)

$$\underline{B}_v := 1.23$$

Mapped Acceleration Parameters:
(ASCE 7-10 - Fig. 22-1 and 22-2)

$$S_s := 0.12 \cdot B \quad S_1 := 0.05 \cdot B$$

Site Coefficient:
(ASCE 7-10 - Tbl. 11.4-1 and 11.4-2)

$$F_a := 1.6 \quad F_v := 2.4$$

Spectral response acceleration for short period:
(ASCE 7-10 - Eq. 11.4-1)

$$S_{MS} := F_a \cdot S_s = 0.236$$

Spectral response acceleration for 1 second:
(ASCE 7-10 - Eq. 11.4-2)

$$S_{M1} := F_v \cdot S_1 = 0.148$$

Design Spectral Acceleration Parameters:
(ASCE 7-10 - Eq. 11.4-3 and 11.4-4)

$$S_{DS} := \frac{2}{3} \cdot S_{MS} = 0.157$$

$$S_{D1} := \frac{2}{3} \cdot S_{M1} = 0.098$$

Design Response Spectrum:
(ASCE 7-10 - Eq. 11.4-5 to 11.4-7)

$$T_S := \frac{S_{D1}}{S_{DS}} = 0.625$$

$$T_0 := 0.2 \frac{S_{D1}}{S_{DS}} = 0.125$$

$$T_L := 12$$

$$S_a(T) := \begin{cases} S_{DS} \cdot \left(0.4 + 0.6 \cdot \frac{T}{T_0} \right) & \text{if } T < T_0 \\ S_{DS} & \text{if } T_0 \leq T \leq T_S \\ \frac{S_{D1}}{T} & \text{if } T_S < T \leq T_L \\ \frac{S_{D1} \cdot T_L}{T^2} & \text{if } T_L < T \end{cases}$$

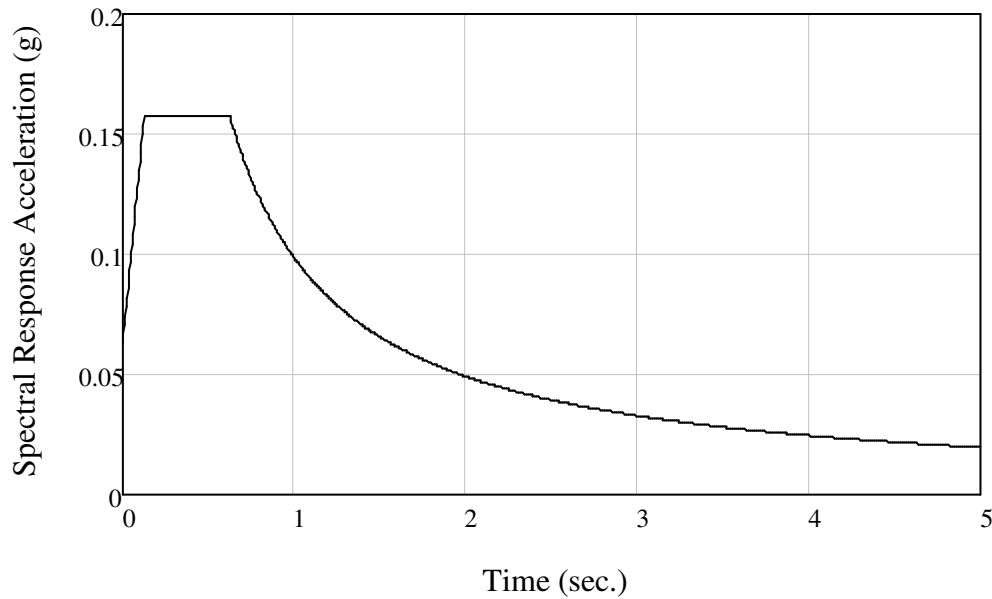


Figure B-7: Design response spectrum.

Response Modification Coefficient:
(ASCE 7-10 - Tbl. 12.2-1)

$$R_s := 1.5$$

Seismic Response Coefficient:
(ASCE 7-10 - Eq. 12.8-2 to 12.8-5)

$$C_{s,\text{lim}}(T) := \begin{cases} \frac{S_{D1}}{T \cdot \left(\frac{R}{I}\right)} & \text{if } T \leq T_L \\ \frac{S_{D1} \cdot T_L}{T^2 \cdot \left(\frac{R}{I}\right)} & \text{if } T > T_L \end{cases}$$

$$C_{sn} := \frac{S_{DS}}{\left(\frac{R}{I}\right)} = 0.105$$

$$C_s(T) := \begin{cases} 0.051 & \text{if } 0.051 < C_{s,\text{lim}}(T) \\ 0.01 & \text{if } C_{s,\text{lim}}(T) < 0.01 \\ C_{s,\text{lim}}(T) & \text{otherwise} \end{cases}$$

Seismic Base Shear:
(ASCE 7-10 - Eq. 12.8-1)

$$V := C_{sn} \cdot W_{\text{tot}} = 354.872 \cdot \text{kip}$$

Percentage of Wind to Seismic Force:

$$\frac{S_{w1}(0, V_1) + F_x \cdot V_1}{V} = 1.401$$

P-M Effect:

Tower Deflection:
(From SAP model)

$$\Delta_x := 0.68\text{ft} \quad \Delta_y := 0.64\text{ft}$$

Additional Moment from deflection:

$$M_{x\text{add}} := W_{\text{turbine}} \cdot \Delta_x = 472.097 \cdot \text{kip} \cdot \text{ft}$$

$$M_{y\text{add}} := W_{\text{turbine}} \cdot \Delta_y = 444.326 \cdot \text{kip} \cdot \text{ft}$$

Percentage of added moment:

$$\delta_{x\text{add}} := \frac{M_{x\text{add}}}{M_{x.V1(0)}} = 0.011$$

$$\delta_{y\text{add}} := \frac{M_{y\text{add}}}{M_{y.V1(0)}} = 0.014$$

Negligible effect

Load Combinations:

(ASCE 7-10 - Art. 2.3.2 and 2.4.1)
(ASCE/AWEA-RP 2011 - Tbl. 5-4)

D: Dead Load

T: Turbine Load

W: Wind Load

E: Seismic Load

Ultimate Loads:

ULT 4: $1.2D + 1.0W + 1.35T$

ULT 5: $1.2D + 1.0E$

ULT 6: $0.9D + 1.0W + 1.35T$

ULT 7: $0.9D + 1.0E$

Service Loads:

SER 5-1: $D + 0.6W + 1.0T$

SER 5-2: $D + 0.7E$

SER 7: $0.6D + 0.6W + 1.0T$

SER 8: $0.6D + 0.7E$

Design

Table B-3: Ultimate loads acting on segment 1 columns.

Segment 1 Columns				
Ultimate Load Combination	Max/Min	Axial	Shear	Moment
		Kip	Kip	Kip-ft
ULT4-C1	Axial	-4412.15	34.29	896.54
		2603.62	11.30	1105.12
	Shear	-3659.80	4.10	1403.51
		-1362.45	55.44	1330.82
	Moment	-4331.37	43.82	654.47
		-3657.23	5.84	1406.12
ULT4-C2	Axial	-4518.25	32.64	815.63
		1906.30	32.02	667.43
	Shear	-4210.69	10.31	965.60
		-4115.31	44.98	1252.82
	Moment	1900.54	30.94	656.03
		-4103.80	44.46	1419.24
ULT5-C1	Axial	-2956.44	11.34	388.97
		7.32	18.55	538.14
	Shear	-0.05	6.03	476.35
		-2847.74	23.10	495.16
	Moment	-2824.81	22.47	266.87
		-2430.45	12.17	694.38
ULT5-C2	Axial	-2712.21	13.59	421.00
		608.91	10.06	445.74
	Shear	-831.90	2.37	490.69
		445.38	22.38	525.56
	Moment	-2584.89	20.38	281.96
		-2212.72	13.98	666.05
ULT6-C1	Axial	-4128.79	35.65	910.76
		2811.59	11.28	1104.95
	Shear	-3464.67	3.11	1404.09
		-1096.40	54.24	1086.77
	Moment	-4061.96	43.31	656.34
		-3464.67	3.11	1404.09

ULT6-C2	Axial	-4234.90	32.37	827.07
		2169.96	31.45	654.17
	Shear	-3993.15	10.44	966.59
		-3911.13	41.62	1256.91
	Moment	2169.96	31.45	654.17
		-3902.48	41.23	1405.97
ULT7-C1	Axial	-2673.09	12.71	404.80
		208.63	15.88	545.04
	Shear	207.92	6.08	476.27
		-2583.54	22.65	491.31
	Moment	-2566.31	21.61	269.60
		-2229.13	8.67	680.62
ULT7-C2	Axial	-2428.86	14.53	433.44
		816.88	10.11	445.58
	Shear	-623.92	2.37	490.69
		728.73	21.17	511.95
	Moment	-2326.39	19.54	284.18
		-2011.41	10.98	653.50

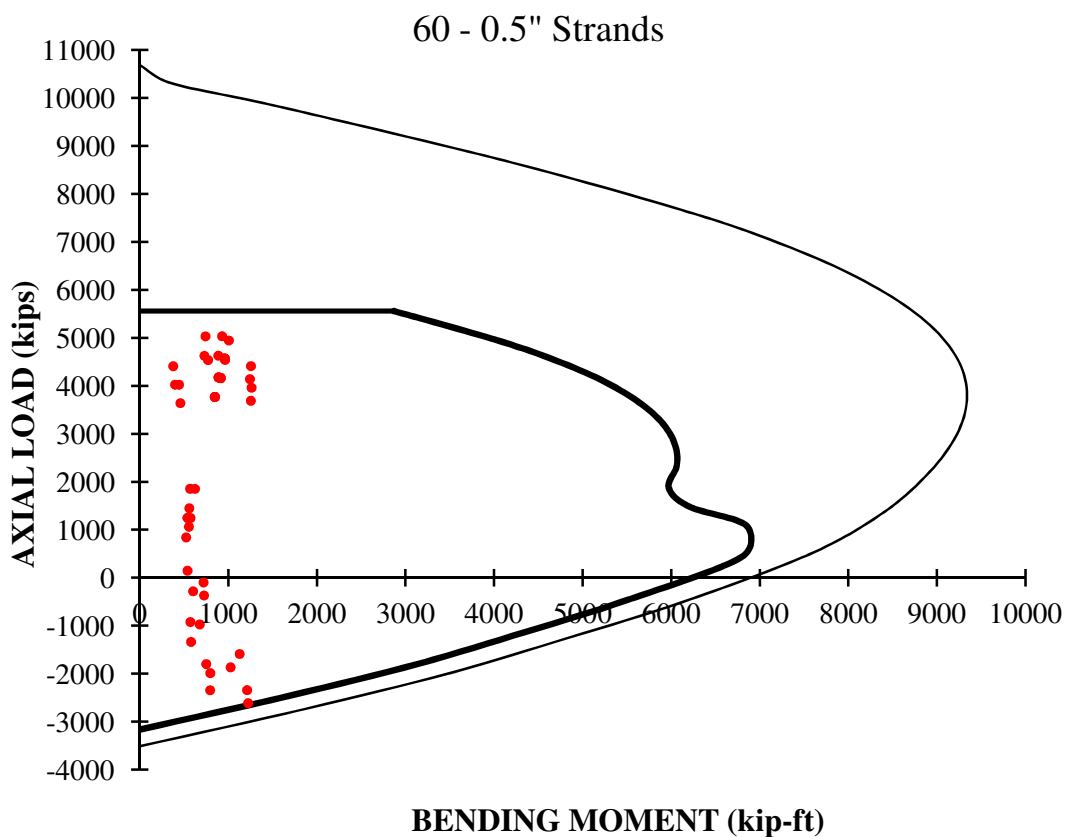


Figure B-8: Segments 1 columns interaction diagram.

Table B-4: Segments 1 column properties.

Service Check						
Prestress	Area	Inertia	y	f_c	Stress Limits	
Kip	in ²	in ⁴	in	ksi	ksi	
-2109.24	1811.80	2.8E+10	31.18	8.00	-4.80	0.67
Shear Check						
b_w	d_p	ϕ	V_c limits		Shear Rft (in ²)	
in	in		Kip		C-Shape	Spiral
28.43	58.35	0.75	296.70	741.75	0.76	0.31
					#6 - 24"	W16 - 12"

Table B-5: Service and operational loads check for segment 1 columns.

Segment 1 Columns							
Load Combination		Axial	Moment	Stress Range		Comp. stress	Tens. stress
		Kip	Kip-ft	ksi			
SER5-1-C1	Axial	-3133.08	579.19	-2.89	-2.89	Safe	No tension
		1761.15	798.10	-0.19	-0.19	Safe	No tension
	Shear	1753.52	783.44	-0.20	-0.20	Safe	No tension
		-1169.83	927.14	-1.81	-1.81	Safe	No tension
	Moment	-3072.30	472.80	-2.86	-2.86	Safe	No tension
-2613.67		993.31	-2.61	-2.61	Safe	No tension	
SER5-1-C2	Axial	-3351.47	522.61	-3.01	-3.01	Safe	No tension
		1168.66	755.33	-0.52	-0.52	Safe	No tension
	Shear	-3119.96	701.49	-2.89	-2.89	Safe	No tension
		-3052.98	873.85	-2.85	-2.85	Safe	No tension
	Moment	1110.91	477.13	-0.55	-0.55	Safe	No tension
-3043.40		1020.87	-2.84	-2.84	Safe	No tension	
SER5-2-C1	Axial	-2220.63	263.84	-2.39	-2.39	Safe	No tension
		-102.25	373.14	-1.22	-1.22	Safe	No tension
	Shear	-133.14	297.82	-1.24	-1.24	Safe	No tension
		-2134.32	348.66	-2.34	-2.34	Safe	No tension
	Moment	-2115.24	185.36	-2.33	-2.33	Safe	No tension
-1808.69		493.40	-2.16	-2.16	Safe	No tension	
SER5-2-C2	Axial	-2049.67	288.18	-2.30	-2.30	Safe	No tension
		315.32	312.10	-0.99	-0.99	Safe	No tension
	Shear	-693.25	343.48	-1.55	-1.55	Safe	No tension
		160.64	375.20	-1.08	-1.08	Safe	No tension
	Moment	-1947.29	196.20	-2.24	-2.24	Safe	No tension
-1656.28		472.95	-2.08	-2.08	Safe	No tension	
SER7-C1	Axial	-2755.27	597.48	-2.68	-2.68	Safe	No tension
		2038.45	797.87	-0.04	-0.04	Safe	No tension
	Shear	-2346.55	975.62	-2.46	-2.46	Safe	No tension
		-897.60	927.65	-1.66	-1.66	Safe	No tension
	Moment	-2713.09	475.23	-2.66	-2.66	Safe	No tension
2029.26		979.71	-0.04	-0.04	Safe	No tension	

SER7-C2	Axial	-2973.67	538.56	-2.81	-2.81	Safe	No tension
		1470.47	488.90	-0.35	-0.35	Safe	No tension
	Shear	1420.87	899.90	-0.38	-0.38	Safe	No tension
		-2780.74	879.39	-2.70	-2.70	Safe	No tension
	Moment	1470.12	474.69	-0.35	-0.35	Safe	No tension
-2774.98		1003.04	-2.70	-2.70	Safe	No tension	
SER8-C1	Axial	-1842.83	284.95	-2.18	-2.18	Safe	No tension
		166.34	333.38	-1.07	-1.07	Safe	No tension
	Shear	166.34	333.38	-1.07	-1.07	Safe	No tension
		-1782.06	343.53	-2.15	-2.15	Safe	No tension
	Moment	-1770.57	188.99	-2.14	-2.14	Safe	No tension
-1540.26		475.06	-2.01	-2.01	Safe	No tension	
SER8-C2	Axial	-1671.87	304.66	-2.09	-2.09	Safe	No tension
		592.62	311.89	-0.84	-0.84	Safe	No tension
	Shear	-415.95	343.48	-1.39	-1.39	Safe	No tension
		538.45	357.01	-0.87	-0.87	Safe	No tension
	Moment	-1602.62	199.15	-2.05	-2.05	Safe	No tension
576.91		456.32	-0.85	-0.85	Safe	No tension	
OPR5-1-C1	Axial	-3076.01	383.70	-2.86	-2.86	Safe	No tension
		637.14	720.99	-0.81	-0.81	Safe	No tension
	Shear	-2802.27	646.49	-2.71	-2.71	Safe	No tension
		635.15	739.32	-0.81	-0.81	Safe	No tension
	Moment	-76.52	345.07	-1.21	-1.21	Safe	No tension
-2733.22		875.65	-2.67	-2.67	Safe	No tension	
OPR5-1-C2	Axial	-2075.67	453.70	-2.31	-2.31	Safe	No tension
		1169.19	702.01	-0.52	-0.52	Safe	No tension
	Shear	1141.57	553.14	-0.53	-0.53	Safe	No tension
		-1877.83	700.43	-2.20	-2.20	Safe	No tension
	Moment	-1631.66	178.95	-2.06	-2.06	Safe	No tension
-1868.30		713.40	-2.20	-2.20	Safe	No tension	
OPR7-C1	Axial	-2698.21	402.67	-2.65	-2.65	Safe	No tension
		905.57	733.31	-0.66	-0.66	Safe	No tension
	Shear	-2517.37	648.74	-2.55	-2.55	Safe	No tension
		904.38	748.00	-0.67	-0.66	Safe	No tension
	Moment	290.28	345.45	-1.00	-1.00	Safe	No tension
-2464.79		857.42	-2.52	-2.52	Safe	No tension	
OPR7-C2	Axial	-1697.86	458.69	-2.10	-2.10	Safe	No tension
		1437.92	600.18	-0.37	-0.37	Safe	No tension

Shear	-1045.63	679.39	-1.74	-1.74	Safe	No tension
	-1605.59	703.59	-2.05	-2.05	Safe	No tension
Moment	-1253.86	188.88	-1.86	-1.86	Safe	No tension
	1437.61	720.19	-0.37	-0.37	Safe	No tension

Table B-6: Shear check for segment 1 columns.

Segment 1 Columns							
Ultimate Load Combination	Max/Min	Axial	Shear	Moment	V _c	V _s	Shear
		Kip	Kip	Kip-ft	Kip	Kip	
ULT4-C1	Axial	-4412.1	34.3	896.5	304.94	111.26	Safe
		2603.6	11.3	1105.1	0.00	111.26	Safe
	Shear	-3659.8	4.1	1403.5	296.70	111.26	Safe
		-1362.4	55.4	1330.8	324.20	111.26	Safe
	Moment	-4331.4	43.8	654.5	466.97	111.26	Safe
-3657.2		5.8	1406.1	296.70	111.26	Safe	
ULT4-C2	Axial	-4518.3	32.6	815.6	314.96	111.26	Safe
		1906.3	32.0	667.4	0.00	111.26	Safe
	Shear	-4210.7	10.3	965.6	296.70	111.26	Safe
		-4115.3	45.0	1252.8	296.70	111.26	Safe
	Moment	1900.5	30.9	656.0	0.00	111.26	Safe
-4103.8		44.5	1419.2	296.70	111.26	Safe	
ULT5-C1	Axial	-2956.4	11.3	389.0	296.70	111.26	Safe
		7.3	18.6	538.1	0.00	111.26	Safe
	Shear	-0.1	6.0	476.4	296.70	111.26	Safe
		-2847.7	23.1	495.2	352.39	111.26	Safe
	Moment	-2824.8	22.5	266.9	564.28	111.26	Safe
-2430.5		12.2	694.4	296.70	111.26	Safe	
ULT5-C2	Axial	-2712.2	13.6	421.0	296.70	111.26	Safe
		608.9	10.1	445.7	0.00	111.26	Safe
	Shear	-831.9	2.4	490.7	296.70	111.26	Safe
		445.4	22.4	525.6	0.00	111.26	Safe
	Moment	-2584.9	20.4	282.0	497.06	111.26	Safe
-2212.7		14.0	666.0	296.70	111.26	Safe	

ULT6-C1	Axial	-4128.8	35.7	910.8	310.02	111.26	Safe
		2811.6	11.3	1104.9	0.00	111.26	Safe
	Shear	-3464.7	3.1	1404.1	296.70	111.26	Safe
		-1096.4	54.2	1086.8	370.75	111.26	Safe
	Moment	-4062.0	43.3	656.3	461.52	111.26	Safe
-3464.7		3.1	1404.1	296.70	111.26	Safe	
ULT6-C2	Axial	-4234.9	32.4	827.1	309.93	111.26	Safe
		2170.0	31.4	654.2	0.00	111.26	Safe
	Shear	-3993.2	10.4	966.6	296.70	111.26	Safe
		-3911.1	41.6	1256.9	296.70	111.26	Safe
	Moment	2170.0	31.4	654.2	0.00	111.26	Safe
-3902.5		41.2	1406.0	296.70	111.26	Safe	
ULT7-C1	Axial	-2673.1	12.7	404.8	296.70	111.26	Safe
		208.6	15.9	545.0	0.00	111.26	Safe
	Shear	207.9	6.1	476.3	0.00	111.26	Safe
		-2583.5	22.7	491.3	349.27	111.26	Safe
	Moment	-2566.3	21.6	269.6	541.45	111.26	Safe
-2229.1		8.7	680.6	296.70	111.26	Safe	
ULT7-C2	Axial	-2428.9	14.5	433.4	296.70	111.26	Safe
		816.9	10.1	445.6	0.00	111.26	Safe
	Shear	-623.9	2.4	490.7	296.70	111.26	Safe
		728.7	21.2	511.9	0.00	111.26	Safe
	Moment	-2326.4	19.5	284.2	477.23	111.26	Safe
		-2011.4	11.0	653.5	296.70	111.26	Safe

Table B-7: Ultimate loads acting on segment 2 columns.

Segment 2 Columns				
Ultimate Load Combination	Max/Min	Axial	Shear	Moment
		Kip	Kip	Kip-ft
ULT4-C1	Axial	-3655.05	126.62	1406.30
		2602.55	83.11	949.71
	Shear	-1349.70	21.05	1219.04
		-3652.77	126.70	1300.93
	Moment	1800.80	81.98	681.52
		-3499.24	94.61	1612.21
ULT4-C2	Axial	-4102.62	107.72	1419.39
		1857.67	81.72	956.09
	Shear	-157.18	28.06	1158.47
		-4100.35	107.80	1312.28
	Moment	-2864.41	78.38	675.21
		1757.08	82.80	1519.09
ULT5-C1	Axial	-2429.32	75.25	694.38
		19.81	28.94	394.27
	Shear	18.14	17.38	458.01
		-2429.32	75.25	694.38
	Moment	-1569.19	42.15	234.76
		-2334.49	50.26	762.06
ULT5-C2	Axial	-2211.74	67.46	666.15
		612.58	36.31	396.83
	Shear	-552.94	18.66	358.48
		-2211.74	67.46	666.15
	Moment	-1433.05	37.64	271.12
		-2126.25	45.12	734.70
ULT6-C1	Axial	-3453.73	122.88	1394.87
		2801.02	86.87	944.84
	Shear	-1142.12	20.92	1136.61
		-3452.03	122.94	1292.91
	Moment	1939.04	81.98	681.44
		-3304.21	94.48	1612.16
ULT6-C2	Axial	-3901.31	104.03	1406.12
		2056.13	85.56	952.97
	Shear	43.57	25.29	1160.59
		-3899.60	104.09	1302.66

ULT7-C1	Moment	-2726.17	78.38	675.29
		1952.11	82.94	1519.13
	Axial	-2228.00	71.51	680.62
		216.61	20.64	455.87
	Shear	216.61	20.64	455.87
		-2228.00	71.51	680.62
Moment	-1430.95	42.15	234.84	
	-2139.46	50.12	762.00	
ULT7-C2	Axial	-2010.43	63.73	653.60
		811.05	40.10	392.70
	Shear	-595.40	16.38	480.76
		-2010.43	63.73	653.60
	Moment	-1294.81	37.64	271.18
		-1931.23	44.99	734.66

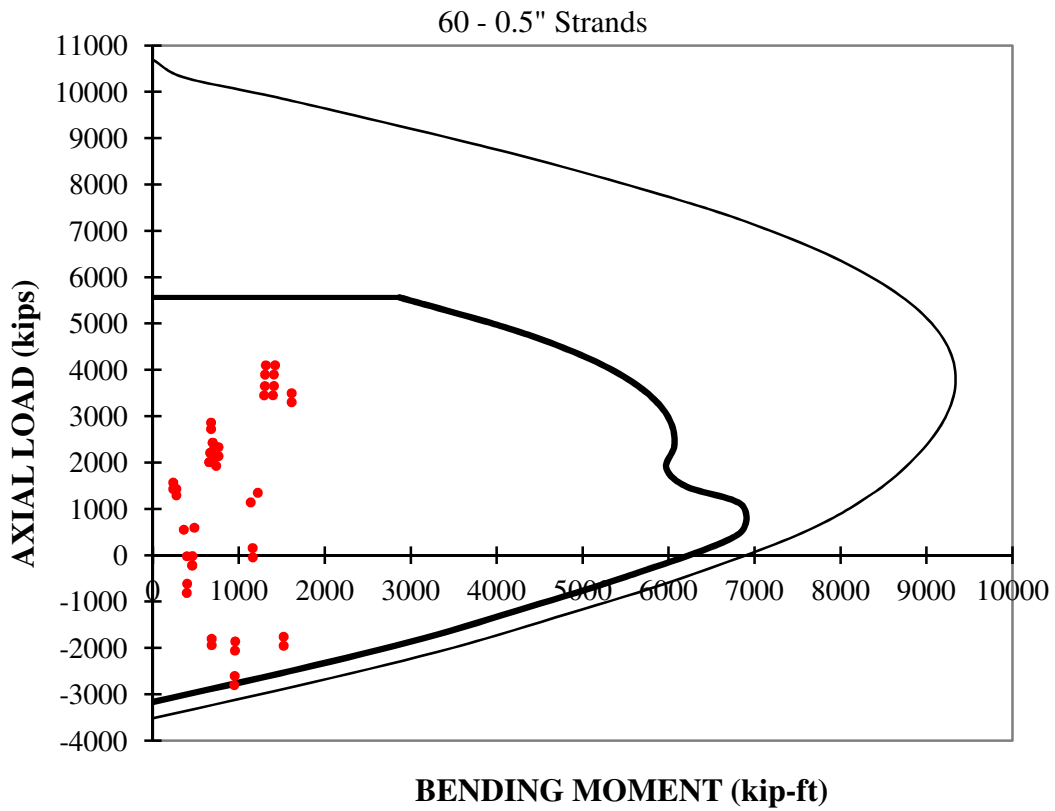


Figure B-9: Segments 2 columns interaction diagram.

Table B-8: Segment 2 column properties.

Service Check						
Prestress	Area	Inertia	y	f_c	Stress Limits	
Kip	in ²	in ⁴	in	ksi	ksi	
-2109.24	1811.80	2.8E+10	31.18	8.00	-4.80	0.67
Shear Check						
b_w	d_p	ϕ	V_c limits		Shear Rft (in ²)	
in	in		Kip		C-Shape	Spiral
28.43	58.35	0.75	296.70	741.75	0.76	0.31
					#6 - 24"	W16 - 12"

Table B-9: Service and operational loads check for segment 2 columns.

Segment 2 Columns							
Load Combination		Axial	Moment	Stress Range		Comp. stress	Tens. stress
		Kip	Kip-ft	ksi			
SER5-1-C1	Axial	-2862.01	888.35	-2.74	-2.74	Safe	No tension
		1549.08	806.17	-0.31	-0.31	Safe	No tension
	Shear	-1274.51	812.11	-1.87	-1.87	Safe	No tension
		-2860.11	809.95	-2.74	-2.74	Safe	No tension
Moment	970.56	681.45	-0.63	-0.63	Safe	No tension	
	-2862.01	888.35	-2.74	-2.74	Safe	No tension	
SER5-1-C2	Axial	-3298.27	899.61	-2.98	-2.98	Safe	No tension
		933.56	763.62	-0.65	-0.65	Safe	No tension
	Shear	-67.27	711.74	-1.20	-1.20	Safe	No tension
		-3296.37	809.60	-2.98	-2.98	Safe	No tension
Moment	-1997.92	647.85	-2.27	-2.27	Safe	No tension	
	-3298.27	899.61	-2.98	-2.98	Safe	No tension	
SER5-2-C1	Axial	-2559.25	610.01	-2.58	-2.58	Safe	No tension
		-65.59	534.23	-1.20	-1.20	Safe	No tension
	Shear	-130.48	364.71	-1.24	-1.24	Safe	No tension
		-2559.25	610.01	-2.58	-2.58	Safe	No tension
Moment	-1520.64	317.92	-2.00	-2.00	Safe	No tension	
	-2559.25	610.01	-2.58	-2.58	Safe	No tension	

SER5-2-C2	Axial	-2337.71	589.73	-2.45	-2.45	Safe	No tension
		528.76	477.79	-0.87	-0.87	Safe	No tension
	Shear	-572.79	384.92	-1.48	-1.48	Safe	No tension
		-2337.71	589.73	-2.45	-2.45	Safe	No tension
	Moment	-1396.42	329.97	-1.93	-1.93	Safe	No tension
-2337.71		589.73	-2.45	-2.45	Safe	No tension	
SER7-C1	Axial	-2499.85	875.45	-2.54	-2.54	Safe	No tension
		1910.49	811.68	-0.11	-0.11	Safe	No tension
	Shear	-959.41	811.42	-1.69	-1.69	Safe	No tension
		-2498.71	805.52	-2.54	-2.54	Safe	No tension
	Moment	1180.20	677.11	-0.51	-0.51	Safe	No tension
-2499.85		875.45	-2.54	-2.54	Safe	No tension	
SER7-C2	Axial	-2936.10	884.12	-2.78	-2.78	Safe	No tension
		1294.96	767.87	-0.45	-0.45	Safe	No tension
	Shear	-2746.48	814.31	-2.68	-2.68	Safe	No tension
		-2934.96	804.03	-2.78	-2.78	Safe	No tension
	Moment	-1788.28	652.21	-2.15	-2.15	Safe	No tension
-2936.10		884.12	-2.78	-2.78	Safe	No tension	
SER8-C1	Axial	-2197.09	593.95	-2.38	-2.38	Safe	No tension
		284.80	484.19	-1.01	-1.01	Safe	No tension
	Shear	79.16	362.57	-1.12	-1.12	Safe	No tension
		-2197.09	593.95	-2.38	-2.38	Safe	No tension
	Moment	-1283.28	322.72	-1.87	-1.87	Safe	No tension
-2197.09		593.95	-2.38	-2.38	Safe	No tension	
SER8-C2	Axial	-1975.54	575.30	-2.25	-2.25	Safe	No tension
		890.17	482.77	-0.67	-0.67	Safe	No tension
	Shear	-343.68	384.90	-1.35	-1.35	Safe	No tension
		-1975.54	575.30	-2.25	-2.25	Safe	No tension
	Moment	-1159.05	333.95	-1.80	-1.80	Safe	No tension
-1975.54		575.30	-2.25	-2.25	Safe	No tension	
OPR5-1-C1	Axial	-2985.46	768.18	-2.81	-2.81	Safe	No tension
		429.34	590.91	-0.93	-0.93	Safe	No tension
	Shear	-140.68	666.93	-1.24	-1.24	Safe	No tension
		-2983.56	675.12	-2.81	-2.81	Safe	No tension
	Moment	-1911.44	474.78	-2.22	-2.22	Safe	No tension
-2985.46		768.18	-2.81	-2.81	Safe	No tension	
OPR5-1-C2	Axial	-2114.14	636.71	-2.33	-2.33	Safe	No tension
		953.83	584.89	-0.64	-0.64	Safe	No tension

	Shear	-1448.42	615.07	-1.96	-1.96	Safe	No tension
		527.96	581.17	-0.87	-0.87	Safe	No tension
	Moment	-1501.08	460.90	-1.99	-1.99	Safe	No tension
		-2114.14	636.71	-2.33	-2.33	Safe	No tension
OPR7-C1	Axial	-2623.29	752.24	-2.61	-2.61	Safe	No tension
		777.94	623.05	-0.73	-0.73	Safe	No tension
	Shear	197.44	668.92	-1.06	-1.06	Safe	No tension
		-2622.15	669.32	-2.61	-2.61	Safe	No tension
	Moment	-1674.07	479.45	-2.09	-2.09	Safe	No tension
		-2623.29	752.24	-2.61	-2.61	Safe	No tension
OPR7-C2	Axial	-1751.97	625.21	-2.13	-2.13	Safe	No tension
		1315.23	590.68	-0.44	-0.44	Safe	No tension
	Shear	-1101.19	589.64	-1.77	-1.77	Safe	No tension
		750.35	587.93	-0.75	-0.75	Safe	No tension
	Moment	726.85	463.13	-0.76	-0.76	Safe	No tension
		-1635.57	630.85	-2.07	-2.07	Safe	No tension

Table B-10: Shear check for segment 2 columns.

Segment 2 Columns							
Ultimate Load Combination	Max and Min	Axial	Shear	Moment	V_c	V_s	Shear
		Kip	Kip	Kip-ft	Kip	Kip	
ULT4-C1	Axial	-3958.16	145.16	1258.53	740.15	111.26	Safe
		2341.91	72.15	1138.86	0.00	111.26	Safe
	Shear	-1507.22	4.74	1145.02	296.70	111.26	Safe
		-3955.88	145.24	1141.00	741.75	111.26	Safe
	Moment	1429.04	21.03	941.77	0.00	111.26	Safe
		-3958.16	145.16	1258.53	740.15	111.26	Safe
ULT4-C2	Axial	-432.42	41.12	1078.21	304.34	111.26	Safe
		1588.23	70.93	1071.83	0.00	111.26	Safe
	Shear	-45.76	1.97	981.99	296.70	111.26	Safe
		-4410.78	125.79	1129.86	717.52	111.26	Safe
	Moment	-2652.14	29.41	895.46	296.70	111.26	Safe
		-4413.05	125.71	1253.73	655.05	111.26	Safe

ULT5-C1	Axial	-3449.12	142.78	862.27	741.75	111.26	Safe
		97.07	31.91	689.28	0.00	111.26	Safe
	Shear	-66.61	3.54	519.79	296.70	111.26	Safe
		-3449.12	142.78	862.27	741.75	111.26	Safe
	Moment	-2036.71	79.65	456.92	741.75	111.26	Safe
-3449.12		142.78	862.27	741.75	111.26	Safe	
ULT5-C2	Axial	-3132.64	128.23	834.21	741.75	111.26	Safe
		961.89	67.15	685.40	0.00	111.26	Safe
	Shear	-687.35	2.61	549.87	296.70	111.26	Safe
		-3132.64	128.23	834.21	741.75	111.26	Safe
	Moment	-1859.24	71.23	473.66	741.75	111.26	Safe
-3132.64		128.23	834.21	741.75	111.26	Safe	
ULT6-C1	Axial	-3686.53	137.50	1248.60	710.70	111.26	Safe
		2612.97	79.62	1142.93	0.00	111.26	Safe
	Shear	-1270.90	4.53	1144.61	296.70	111.26	Safe
		-3684.82	137.56	1137.57	741.75	111.26	Safe
	Moment	1586.27	22.16	938.54	0.00	111.26	Safe
-3686.53		137.50	1248.60	710.70	111.26	Safe	
ULT6-C2	Axial	-4141.43	118.11	1242.21	625.76	111.26	Safe
		1859.29	78.61	1075.12	0.00	111.26	Safe
	Shear	111.47	2.62	981.05	0.00	111.26	Safe
		-4139.72	118.17	1125.73	681.61	111.26	Safe
	Moment	-2494.91	28.28	898.71	296.70	111.26	Safe
-4141.43		118.11	1242.21	625.76	111.26	Safe	
ULT7-C1	Axial	-3177.50	135.12	850.22	741.75	111.26	Safe
		368.13	38.27	691.39	0.00	111.26	Safe
	Shear	90.62	4.68	518.19	0.00	111.26	Safe
		-3177.50	135.12	850.22	741.75	111.26	Safe
	Moment	-1858.68	77.64	460.52	741.75	111.26	Safe
-3177.50		135.12	850.22	741.75	111.26	Safe	
ULT7-C2	Axial	-2861.01	120.61	823.39	741.75	111.26	Safe
		1232.95	74.72	689.13	0.00	111.26	Safe
	Shear	-515.52	2.51	549.86	296.70	111.26	Safe
		-2861.01	120.61	823.39	741.75	111.26	Safe
	Moment	-1681.22	69.26	476.64	741.75	111.26	Safe
-2861.01		120.61	823.39	741.75	111.26	Safe	

Table B-11: Ultimate loads acting on segment 3 columns.

Segment 3 Columns				
Ultimate Load Combination	Max/Min	Axial	Shear	Moment
		Kip	Kip	Kip-ft
ULT4-C1	Axial	-2084.25	135.33	1166.35
		1612.70	136.21	486.57
	Shear	-239.76	53.05	453.89
		-303.44	155.78	594.72
	Moment	880.22	122.28	21.89
1351.74		130.47	1570.08	
ULT4-C2	Axial	-2630.50	152.98	1208.30
		962.71	106.67	657.43
	Shear	-254.54	30.69	524.91
		-317.77	202.05	612.03
	Moment	-1716.41	121.40	23.18
-2347.82		128.27	1539.20	
ULT5-C1	Axial	-1436.95	79.19	523.10
		-67.97	32.16	282.18
	Shear	-249.32	18.25	87.66
		-302.91	121.58	108.10
	Moment	-1104.97	56.16	14.88
-291.76		120.47	700.61	
ULT5-C2	Axial	-1315.70	71.08	506.69
		263.32	50.38	211.06
	Shear	-213.79	21.53	51.37
		-301.00	115.10	133.46
	Moment	-361.64	23.36	7.02
-289.85		114.11	691.47	
ULT6-C1	Axial	-1951.28	132.91	1160.12
		1742.82	138.69	482.60
	Shear	-971.21	64.68	779.23
		1735.99	140.01	1033.38
	Moment	986.52	122.47	21.73
1479.61		130.70	1570.61	
ULT6-C2	Axial	-2497.53	150.49	1200.09
		1092.83	109.05	655.77
	Shear	-193.65	33.70	407.43
		-247.78	183.53	472.11

ULT7-C1	Moment	-1610.11	121.20	23.31
		-2219.94	128.04	1538.67
	Axial	-1303.98	76.68	514.73
		62.16	34.07	280.87
	Shear	-174.86	19.55	78.39
		-230.69	102.98	40.65
Moment	-329.18	53.58	3.77	
	-1160.18	61.38	668.28	
ULT7-C2	Axial	-1182.73	68.62	499.15
		393.44	52.81	208.23
	Shear	-204.48	16.34	344.00
		-228.79	96.62	68.04
	Moment	-271.23	23.36	6.89
		-1056.15	55.58	636.71

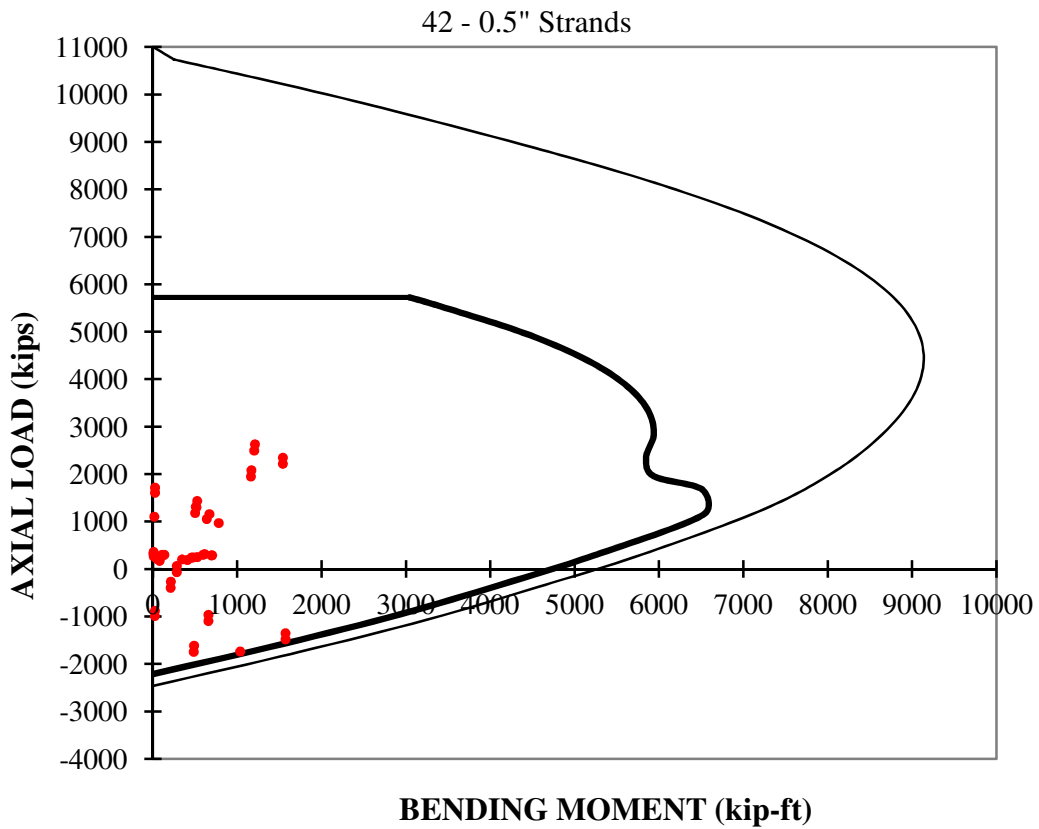


Figure B-10: Segments 3 columns interaction diagram.

Table B-12: Segment 3 column properties.

Service Check						
Prestress	Area	Inertia	y	f_c	Stress Limits	
Kip	in ²	in ⁴	in	ksi	ksi	
-1476.47	1811.80	2.8E+10	31.18	8.00	-4.80	0.67
Shear Check						
b_w	d_p	ϕ	V_c limits		Shear Rft (in ²)	
in	in		Kip		C-Shape	Spiral
28.43	58.35	0.75	296.70	741.75	0.76	0.31
					#6 - 24"	W16 - 12"

Table B-13: Service and operational loads check for segment 3 columns.

Segment 3 Columns							
Load Combination		Axial	Moment	Stress Range		Comp. stress	Tens. stress
		Kip	Kip-ft	ksi			
SER5-1-C1	Axial	-1664.34	750.75	-1.73	-1.73	Safe	No tension
		1029.98	644.18	-0.25	-0.25	Safe	No tension
	Shear	-873.00	671.24	-1.30	-1.30	Safe	No tension
		-235.41	536.20	-0.94	-0.94	Safe	No tension
	Moment	-385.24	48.81	-1.03	-1.03	Safe	No tension
-1664.34		750.75	-1.73	-1.73	Safe	No tension	
SER5-1-C2	Axial	-2115.04	773.53	-1.98	-1.98	Safe	No tension
		516.63	641.99	-0.53	-0.53	Safe	No tension
	Shear	-130.83	202.43	-0.89	-0.89	Safe	No tension
		-237.99	548.85	-0.95	-0.95	Safe	No tension
	Moment	-458.55	45.64	-1.07	-1.07	Safe	No tension
-2115.04		773.53	-1.98	-1.98	Safe	No tension	
SER5-2-C1	Axial	-1371.10	407.86	-1.57	-1.57	Safe	No tension
		-132.62	337.05	-0.89	-0.89	Safe	No tension
	Shear	-213.27	74.20	-0.93	-0.93	Safe	No tension
		-1371.10	407.86	-1.57	-1.57	Safe	No tension
	Moment	-340.03	12.14	-1.00	-1.00	Safe	No tension
-233.77		528.11	-0.94	-0.94	Safe	No tension	

SER5-2-C2	Axial	-1261.65	397.00	-1.51	-1.51	Safe	No tension
		155.70	307.70	-0.73	-0.73	Safe	No tension
	Shear	-356.46	42.20	-1.01	-1.01	Safe	No tension
		-1261.65	397.00	-1.51	-1.51	Safe	No tension
	Moment	-330.92	19.52	-1.00	-1.00	Safe	No tension
-233.41		526.22	-0.94	-0.94	Safe	No tension	
SER7-C1	Axial	-1442.77	743.81	-1.61	-1.61	Safe	No tension
		1250.79	648.03	-0.12	-0.12	Safe	No tension
	Shear	-685.46	671.71	-1.19	-1.19	Safe	No tension
		1250.79	648.03	-0.12	-0.12	Safe	No tension
	Moment	-181.39	41.48	-0.92	-0.92	Safe	No tension
1249.65		748.62	-0.13	-0.13	Safe	No tension	
SER7-C2	Axial	-1893.47	764.15	-1.86	-1.86	Safe	No tension
		737.43	644.56	-0.41	-0.41	Safe	No tension
	Shear	139.41	663.10	-0.74	-0.74	Safe	No tension
		-145.43	342.30	-0.90	-0.90	Safe	No tension
	Moment	-237.45	37.38	-0.95	-0.95	Safe	No tension
-1893.47		764.15	-1.86	-1.86	Safe	No tension	
SER8-C1	Axial	-1149.53	398.29	-1.45	-1.45	Safe	No tension
		77.38	320.52	-0.77	-0.77	Safe	No tension
	Shear	-94.19	75.20	-0.87	-0.87	Safe	No tension
		-1149.53	398.29	-1.45	-1.45	Safe	No tension
	Moment	-231.35	5.08	-0.94	-0.94	Safe	No tension
-1149.53		398.29	-1.45	-1.45	Safe	No tension	
SER8-C2	Axial	-1040.08	388.46	-1.39	-1.39	Safe	No tension
		376.51	311.05	-0.61	-0.61	Safe	No tension
	Shear	-196.81	116.70	-0.92	-0.92	Safe	No tension
		-1040.08	388.46	-1.39	-1.39	Safe	No tension
	Moment	-222.23	9.31	-0.94	-0.94	Safe	No tension
-1040.08		388.46	-1.39	-1.39	Safe	No tension	
OPR5-1-C1	Axial	-1713.00	590.04	-1.76	-1.76	Safe	No tension
		324.60	452.91	-0.64	-0.64	Safe	No tension
	Shear	196.96	437.88	-0.71	-0.71	Safe	No tension
		324.48	250.37	-0.64	-0.64	Safe	No tension
	Moment	-128.45	89.06	-0.89	-0.89	Safe	No tension
-741.99		927.45	-1.22	-1.22	Safe	No tension	
OPR5-1-C2	Axial	-1391.60	536.69	-1.58	-1.58	Safe	No tension
		529.16	419.60	-0.52	-0.52	Safe	No tension

	Shear	-378.61	167.00	-1.02	-1.02	Safe	No tension
		-186.04	729.31	-0.92	-0.92	Safe	No tension
	Moment	-37.53	76.69	-0.84	-0.84	Safe	No tension
		-789.33	973.31	-1.25	-1.25	Safe	No tension
OPR7-C1	Axial	-1491.43	580.79	-1.64	-1.64	Safe	No tension
		545.41	455.92	-0.51	-0.51	Safe	No tension
	Shear	-649.43	733.92	-1.17	-1.17	Safe	No tension
		417.06	223.22	-0.58	-0.58	Safe	No tension
	Moment	-195.42	93.33	-0.92	-0.92	Safe	No tension
		-650.57	739.20	-1.17	-1.17	Safe	No tension
OPR7-C2	Axial	-1170.03	529.26	-1.46	-1.46	Safe	No tension
		749.97	423.43	-0.40	-0.40	Safe	No tension
	Shear	-271.91	169.72	-0.96	-0.96	Safe	No tension
		-232.68	359.48	-0.94	-0.94	Safe	No tension
	Moment	88.05	82.50	-0.77	-0.77	Safe	No tension
		-695.98	792.95	-1.20	-1.20	Safe	No tension

Table B-14: Shear check for segment 3 columns.

Segment 3 Columns							
Ultimate Load Combination	Max and Min	Axial	Shear	Moment	Vc	Vs	Shear
		Kip	Kip	Kip-ft	Kip	Kip	
ULT4-C1	Axial	-2244.25	145.42	1038.35	741.75	111.26	Safe
		1513.51	136.21	890.75	296.16	111.26	Safe
	Shear	-1076.27	1.23	926.41	296.70	111.26	Safe
		-2241.97	145.42	914.89	741.75	111.26	Safe
	Moment	-480.82	115.41	67.50	741.75	111.26	Safe
		-2244.25	145.42	1038.35	741.75	111.26	Safe
ULT4-C2	Axial	-2805.84	165.02	1060.83	741.75	111.26	Safe
		847.50	104.79	882.70	296.40	111.26	Safe
	Shear	-136.27	2.61	275.05	296.70	111.26	Safe
		-286.59	188.09	663.55	741.75	111.26	Safe
	Moment	-578.91	147.71	68.16	741.75	111.26	Safe
		-2805.84	165.02	1060.83	741.75	111.26	Safe

ULT5-C1	Axial	-1832.10	118.82	577.19	741.75	111.26	Safe
		-78.73	44.94	456.31	645.00	111.26	Safe
	Shear	-236.63	1.00	106.57	296.70	111.26	Safe
		-1832.10	118.82	577.19	741.75	111.26	Safe
	Moment	-423.66	81.68	7.51	741.75	111.26	Safe
-281.06		103.59	636.33	741.75	111.26	Safe	
ULT5-C2	Axial	-1675.75	106.49	562.25	741.75	111.26	Safe
		348.61	73.33	441.48	296.57	111.26	Safe
	Shear	-393.61	0.87	166.72	296.70	111.26	Safe
		-1675.75	106.49	562.25	741.75	111.26	Safe
	Moment	-410.63	76.29	19.64	741.75	111.26	Safe
-280.55		97.25	633.71	741.75	111.26	Safe	
ULT6-C1	Axial	-2078.08	141.33	1033.02	741.75	111.26	Safe
		1679.12	140.37	893.62	296.10	111.26	Safe
	Shear	-935.62	0.81	926.74	296.70	111.26	Safe
		-2076.37	141.33	912.84	741.75	111.26	Safe
	Moment	-266.22	40.90	61.51	741.75	111.26	Safe
1677.41		140.37	1033.28	296.10	111.26	Safe	
ULT6-C2	Axial	-2639.66	160.85	1053.83	741.75	111.26	Safe
		1013.11	108.81	884.66	296.34	111.26	Safe
	Shear	119.32	2.92	911.47	296.66	111.26	Safe
		-217.17	174.12	508.64	741.75	111.26	Safe
	Moment	-342.45	34.58	57.55	741.75	111.26	Safe
-2639.66		160.85	1053.83	741.75	111.26	Safe	
ULT7-C1	Axial	-1665.93	114.62	570.01	741.75	111.26	Safe
		86.88	48.20	457.69	296.67	111.26	Safe
	Shear	-147.32	1.66	107.32	296.70	111.26	Safe
		-1665.93	114.62	570.01	741.75	111.26	Safe
	Moment	-342.15	72.75	5.41	741.75	111.26	Safe
-1665.93		114.62	570.01	741.75	111.26	Safe	
ULT7-C2	Axial	-1509.57	102.35	555.85	741.75	111.26	Safe
		514.22	77.42	444.00	296.52	111.26	Safe
	Shear	-295.21	0.69	166.71	296.70	111.26	Safe
		-1509.57	102.35	555.85	741.75	111.26	Safe
	Moment	-329.11	67.48	13.35	741.75	111.26	Safe
-1509.57		102.35	555.85	741.75	111.26	Safe	

Prestressed Concrete Fatigue Design (Model Code 1990)

Operating frequency: 20 RPM for 30 years
 $nf := 5.39 \cdot 10^8$

Fatigue Loads: (From SAP)

Max Tension Case:	$P_t := 63.3 \text{ kip}$	$M_t := 46.4 \text{ kip}\cdot\text{ft}$
Max Compression Case:	$P_c := -1776.9 \text{ kip}$	$M_c := 264.4 \text{ kip}\cdot\text{ft}$
Max Moment Case:	$P_m := -35.4 \text{ kip}$	$M_m := 1023.3 \text{ kip}\cdot\text{ft}$

Concrete and Strands Properties:

$A_c := A_{col} = 1.812 \times 10^3 \text{ in}^2$	$A_s := 60 \cdot 0.217 \text{ in}^2 = 13.02 \text{ in}^2$
$I_{cx} := 28387855285 \text{ in}^4$	$I_{sx} := 191919020 \text{ in}^4$
$S_{cx} := \frac{I_{cx}}{31.1769 \text{ in}} = 9.105 \times 10^8 \text{ in}^3$	$S_{sx} := \frac{I_{sx}}{27.1769 \text{ in}} = 7.062 \times 10^6 \text{ in}^3$

Concrete Fatigue:

Concrete Stresses:

$f_{cmin1} := \frac{P_t}{A_c} - \frac{M_t}{S_{cx}} = 0.035 \text{ ksi}$	$f_{cmax1} := \frac{P_t}{A_c} + \frac{M_t}{S_{cx}} = 0.035 \text{ ksi}$
$f_{cmin2} := \frac{P_c}{A_c} - \frac{M_c}{S_{cx}} = -0.981 \text{ ksi}$	$f_{cmax2} := \frac{P_c}{A_c} + \frac{M_c}{S_{cx}} = -0.981 \text{ ksi}$
$f_{cmin3} := \frac{P_m}{A_c} - \frac{M_m}{S_{cx}} = -0.02 \text{ ksi}$	$f_{cmax3} := \frac{P_m}{A_c} + \frac{M_m}{S_{cx}} = -0.02 \text{ ksi}$

$f_{c,max} := \max(f_{cmax1}, f_{cmax2}, f_{cmax3}) = 0.035 \text{ ksi}$

$f_{c,min} := \min(f_{cmin1}, f_{cmin2}, f_{cmin3}) = -0.981 \text{ ksi}$

Concrete Strength:	$f_c' = 8 \text{ ksi}$
Concrete Reference Strength: (MC90 - Art. 6.7.2)	$f_{cko} := 10 \text{ MPa} = 1.45 \text{ ksi}$
Concrete Material Factor: (MC90 - Art. 1.6.4.4)	$\gamma_{c.fat} := 1.5$
	$\gamma_{Sd} := 1.1$
	$\gamma_{s.fat} := 1.15$
Concrete Age at beginning of loading:	$age := 60 \text{ day}$
Cement Factor: (MC90 - Art. 2.1.6.1) Normal hardening cement	$s_f := 0.25$
Age Factor: (MC90 - Eq. 2.1-54)	$\beta_{cc} := \exp\left(s_f \cdot \sqrt{1 - \frac{28 \text{ day}}{age}}\right) = 1.2$
Fatigue Reference Strength: (MC90 - Art. 6.7.2)	$f_{cd.fat} := 0.85 \cdot \beta_{cc} \cdot \frac{\left[fc' \cdot \left(1 - \frac{fc'}{25 \cdot f_{cko}}\right)\right]}{\gamma_{c.fat}}$
Fatigue Parameter: (MC90 - Eq. 6.7-2)	$\eta_c := 1$
Lower bound value of the characteristic Tensile Strength: (MC90 - Eq. 2.1-2)	$f_{ctk.min} := 0.95 \text{ MPa} \cdot \left(\frac{fc'}{f_{cko}}\right)^{\frac{2}{3}} = 0.43 \text{ ksi}$
Fatigue Reference Design Strength: (MC90 - Eq. 6.7-5)	$f_{ctd.dat} := \frac{f_{ctk.min}}{\gamma_{c.fat}} = 0.287 \text{ ksi}$
Simplified Method Check:	
Concrete Compression Check: (MC90 - Eq. 6.7-4)	$\gamma_{Sd} \cdot \eta_c \cdot f_{c.min} = -1.079 \text{ ksi}$
	Allowable: $0.45 \cdot f_{cd.fat} = 1.908 \text{ ksi}$
	Compression is Safe
Concrete Tension Check: (MC90 - Eq. 6.7-5)	$\gamma_{Sd} \cdot f_{c.max} = 0.038 \text{ ksi}$
	Allowable: $0.33 \cdot f_{ctd.dat} = 0.095 \text{ ksi}$
	Tension is Safe

Strands Fatigue:

Strands Stresses:

$$f_{tmin1} := \frac{P_t}{A_s} - \frac{M_t}{S_{sx}} = 4.862 \text{ ksi}$$

$$f_{tmax1} := \frac{P_t}{A_s} + \frac{M_t}{S_{sx}} = 4.862 \text{ ksi}$$

$$f_{tmin2} := \frac{P_c}{A_s} - \frac{M_c}{S_{sx}} = -136.475 \text{ ksi}$$

$$f_{tmax2} := \frac{P_c}{A_s} + \frac{M_c}{S_{sx}} = -136.474 \text{ ksi}$$

$$f_{tmin3} := \frac{P_m}{A_s} - \frac{M_m}{S_{sx}} = -2.721 \text{ ksi}$$

$$f_{tmax3} := \frac{P_m}{A_s} + \frac{M_m}{S_{sx}} = -2.717 \text{ ksi}$$

$$f_{t,max} := \max(f_{tmax1}, f_{tmax2}, f_{tmax3}) = 4.862 \text{ ksi}$$

$$f_{t,min} := \min(f_{tmin1}, f_{tmin2}, f_{tmin3}) = -136.475 \text{ ksi}$$

Compression:

$$f_{tmin} := 0$$

For pre-tensioned strands
(MC90 - Art. 6.7.2)

$$\zeta := 0.6$$

Rebar Diameter:

$$\phi_s := \frac{4}{8} \text{ in}$$

Strands Equivalent Diameter:
(MC90 - Eq. 6.7-1)

$$\phi_p := 1.6 \sqrt{0.2172 \text{ in}^2} = 0.746 \text{ in}$$

Fatigue Parameter:
(MC90 - Eq. 6.7-1)

$$\eta_s := \frac{1 \cdot (\text{in}^2) + A_s}{1 \cdot (\text{in}^2) + A_s \cdot \sqrt{\left[\zeta \cdot \left(\frac{\phi_s}{\phi_p} \right) \right]}} = 1.514$$

Characteristic Fatigue Strength:
(MC90 - Tbl. 6.7.2)
For prestressed Straight Strands

$$\Delta\sigma_{Rsk} := 95 \text{ MPa} = 13.779 \text{ ksi}$$

$$\Delta\sigma_{RskN} := 160 \text{ MPa} = 23.206 \text{ ksi}$$

$$k_1 := 5$$

$$k_2 := 9$$

Max Stress Range:

$$\Delta\sigma_s := f_{t,max} - f_{t,min} = 4.862 \text{ ksi}$$

Strands Fatigue Check:
(MC90 - Eq. 6.7-5)

$$\gamma_{Sd} \cdot \Delta\sigma_s = 5.348 \text{ ksi}$$

$$\text{Allowable: } \frac{\Delta\sigma_{Rsk}}{\gamma_{s,fat}} = 11.981 \text{ ksi}$$

Strands are Safe

Panels Design

Table B-15: Panels properties.

Panels properties						
b_w	h	d	f_c	L_n	L_n/d	j_d
in	in	in	ksi	ft	---	in
6.00	120.00	108.00	8000.00	20.00	2.22	91.20
Shear and out of plane bending reinforcement						
ϕ Shear	V_c limits		Min Shear Rft	Direct Wind Rft	Rft. Used	V_s
	ksi		in^2	in^2	in^2	Kip
0.75	115.92	289.79	0.18	0.40	0.40	270.00
					W20 - 12"	
In plane bending reinforcement						
ϕ Bending	Min Flexure Rft		y	Flexure rft	ρ_s	ϕM_n
	in^2		in	in^2		k-ft
0.90	2.90	2.16	18.00	2.5+0.4	0.005	1296.86
				8#5		

Table B-16: Panels design for out of plane bending (as slab).

Height (z)	CL Panel Width	K_z	q_z	C_f		G_f	Moment on panels		Flexural Check W20-12" T&B ($\phi Mn=5.4(k-ft)$)	
			(psf)				(k-f) / ft'		EWM C1	EWM C2
(ft)	(ft)		EWM	C1	C2	EWM	EWM C1	EWM C2	EWM C1	EWM C2
240	10.00	1.67	53.67	1.46	1.14	1.04	---	---	---	---
235	10.00	1.66	53.47	1.46	1.14	1.04	1.01	2.18	Safe	Safe
225	10.00	1.65	53.07	1.46	1.14	1.04	1.01	2.16	Safe	Safe
215	10.00	1.64	52.65	1.46	1.14	1.04	1.00	2.14	Safe	Safe
205	10.00	1.62	52.22	1.46	1.14	1.04	0.99	2.13	Safe	Safe
195	10.00	1.61	51.76	1.46	1.14	1.04	0.98	2.11	Safe	Safe
185	10.00	1.59	51.29	1.46	1.14	1.04	0.97	2.09	Safe	Safe
175	10.00	1.58	50.80	1.46	1.14	1.04	0.96	2.07	Safe	Safe
165	10.00	1.56	50.28	1.46	1.14	1.04	0.95	2.05	Safe	Safe
160	10.00	1.55	50.01	1.46	1.14	1.04	---	---	---	---
155	10.31	1.55	49.74	1.46	1.14	1.04	1.00	2.10	Safe	Safe
145	10.94	1.53	49.16	1.46	1.14	1.04	1.11	2.23	Safe	Safe
135	11.56	1.51	48.56	1.46	1.14	1.04	1.23	2.36	Safe	Safe
125	12.19	1.49	47.91	1.46	1.14	1.04	1.35	2.49	Safe	Safe
115	12.81	1.47	47.22	1.46	1.14	1.04	1.46	2.62	Safe	Safe
105	13.44	1.45	46.48	1.46	1.14	1.03	1.58	2.74	Safe	Safe
95	14.06	1.42	45.68	1.46	1.14	1.03	1.70	2.86	Safe	Safe
85	14.69	1.39	44.80	1.46	1.14	1.03	1.82	2.98	Safe	Safe
80	15.00	1.38	44.33	1.46	1.14	1.03	---	---	---	---
75	15.63	1.36	43.84	1.46	1.14	1.03	2.01	3.17	Safe	Safe
65	16.88	1.33	42.76	1.46	1.14	1.03	2.28	3.45	Safe	Safe
55	18.13	1.29	41.54	1.46	1.14	1.03	2.56	3.71	Safe	Safe
45	19.38	1.25	40.11	1.46	1.14	1.02	2.81	3.94	Safe	Safe
35	20.63	1.19	38.40	1.46	1.14	1.02	3.04	4.13	Safe	Safe
25	21.88	1.13	36.21	1.46	1.14	1.02	3.21	4.24	Safe	Safe
15	23.13	1.03	33.14	1.46	1.14	1.01	3.26	4.20	Safe	Safe
5	24.38	0.85	27.37	1.46	1.14	0.99	2.95	3.71	Safe	Safe
0	25.00	0.00	0.00	1.46	1.14	0.00	---	---	---	---

Table B-17: Panels design for shear and in plane bending (as deep beam).

Panel design for shear and in plane bending							
Ultimate Load Combination	Max/Min	Axial	Shear	Moment	V _c	Check shear	Check bending
		Kip	Kip	Kip-ft	Kip		
ULT4-C1	Axial	-35.3	45.7	406.2	121.93	Safe	Safe
		56.2	13.8	234.5	115.92	Safe	Safe
	Shear	-0.9	-172.3	-866.9	248.18	Safe	Safe
		1.1	119.0	-659.2	243.23	Safe	Safe
	Moment	-0.9	-172.3	-866.9	248.18	Safe	Safe
		-0.9	-163.3	811.6	239.53	Safe	Safe
ULT4-C2	Axial	-31.2	-31.8	-160.1	247.90	Safe	Safe
		46.6	-106.5	-388.0	289.79	Safe	Safe
	Shear	-0.9	-119.0	-498.3	275.73	Safe	Safe
		0.5	165.5	-786.1	237.89	Safe	Safe
	Moment	0.5	165.5	-786.1	237.89	Safe	Safe
		0.5	156.5	823.7	240.51	Safe	Safe
ULT5-C1	Axial	-15.9	11.8	175.7	115.92	Safe	Safe
		37.7	-46.0	-114.6	289.79	Safe	Safe
	Shear	-0.4	-68.8	-302.5	268.86	Safe	Safe
		-0.4	68.8	-302.5	234.90	Safe	Safe
	Moment	-9.3	68.8	-311.2	236.03	Safe	Safe
		-0.4	59.8	340.2	226.48	Safe	Safe
ULT5-C2	Axial	-20.7	3.9	127.4	115.92	Safe	Safe
		40.6	19.5	221.7	116.37	Safe	Safe
	Shear	-0.1	-78.7	-376.7	256.14	Safe	Safe
		0.3	41.6	-234.5	243.75	Safe	Safe
	Moment	-5.3	-78.7	-381.8	254.00	Safe	Safe
		-0.1	-69.7	365.2	241.39	Safe	Safe
ULT6-C1	Axial	-33.1	47.4	409.2	129.98	Safe	Safe
		47.8	14.9	214.1	115.92	Safe	Safe
	Shear	-0.8	-171.2	-865.5	247.37	Safe	Safe
		1.1	117.8	-658.0	243.48	Safe	Safe
	Moment	-0.8	-171.2	-865.5	247.37	Safe	Safe
		-0.8	-164.5	813.0	239.35	Safe	Safe

ULT6-C2	Axial	-29.0	-30.1	-157.1	242.15	Safe	Safe
		38.2	-105.3	-408.7	285.88	Safe	Safe
	Shear	-0.9	-117.8	-497.2	274.74	Safe	Safe
		0.5	164.4	-784.7	238.07	Safe	Safe
	Moment	0.5	164.4	-784.7	238.07	Safe	Safe
0.5		157.6	825.2	241.44	Safe	Safe	
ULT7-C1	Axial	-13.5	13.6	173.3	115.92	Safe	Safe
		29.3	-44.9	-134.9	289.79	Safe	Safe
	Shear	-0.4	-67.6	-301.1	267.16	Safe	Safe
		-0.4	67.6	-301.1	235.37	Safe	Safe
	Moment	-8.0	67.6	-308.5	236.33	Safe	Safe
-0.4		60.9	341.6	229.16	Safe	Safe	
ULT7-C2	Axial	-18.4	15.0	157.1	116.93	Safe	Safe
		32.2	20.6	201.3	117.40	Safe	Safe
	Shear	-0.1	-77.6	-375.3	254.47	Safe	Safe
		0.3	40.5	-233.1	244.41	Safe	Safe
	Moment	-3.9	-77.5	-379.0	252.84	Safe	Safe
-0.1		-70.8	366.7	240.97	Safe	Safe	

Panels Connection Design Sample:

$$P_u := 57\text{kip} \quad \theta_p := 90\text{deg}$$

$$S_u := 175\text{kip} \quad \theta_s := 0\text{deg}$$

$$M_u := 870\text{kip}\cdot\text{ft} \quad \theta_m := 85\text{deg}$$

Use: (8 - 1 1/2") A490-N Grade 60 Bolts:

$$\phi V_n := 79.5\text{kip}$$

$$\phi T_n := 150\text{kip}$$

$$n := 8$$

Shear on Bolts from applied shear:

$$s_b := \frac{\sqrt{S_u^2 + P_u^2}}{n} = 23.006\cdot\text{kip}$$

$$\theta_b := 18\text{deg}$$

Shear on Bolts from applied moment:

Determine "r":

$$r_1 := 50.5418n \quad r_2 := 51.8833n$$

$$r_3 := 70.1882n \quad r_4 := 71.5492n$$

$$m_b := \frac{M_u \cdot r_4}{2 \cdot (r_1^2 + r_2^2 + r_3^2 + r_4^2)} = 24.424\cdot\text{kip}$$

Max Shear on one Bolt:

$$\theta := 67\text{deg}$$

$$S_b := \sqrt{s_b^2 + m_b^2 + 2 \cdot s_b \cdot m_b \cdot \cos(\theta)} = 39.559\cdot\text{kip}$$

$$\text{Check Shear on bolts: } DCR_{sh} := \frac{S_b}{\phi V_n} = 0.498$$

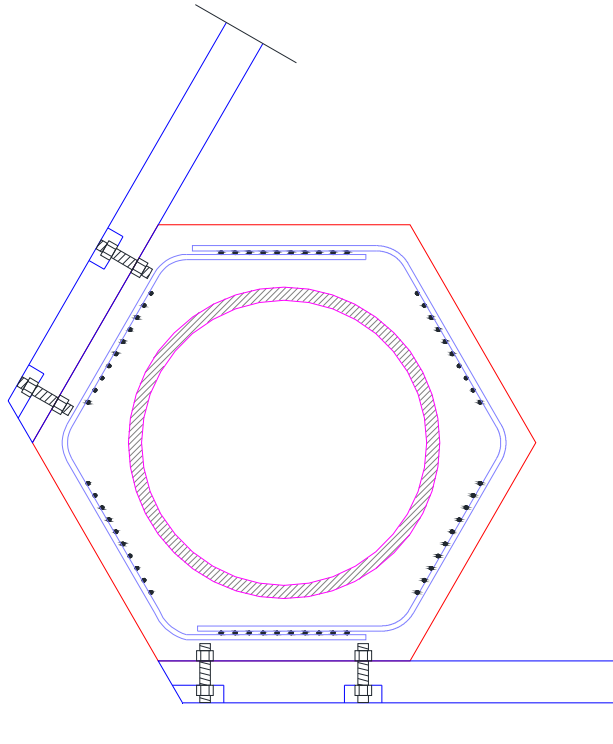


Figure B-11: Panel connection cross section details.

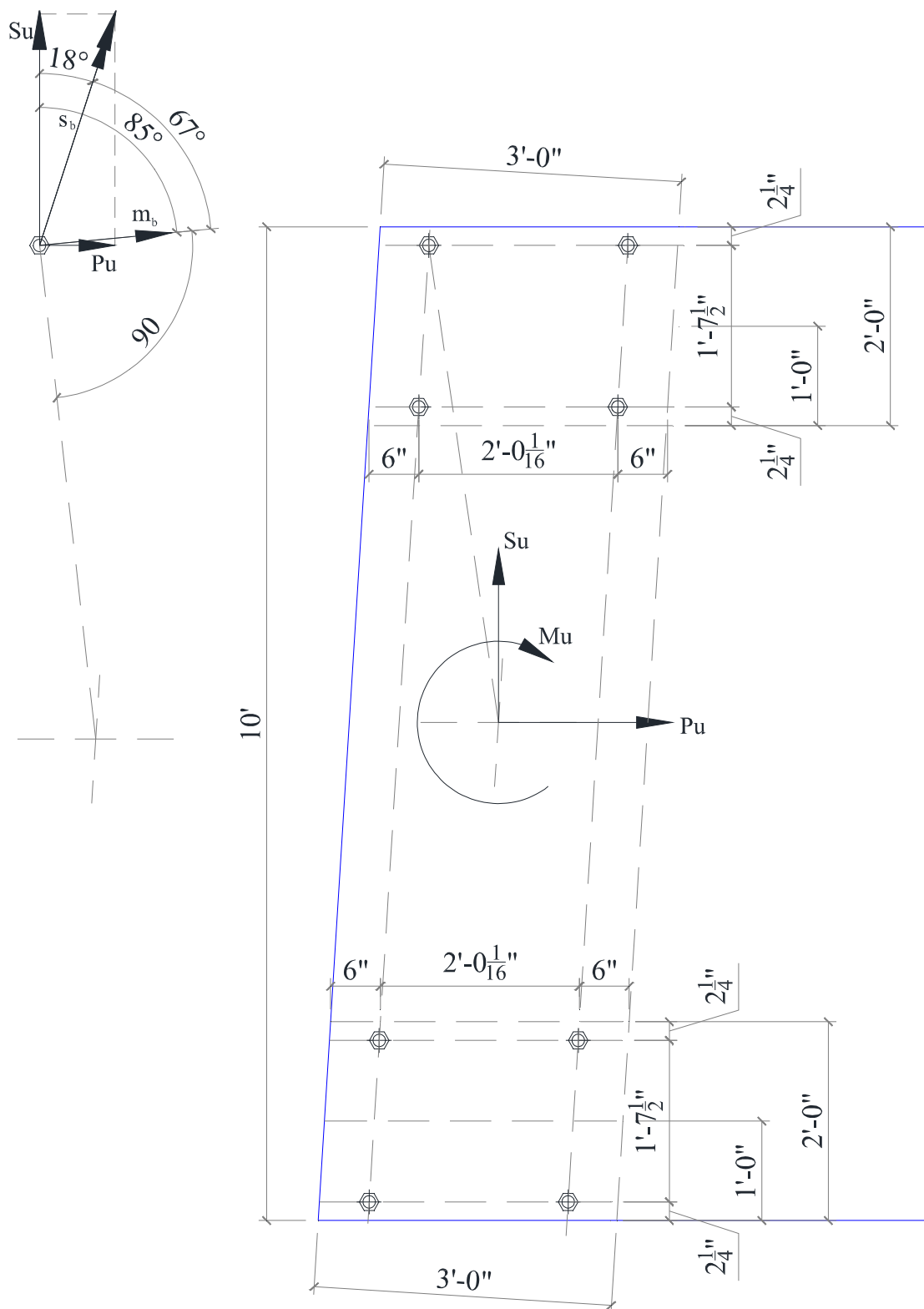


Figure B-12: Panel connection elevation details.

Table B-18: Panels connection properties.

Panel Connection bolts properties					
No. of Bolts	□	Bolt type	Bolt grade	ϕV_n	ϕT_n
	in			Kip	Kip
8	1.50	A490-N	60	79.50	150.00

Table B-19: Panels connection design.

Panel Connection design						
Ultimate Load Combination	Max and Min	Axial	Shear	Moment	Total shear on one bolt	Shear Check
		Kip	Kip	Kip-ft	Kip	
ULT4-C1	Axial	-35.3	45.7	406.2	17.61	Safe
		56.2	13.8	234.5	13.03	Safe
	Shear	-0.9	-172.3	-866.9	43.25	Safe
		1.1	119.0	-659.2	31.48	Safe
	Moment	-0.9	-172.3	-866.9	43.25	Safe
-0.9		-163.3	811.6	40.73	Safe	
ULT4-C2	Axial	-31.2	-31.8	-160.1	9.49	Safe
		46.6	-106.5	-388.0	23.99	Safe
	Shear	-0.9	-119.0	-498.3	27.20	Safe
		0.5	165.5	-786.1	40.30	Safe
	Moment	0.5	165.5	-786.1	40.30	Safe
0.5		156.5	823.7	40.25	Safe	
ULT5-C1	Axial	-15.9	11.8	175.7	7.03	Safe
		37.7	-46.0	-114.6	10.14	Safe
	Shear	-0.4	-68.8	-302.5	16.11	Safe
		-0.4	68.8	-302.5	16.11	Safe
	Moment	-9.3	68.8	-311.2	16.41	Safe
-0.4		59.8	340.2	16.06	Safe	
ULT5-C2	Axial	-20.7	3.9	127.4	5.86	Safe
		40.6	19.5	221.7	11.17	Safe
	Shear	-0.1	-78.7	-376.7	19.24	Safe
		0.3	41.6	-234.5	11.12	Safe
	Moment	-5.3	-78.7	-381.8	19.39	Safe
-0.1		-69.7	365.2	17.88	Safe	

ULT6-C1	Axial	-33.1	47.4	409.2	17.70	Safe
		47.8	14.9	214.1	11.57	Safe
	Shear	-0.8	-171.2	-865.5	43.08	Safe
		1.1	117.8	-658.0	31.32	Safe
	Moment	-0.8	-171.2	-865.5	43.08	Safe
-0.8		-164.5	813.0	40.90	Safe	
ULT6-C2	Axial	-29.0	-30.1	-157.1	9.09	Safe
		38.2	-105.3	-408.7	24.03	Safe
	Shear	-0.9	-117.8	-497.2	27.04	Safe
		0.5	164.4	-784.7	40.13	Safe
	Moment	0.5	164.4	-784.7	40.13	Safe
0.5		157.6	825.2	40.42	Safe	
ULT7-C1	Axial	-13.5	13.6	173.3	6.89	Safe
		29.3	-44.9	-134.9	9.93	Safe
	Shear	-0.4	-67.6	-301.1	15.94	Safe
		-0.4	67.6	-301.1	15.94	Safe
	Moment	-8.0	67.6	-308.5	16.18	Safe
-0.4		60.9	341.6	16.23	Safe	
ULT7-C2	Axial	-18.4	15.0	157.1	6.98	Safe
		32.2	20.6	201.3	9.83	Safe
	Shear	-0.1	-77.6	-375.3	19.07	Safe
		0.3	40.5	-233.1	10.95	Safe
	Moment	-3.9	-77.5	-379.0	19.18	Safe
-0.1		-70.8	366.7	18.05	Safe	

Columns Splice Design:

Column design: 60-0.6" Strands

$$a_{\text{strand}} := 0.217 \text{in}^2$$

$$n_1 := 60$$

$$F_{u,\text{strand}} := 207 \text{ksi}$$

$$F_1 := n_1 \cdot a_{\text{strand}} \cdot F_{u,\text{strand}} = 2.695 \times 10^3 \cdot \text{kip}$$

Use 6 Threaded Bars:

$$F_{\text{bar}} := \frac{F_1}{6} = 449.19 \cdot \text{kip}$$

Use 2-1/4" (57mm) 150 ksi Threaded Bars: $F_u = 613 \text{ kips}$

Table B-20: Base connection design.

Base Connection					
Ultimate Load Combination	Axial	Shear	Moment	Force on bolts	6 - 2 1/4" threaded bars (Fu=613kips)
	Kip	Kip	Kip-ft	Kip	
ULT4-C1	-4398.24	351.68	897.19	-558.30	Safe
	-1379.24	66.73	1085.91	-18.37	Safe
	2384.88	183.99	1012.94	594.77	Safe
ULT4-C2	-742.95	86.00	961.92	63.53	Safe
	-4507.07	319.36	812.39	-592.95	Safe
	1857.41	170.36	915.94	487.96	Safe
ULT5-C1	-222.32	17.55	538.32	67.79	Safe
	-222.32	17.55	538.32	67.79	Safe
	-2947.96	224.12	388.97	-415.57	Safe
ULT5-C2	442.78	52.97	524.91	176.03	Safe
	-2704.52	204.59	420.19	-368.91	Safe
	-1130.87	78.73	527.88	-85.66	Safe
ULT6-C1	-1096.53	51.53	1082.68	28.12	Safe
	2667.60	202.65	1001.04	639.57	1.04
	-4115.53	332.64	911.40	-508.41	Safe
ULT6-C2	-460.23	68.36	962.87	110.83	Safe
	-4224.35	300.42	823.87	-543.59	Safe
	2140.13	189.39	901.70	532.31	Safe
ULT7-C1	60.39	24.26	529.98	113.29	Safe
	60.39	24.26	529.98	113.29	Safe
	-2665.24	205.09	404.80	-365.36	Safe
ULT7-C2	725.50	71.76	511.28	220.50	Safe
	-2421.80	185.57	432.65	-319.37	Safe
	-848.15	60.53	526.21	-38.87	Safe

APPENDIX C

C. 240 FT STEEL TOWER DESIGN

Geometry and Dimensions

Tower Height:	$H_t := 240\text{ft}$
Segment Height:	$H_{\text{seg}} := 80\text{ft}$
Number of Segments:	$N_{\text{seg}} := 3$
Base Outer Diameter:	$D_{\text{base}} := 216\text{in} = 18\text{ft}$
Wall Thickness:	$th_{\text{base}} := 1.8\text{in}$
Top Outer Diameter:	$D_{\text{top}} := 120\text{in} = 10\text{ft}$
Wall Thickness:	$th_{\text{top}} := 1.0\text{in}$

Steel Properties

Steel Yield Stress:	$f_y := 50\cdot\text{ksi}$
Steel Density:	$\rho_s := 490 \frac{\text{lbf}}{\text{ft}^3}$
Steel Elastic Modulus:	$E_s := 28500\text{ksi}$

3.6 MW Wind Turbine

Turbine Head Weight: (<i>WindPACT Report, 2005</i>)	$W_{\text{turbine}} := 694.26\cdot\text{kip}$
--	---

Tower Profile

Variations along the Height:

$$D(z) := D_{\text{top}} + \left(\frac{D_{\text{base}} - D_{\text{top}}}{H_t} \right) \cdot (H_t - z)$$

$$\text{th}(z) := \text{th}_{\text{top}} + \left(\frac{\text{th}_{\text{base}} - \text{th}_{\text{top}}}{H_t} \right) \cdot (H_t - z)$$

$$A_s(z) := \frac{\pi}{4} \cdot [D(z)^2 - (D(z) - 2 \cdot \text{th}(z))^2]$$

$$I_x(z) := \frac{\pi}{64} \cdot [D(z)^4 - (D(z) - 2 \cdot \text{th}(z))^4]$$

$$S(z) := \frac{2 \cdot I_x(z)}{D(z)}$$

$$W(z) := A_s(z) \cdot \rho_s$$

$$R_t(z) := \frac{D(z) - \text{th}(z)}{2}$$

Tower Weights

Miscellaneous Additional Weights:
(Connections, bolts and steel plates)

$$W_{\text{misc}} := 250 \text{kip} \quad (\text{Assumed})$$

Steel Weight:

$$W_t(z) := \int_z^{H_t} W(x) \, dx$$

Total Tower Weight:

$$W_{\text{tot}}(z) := W_{\text{turbine}} + W_t(z) + W_{\text{misc}}$$

$$W_{\text{tot}}(0) = 1.559 \times 10^3 \cdot \text{kip}$$

$$W_{\text{tot}}(0) = 779.476 \cdot \text{tonf}$$

Wind Loading (Mid-West)

Direct Wind on the Tower:

Building Category: II
(ASCE 7-10 - Tbl. 1.5-1)
(Draft 4.4)

Wind Importance Factor: $I := 1.0$
(ASCE 7-10 - Tbl. 1.5-2)

Basic Wind Speed: $V_w := 115 \text{ mph} = 51.41 \cdot \frac{\text{m}}{\text{s}}$
(ASCE 7-10 - Fig. 26.5-1A)

Design Wind Speeds:

Extreme 3-sec gust at reference height (33-ft from ground):

Non Operational Load Case (EWM): $V_1 := 115 \text{ mph}$ Extreme wind speed model
Operational Load Case (EOG): $V_2 := 49.7 \text{ mph}$ Extreme operational gust

At Hub Level:

Non Operational Load Case (EWM): $V_{1_EWM} := \left[V_1 \cdot \left(\frac{33 \text{ ft}}{H_t} \right)^{-0.11} \right] = 143.049 \cdot \text{mph}$

Operational Load Case (EOG): $V_{2_EOG} := \left[V_2 \cdot \left(\frac{33 \text{ ft}}{H_t} \right)^{-0.2} \right] = 73.909 \cdot \text{mph}$

Directional Factor: $K_d := 0.95$
(ASCE 7-10 - Tbl. 26.6-1)

Terrain Exposure Constants:
(ASCE 7-10 - Art. 26.7.3)
(ASCE 7-10 - Tbl. 26.9-1)

Exposure Category: " D "

$$\alpha_{\text{ex}} := 11.5$$

$$c_{\text{ex}} := 0.15$$

$$b_{\text{ex}} := 0.8$$

$$z_{\text{g.ex}} := 700 \text{ ft}$$

$$z_{\text{min.ex}} := 7 \text{ ft}$$

$$l_{\text{ex}} := 650 \text{ ft}$$

$$\varepsilon_{\text{ex}} := \frac{1}{8.0}$$

$$\alpha'_{\text{ex}} := \frac{1}{9.0}$$

Topographic Factor:

(ASCE 7-10 - Art. 26.8)
(No hills)

$$K_{zt} := 1.0$$

Gust-Effects:

Flexible Structure:

(ASCE 7-10 - Art. 26.2)

Equivalent Height of Structure:

(ASCE 7-10 - Eq. 26.9-7)

$$n < 1.0\text{Hz}$$

$$z_{eq} := 0.6 \cdot H_t = 144 \text{ ft} \quad z > z_{\min.ex} \quad \text{ok}$$

Intensity of Turbulence:

(ASCE 7-10 - Eq. 26.9-7)

$$I_z(z) := c_{ex} \left(\frac{33\text{ft}}{z} \right)^{\frac{1}{6}}$$

Integral Length scale of turbulence:

(ASCE 7-10 - Eq. 26.9-9)

$$L_z(z) := l_{ex} \cdot \left(\frac{z}{33\text{ft}} \right)^{\varepsilon_{ex}}$$

Background Response:

(ASCE 7-10 - Eq. 26.9-8)

$$Q(z) := \sqrt{\frac{1}{1 + 0.63 \cdot \left(\frac{D(z) + H_t}{L_z(z)} \right)^{0.63}}}$$

Peak Factor for Background Response:

(ASCE 7-10 - Eq. 26.9-10)

$$g_Q := 3.4$$

Peak Factor for Wind Response:

(ASCE 7-10 - Eq. 26.9-10)

$$g_v := 3.4$$

Natural Frequency of the Tower:

(ASCE 7-10 - Eq. 26.9-4)

$$n_a := \frac{75\text{ft}}{H_t} = 0.313 \quad n_1 = 0.34 \text{ Hz}$$

Peak Factor for Resonant Response:

(ASCE 7-10 - Eq. 26.9-11)

$$g_R := \sqrt{2 \cdot \ln \left(3600 \cdot \frac{n_1}{\text{Hz}} \right)} + \frac{0.577}{\sqrt{2 \cdot \ln \left(3600 \cdot \frac{n_1}{\text{Hz}} \right)}}$$

$$g_R = 3.902$$

Mean Hourly Velocity:

(ASCE 7-10 - Eq. 26.9-16)

$$V_z(z, v) := b_{ex} \cdot \left(\frac{z}{33\text{ft}} \right)^{\alpha'_{ex}} \cdot \left(\frac{88}{60} \right) \cdot v$$

$$V_z(z_{eq}, V_1) = 158.933 \cdot \text{mph} \quad (\text{EWM})$$

$$V_z(z_{eq}, V_2) = 68.687 \cdot \text{mph} \quad (\text{EOG})$$

Reduced Frequency:

(ASCE 7-10 - Eq. 26.9-14)

$$N_1(z, v) := \frac{n_1 \cdot L_z(z)}{V_z(z, v)}$$

$$N_1(z_{eq}, V_1) = 1.048 \quad (\text{EWM})$$

$$N_1(z_{eq}, V_2) = 2.424 \quad (\text{EOG})$$

Damping Factor: $\beta := 2\%$ (ASCE-AWEA - Art. 5.4.4)

Resonant Response Factor: (ASCE 7-10 - Eq. 26.9-12)

$$\eta_{Rh}(z, v) := 4.6 \cdot n_1 \cdot \frac{H_t}{V_z(z, v)} \quad (\text{ASCE 7-10 - Eq. 26.9-15a})$$

$$\eta_{RB}(z, v) := 4.6 \cdot n_1 \cdot \frac{D(z)}{V_z(z, v)} \quad (\text{ASCE 7-10 - Eq. 26.9-15a})$$

$$\eta_{RL}(z, v) := 4.6 \cdot n_1 \cdot \frac{D(z)}{V_z(z, v)} \quad (\text{ASCE 7-10 - Eq. 26.9-15a})$$

$$R_h(z, v) := \frac{1}{\eta_{Rh}(z, v)} - \frac{\left[1 - e^{(-2 \cdot \eta_{Rh}(z, v))}\right]}{2(\eta_{Rh}(z, v))^2} \quad R_h(z_{eq}, V_1) = 0.459$$

$$R_h(z_{eq}, V_2) = 0.249$$

$$R_B(z, v) := \frac{1}{\eta_{RB}(z, v)} - \frac{\left[1 - e^{(-2 \cdot \eta_{RB}(z, v))}\right]}{2(\eta_{RB}(z, v))^2} \quad R_B(z_{eq}, V_1) = 0.948$$

$$R_B(z_{eq}, V_2) = 0.885$$

$$R_L(z, v) := \frac{1}{\eta_{RL}(z, v)} - \frac{\left[1 - e^{(-2 \cdot \eta_{RL}(z, v))}\right]}{2(\eta_{RL}(z, v))^2} \quad R_L(z_{eq}, V_1) = 0.948$$

$$R_L(z_{eq}, V_2) = 0.885$$

$$R_n(z, v) := \frac{7.47 \cdot N_1(z, v)}{\frac{5}{(1 + 10.3 \cdot N_1(z, v))^3}} \quad (\text{ASCE 7-10 - Eq. 26.9-13})$$

$$R_n(z_{eq}, V_1) = 0.128$$

$$R_n(z_{eq}, V_2) = 0.08$$

$$R_{\text{eff}}(z, v) := \sqrt{\frac{1}{\beta} \cdot R_n(z, v) \cdot R_h(z, v) \cdot R_B(z, v) \cdot (0.53 + 0.47 \cdot R_L(z, v))} \quad (\text{ASCE 7-10 - Eq. 26.9-12})$$

$$R(z_{eq}, V_1) = 1.649$$

$$R(z_{eq}, V_2) = 0.911$$

Gust - Effect Factor:

(ASCE 7-10 - Eq. 26.9-10)

$$G_f(z, v) := 0.925 \cdot \left(\frac{1 + 1.7 \cdot I_z(z) \cdot \sqrt{g_Q^2 \cdot Q(z)^2 + g_R^2 \cdot R(z, v)^2}}{1 + 1.7 \cdot g_v \cdot I_z(z)} \right)$$

$$G_f(z_{eq}, V_1) = 1.331$$

$$G_f(z_{eq}, V_2) = 1.061$$

Enclosure Classification:
(ASCE 7-10 - Art. 26.10)

Enclosed Building (Openings less than 10 %)

Velocity Pressure Coefficient:
(ASCE 7-10 - Tbl. 29.3-1)

$$K_z(z) := \begin{cases} 2.01 \cdot \left(\frac{15\text{ft}}{z_{g,ex}}\right)^{\frac{2}{\alpha_{ex}}} & \text{if } z < 15\text{ft} \\ 2.01 \cdot \left(\frac{z}{z_{g,ex}}\right)^{\frac{2}{\alpha_{ex}}} & \text{if } 15\text{ft} \leq z \leq z_{g,ex} \end{cases}$$

(ASCE 7-10 - Eq. 29.3-1) $q_z(z, v) := K_z(z) \cdot K_{zt} \cdot K_d \cdot \left(\frac{v}{\text{mph}}\right)^2 \cdot 0.00256 \cdot (\text{psf})$

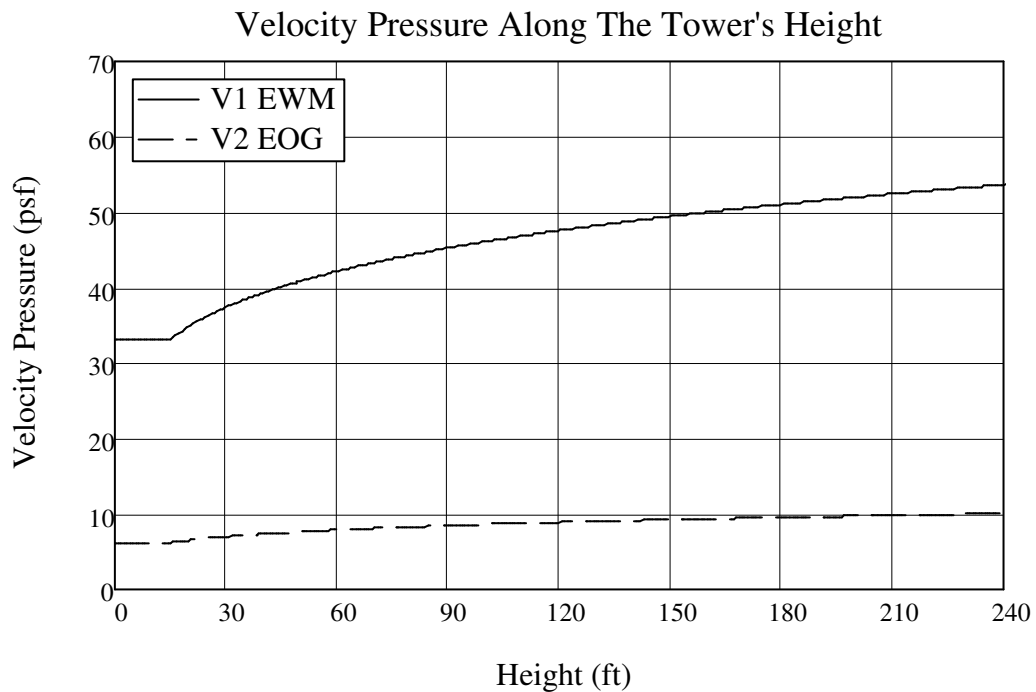


Figure C-1: Velocity pressure along the tower's height.

Force Coefficient:
(ASCE 7-10 - Tbl. 29.5-1)

$$\frac{H_t}{D(0)} = 13.333$$

Table C-1: Force coefficient for the circular tower*.

Cross Section	h/D**			h/D=13.33
	1	7	25	
Round	0.5	0.6	0.7	0.64

* Based on ASCE-07 Table 29.5-1 for moderately smooth towers

** h : Tower Height

** D : Least Structure Dimension

$$C_f := 0.64$$

Force along the Tower:
(ASCE 7-10 - Eq. 29.5-1)

$$F := q_z \cdot G_f \cdot C_f \cdot A_f$$

$$F_w(z, v) := q_z(z, v) \cdot G_f(z, v) \cdot C_f \cdot D(z) \quad dz$$

Shearing Force along the Tower:

$$S_w(z, v) := \int_z^{H_t} F_w(x, v) \, dx$$

Base Shear (EWM):

$$S_w(0, V_1) = 129.241 \cdot \text{kip}$$

Base Shear (EOG):

$$S_w(0, V_2) = 19.091 \cdot \text{kip}$$

Bending Moment along the Tower:

$$M_w(z, v) := \int_z^{H_t} F_w(x, v) \cdot (x - z) \, dx$$

Base Moment (EWM):

$$M_w(0, V_1) = 1.517 \times 10^4 \cdot \text{kip} \cdot \text{ft}$$

Base Moment (EOG):

$$M_w(0, V_2) = 2.259 \times 10^3 \cdot \text{kip} \cdot \text{ft}$$

Wind Turbine Load: (WindPact Report)

Coordinate System: x : Downwind, y : Lateral, and z : Gravity.

Turbine Offset: offset := 0ft

Straining Actions on Top of the Tower:

$F_{x.T.V1} := 143\text{kip}$	$F_{x.T.V2} := 269\text{kip}$
$F_{y.T.V1} := 198\text{kip}$	$F_{y.T.V2} := 18\text{kip}$
$F_{z.T.V1} := 709\text{kip}$	$F_{z.T.V2} := 703\text{kip}$
$M_{x.T.V1} := 10458\text{kip}\cdot\text{ft}$	$M_{x.T.V2} := 3143\text{kip}\cdot\text{ft}$
$M_{y.T.V1} := 6601\text{kip}\cdot\text{ft}$	$M_{y.T.V2} := 6601\text{kip}\cdot\text{ft}$
$M_{z.T.V1} := 2534\text{kip}\cdot\text{ft}$	$M_{z.T.V2} := 1178\text{kip}\cdot\text{ft}$

Fatigue Range:

$\Delta F_{x.T} := 32\text{kip}$	$\Delta M_{z.T} := 1637\text{kip}\cdot\text{ft}$
$\Delta M_{x.T} := 319\text{kip}\cdot\text{ft}$	$\Delta M_{y.T} := 1600\text{kip}\cdot\text{ft}$

Extreme 3-sec gust at reference height (33-ft from ground):

(ASCE 7-05 - Fig. 6-1) $V_{mw} := 40 \frac{\text{m}}{\text{s}}$

Reference wind speed over 10 min at hub height:

(ASCE/AWEA-RP2011 - Eq. C5-6) $V_{ref} := V_{mw} \cdot \left(\frac{H_t}{z_{g.ex}} \right)^{\alpha_{ex}} = 36.445 \cdot \frac{\text{m}}{\text{s}}$

Extreme 3-sec gust at hub height:

(ASCE/AWEA-RP2011 - Eq. C5-4) $V_{e50}(z) := 1.4 \cdot V_{ref} \cdot \left(\frac{z}{H_t} \right)^{0.11}$

$$V_{e50}(240\text{ft}) = 51.023 \cdot \frac{\text{m}}{\text{s}}$$

Class II wind Turbine:

(ASCE/AWEA-RP2011 - Eq. C5-4) $V_t := 59.5 \frac{\text{m}}{\text{s}}$

Speed Modification Factor:

$$c_{sa} := \left(\frac{V_{e50}(240\text{ft})}{V_t} \right)^2 = 0.735$$

Take $c_{sa} := 0.75$

Wind Turbine Load Distribution along the Tower:

$$F_{x.V1} := F_{x.T.V1} \cdot c \qquad F_{x.V2} := F_{x.T.V2}$$

$$F_{y.V1} := F_{y.T.V1} \cdot c \qquad F_{y.V2} := F_{y.T.V2}$$

$$F_{z.V1} := F_{z.T.V1} \cdot c \qquad F_{z.V2} := F_{z.T.V2}$$

$$M_{x.V1}(z) := M_{x.T.V1} \cdot c + F_{y.V1} \cdot (H_t - z)$$

$$M_{x.V2}(z) := M_{x.T.V2} + F_{y.V2} \cdot (H_t - z)$$

$$M_{y.V1}(z) := M_{y.T.V1} \cdot c + F_{x.V1} \cdot (H_t - z)$$

$$M_{y.V2}(z) := M_{y.T.V2} + F_{x.V2} \cdot (H_t - z)$$

$$M_{z.V1}(z) := M_{z.T.V1} \cdot c$$

$$M_{z.V2}(z) := M_{z.T.V2}$$

$$\Delta M_t(z) := \sqrt{(\Delta M_{x.T})^2 + (\Delta M_{y.T})^2}$$

$$\Delta M(z) := \Delta M_t(z) + \Delta F_{x.T} \cdot (H_t - z)$$

$$F_{T.V1}(z) := \sqrt{F_{x.V1}^2 + (F_{y.V1} + S_w(z, V_1))^2}$$

$$F_{T.V2}(z) := \sqrt{F_{x.V2}^2 + (F_{y.V2} + S_w(z, V_2))^2}$$

$$M_{T.V1}(z) := \sqrt{M_{x.V1}(z)^2 + (M_{y.V1}(z) + M_w(z, V_1))^2}$$

$$M_{T.V2}(z) := \sqrt{M_{x.V2}(z)^2 + (M_{y.V2}(z) + M_w(z, V_2))^2}$$

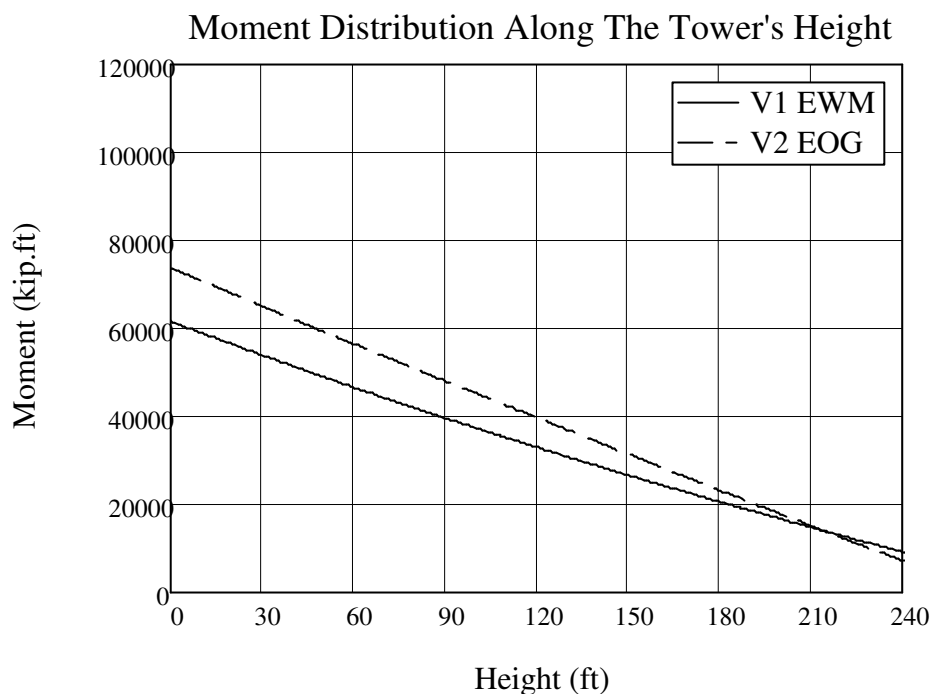


Figure C-2: Moment distribution along the tower's height.

Seismic Loading (Mid-West)

Seismic Importance Factor: (ASCE 7-10 - Tbl. 1.5-2)	$I = 1$	
Site Class: (ASCE 7-10 - Art. 11.4.2)	Soil Class "D"	
Damping Adjustment Factor: (ASCE-AWEA - Tbl. 5-6)	$B := 1.23$	
Mapped Acceleration Parameters: (ASCE 7-10 - Fig. 22-1 and 22-2)	$S_s := 0.12 \cdot B$	$S_1 := 0.05 \cdot B$
Site Coefficient: (ASCE 7-10 - Tbl. 11.4-1 and 11.4-2)	$F_a := 1.6$	$F_v := 2.4$
Spectral response acceleration for short period: (ASCE 7-10 - Eq. 11.4-1)	$S_{MS} := F_a \cdot S_s = 0.236$	
Spectral response acceleration for 1 second: (ASCE 7-10 - Eq. 11.4-2)	$S_{M1} := F_v \cdot S_1 = 0.148$	
Design Spectral Acceleration Parameters: (ASCE 7-10 - Eq. 11.4-3 and 11.4-4)	$S_{DS} := \frac{2}{3} \cdot S_{MS} = 0.157$	
	$S_{D1} := \frac{2}{3} \cdot S_{M1} = 0.098$	

Design Response Spectrum:
(ASCE 7-10 - Eq. 11.4-5 to 11.4-7)

$$T_S := \frac{S_{D1}}{S_{DS}} = 0.625$$

$$T_0 := 0.2 \frac{S_{D1}}{S_{DS}} = 0.125$$

$$T_L := 12$$

$$S_a(T) := \begin{cases} S_{DS} \cdot \left(0.4 + 0.6 \cdot \frac{T}{T_0} \right) & \text{if } T < T_0 \\ S_{DS} & \text{if } T_0 \leq T \leq T_S \\ \frac{S_{D1}}{T} & \text{if } T_S < T \leq T_L \\ \frac{S_{D1} \cdot T_L}{T^2} & \text{if } T_L < T \end{cases}$$

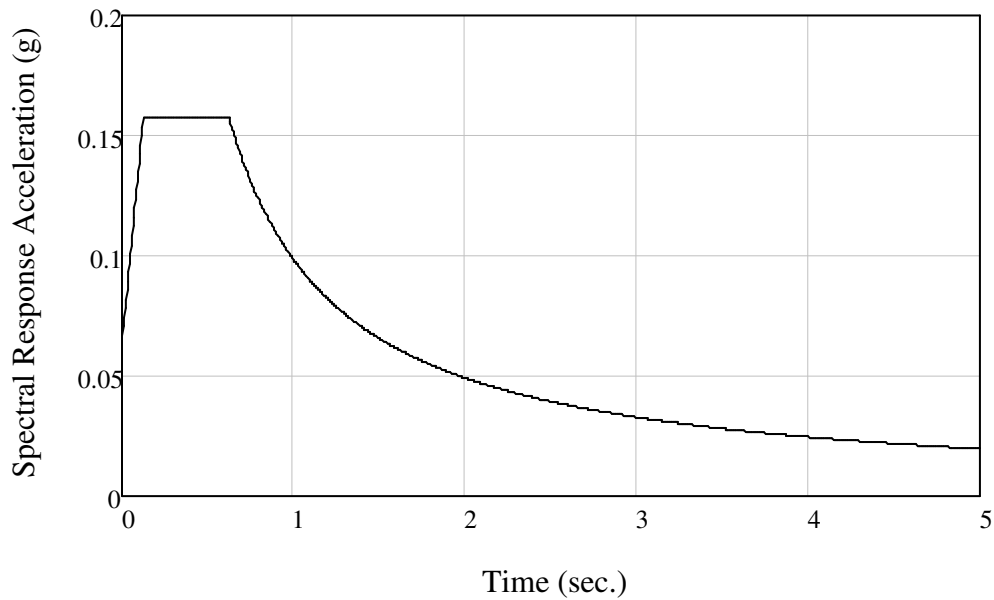


Figure C-3: Design Response spectrum.

Response Modification Coefficient:
(ASCE 7-10 - Tbl. 12.2-1)

$$R := 1.5$$

Seismic Response Coefficient:
(ASCE 7-10 - Eq. 12.8-2 to 12.8-5)

$$C_{s,\text{lim}}(T) := \begin{cases} \frac{S_{D1}}{T \cdot \left(\frac{R}{I}\right)} & \text{if } T \leq T_L \\ \frac{S_{D1} \cdot T_L}{T^2 \cdot \left(\frac{R}{I}\right)} & \text{if } T > T_L \end{cases}$$

$$C_{\text{sn}} := \frac{S_{DS}}{\left(\frac{R}{I}\right)} = 0.105$$

$$C_s(T) := \begin{cases} 0.051 & \text{if } 0.051 < C_{s,\text{lim}}(T) \\ 0.01 & \text{if } C_{s,\text{lim}}(T) < 0.01 \\ C_{s,\text{lim}}(T) & \text{otherwise} \end{cases}$$

Seismic Base Shear:
(ASCE 7-10 - Eq. 12.8-1)

$$V_{\text{eq}}(z) := C_{\text{sn}} \cdot W_{\text{tot}}(z)$$

Percentage of Wind to Seismic Force:

$$\frac{F_{T,V1}(0)}{V_{\text{eq}}(0)} = 1.82$$

P-M effect:

Tower Deflection:

$$\Delta(z) := \int_0^z \frac{M_{T,V1}(x)}{E_s \cdot I_x(x)} \cdot (z-x) dx$$

$$\Delta(240\text{ft}) = 1.701 \text{ ft}$$

Additional Moment from deflection: $M_{\text{add}} := W_{\text{turbine}} \cdot \Delta(240\text{ft}) = 1.181 \times 10^3 \cdot \text{kip}\cdot\text{ft}$

Percentage of added moment: $\delta_{\text{add}} := \frac{M_{\text{add}}}{M_{T,V1}(0)} = 0.019$

Negligible effect

Load Combinations:

(ASCE 7-10 - Art. 2.3.2 and 2.4.1)
(ASCE/AWEA-RP2011 - Tbl. 5-4)

Ultimate Loads:

ULT 4:	1.2D +1.0W+1.35T
ULT 5:	1.2D +1.0E
ULT 6:	0.9D +1.0W+1.35T
ULT 7:	0.9D +1.0E

Service Loads:

SER 5-1:	D +0.6W+1.0T
SER 5-2:	D +0.7E
SER 7:	0.6D +0.6W+1.0T
SER 8:	0.6D +0.7E

Ultimate Load:

Load Factors:	$\gamma_{DL,umax} := 1.2$
	$\gamma_{DL,umin} := 0.9$
	$\gamma_{WLu} := 1.0$
	$\gamma_{TLu} := 1.35$

Service Load:

Load Factors:	$\gamma_{DL,smax} := 1.0$
	$\gamma_{DL,smin} := 0.6$
	$\gamma_{WLS} := 0.6$

Ultimate Load (EWM):

$$P_u(z, \gamma_{DL}) := \gamma_{DL}(W_{tot}(z))$$

$$V_u(z) := \sqrt{(\gamma_{TLu} \cdot F_{x,V1})^2 + (\gamma_{TLu} \cdot F_{y,V1} + \gamma_{WLu} \cdot S_w(z, V_1))^2}$$

$$M_u(z) := \sqrt{(\gamma_{TLu} \cdot M_{x,V1}(z))^2 + (\gamma_{TLu} \cdot M_{y,V1}(z) + \gamma_{WLu} \cdot M_w(z, V_1))^2}$$

$$M_{z,u}(z) := \gamma_{TLu} \cdot M_{z,V1}(z)$$

Service Load (EWM):

$$P_s(z, \gamma_{DL}) := \gamma_{DL}(W_{tot}(z))$$

$$V_s(z) := \sqrt{(F_{x,V1})^2 + (F_{y,V1} + \gamma_{WLS} \cdot S_w(z, V_1))^2}$$

$$M_s(z) := \sqrt{(M_{x,V1}(z))^2 + (M_{y,V1}(z) + \gamma_{WLS} \cdot M_w(z, V_1))^2}$$

$$M_{z,s}(z) := M_{z,V1}(z)$$

Operation Load (EOG):

$$P_o(z, \gamma_{DL}) := \gamma_{DL}(W_{tot}(z))$$

$$V_o(z) := \sqrt{(F_x \cdot V_2)^2 + (F_y \cdot V_2 + \gamma_{WLS} \cdot S_w(z, V_2))^2}$$

$$M_o(z) := \sqrt{(M_x \cdot V_2(z))^2 + (M_y \cdot V_2(z) + \gamma_{WLS} \cdot M_w(z, V_2))^2}$$

$$M_{z,o}(z) := M_z \cdot V_2(z)$$

Straining Actions at Base:

Ultimate Load (EWM):

$$P_u(0, \gamma_{DL,umax}) = 1.871 \times 10^3 \cdot \text{kip}$$

$$P_u(0, \gamma_{DL,umin}) = 1.403 \times 10^3 \cdot \text{kip}$$

$$V_u(0) = 360.105 \cdot \text{kip}$$

$$M_u(0) = 8.155 \times 10^4 \cdot \text{kip}\cdot\text{ft}$$

$$M_{z,u}(0) = 2.566 \times 10^3 \cdot \text{kip}\cdot\text{ft}$$

Service Load (EWM):

$$P_s(0, \gamma_{DL,smax}) = 1.559 \times 10^3 \cdot \text{kip}$$

$$P_s(0, \gamma_{DL,smin}) = 935.371 \cdot \text{kip}$$

$$V_s(0) = 250.197 \cdot \text{kip}$$

$$M_s(0) = 5.894 \times 10^4 \cdot \text{kip}\cdot\text{ft}$$

$$M_{z,s}(0) = 1.901 \times 10^3 \cdot \text{kip}\cdot\text{ft}$$

Operation Load (EOG):

$$P_o(0, \gamma_{DL,smax}) = 1.559 \times 10^3 \cdot \text{kip}$$

$$P_o(0, \gamma_{DL,smin}) = 935.371 \cdot \text{kip}$$

$$V_o(0) = 270.608 \cdot \text{kip}$$

$$M_o(0) = 7.29 \times 10^4 \cdot \text{kip}\cdot\text{ft}$$

$$M_{z,o}(0) = 1.178 \times 10^3 \cdot \text{kip}\cdot\text{ft}$$

Tower Design (ASD):

Axial Stress:
$$f_{a.\max}(z) := \frac{P_s(z, \gamma \text{DL.smax})}{A_s(z)}$$

$$f_{a.\max}(0) = 1.279 \cdot \text{ksi}$$

$$f_{a.\min}(z) := \frac{P_s(z, \gamma \text{DL.smin})}{A_s(z)}$$

$$f_{a.\min}(0) = 0.767 \cdot \text{ksi}$$

Bending Stress:
$$f_b(z) := \frac{M_s(z)}{S(z)}$$

$$f_b(0) = 10.995 \cdot \text{ksi}$$

Shear Stress:
$$f_v(z) := \frac{V_s(z)}{\pi \cdot \text{th}(z) \cdot R_t(z)}$$

$$f_v(0) = 0.413 \cdot \text{ksi}$$

Shear Stress from Torsion:
$$f_{vt}(z) := \frac{M_{z.s}(z) \cdot D(z)}{4 \cdot I_x(z)}$$

$$f_{vt}(0) = 0.177 \cdot \text{ksi}$$

Max and Min Normal Stress:
$$f_{n.\max}(z) := f_{a.\max}(z) + f_b(z)$$

$$f_{n.\max}(0) = 12.274 \cdot \text{ksi}$$

$$f_{n.\min}(z) := f_{a.\min}(z) - f_b(z)$$

$$f_{n.\min}(0) = -10.228 \cdot \text{ksi}$$

Max Shear Stress:
$$f_{v.\max}(z) := f_v(z) + f_{vt}(z)$$

$$f_{v.\max}(0) = 0.59 \cdot \text{ksi}$$

Combined Stress:
$$\sigma_w(z) := \sqrt{(f_{n.\max}(z))^2 + 3 \cdot (f_{v.\max}(z))^2}$$

$$\sigma_w(0) = 12.317 \cdot \text{ksi}$$

Allowable Bending Stress: $F_{b.all} := 0.6 \cdot f_y = 30 \cdot \text{ksi}$

Allowable Shear Stress: $F_{v.all} := 0.4 \cdot f_y = 20 \cdot \text{ksi}$

Allowable Compressive Stress: $k := 2$

$$r(z) := \sqrt{\frac{I_x(z)}{A_s(z)}}$$

$$KLr := k \cdot \frac{(H_t)}{r(0)} = 76.056$$

$$Cc := \sqrt{\frac{2 \cdot \pi^2 \cdot E_s}{f_y}} = 106.072$$

$$F_{c.all} := \begin{cases} \frac{\left[\left(1 - \frac{KLr^2}{2 \cdot Cc^2} \right) \cdot f_y \right]}{\frac{5}{3} + \frac{3 \cdot KLr}{8 \cdot Cc} - \frac{KLr^3}{8 \cdot Cc^3}} & \text{if } KLr \leq Cc \\ \frac{12 \cdot \pi^2 \cdot E_s}{23 \cdot KLr^2} & \text{otherwise} \end{cases}$$

$$F_{c.all} = 19.66 \cdot \text{ksi}$$

Check Design:

$$\text{Compression}(z) := \frac{f_{a.max}(z)}{F_{c.all}}$$

$$\text{Shear}(z) := \frac{f_{v.max}(z)}{F_{v.all}}$$

$$\text{Combined}(z) := \frac{f_{a.max}(z)}{F_{c.all}} + \frac{f_b(z)}{F_{b.all}}$$

Check Buckling Stresses:

Elastic Tube Buckling:

$$\sigma_{cr}(z) := 0.605 \cdot E_s \cdot \frac{2 \cdot th(z)}{D(z)}$$

Reduction Coefficient for Axial:

$$\alpha_0(z) := \begin{cases} \frac{0.83}{\sqrt{1 + 0.01 \cdot \frac{D(z)}{2 \cdot th(z)}}} & \text{if } \frac{D(z)}{2 \cdot th(z)} < 212 \\ \frac{0.7}{\sqrt{1 + 0.01 \cdot \frac{D(z)}{2 \cdot th(z)}}} & \text{if } \frac{D(z)}{2 \cdot th(z)} \geq 212 \end{cases}$$

Reduction Coefficient for Bending:

$$\alpha_B(z) := 0.1887 + 0.8113 \cdot \alpha_0(z)$$

Combined Buckling Stress:

$$\sigma_u(z) := \begin{cases} fy \cdot \left[1 - 0.4123 \cdot \left(\frac{fy}{\alpha_B(z) \cdot \sigma_{cr}(z)} \right)^{0.6} \right] & \text{if } \alpha_B(z) \cdot \sigma_{cr}(z) > \frac{fy}{2} \\ (0.75 \cdot \alpha_B(z) \cdot \sigma_{cr}(z)) & \text{if } \alpha_B(z) \cdot \sigma_{cr}(z) \leq \frac{fy}{2} \end{cases}$$

$$DCR_b(z) := \frac{\sigma_u(z)}{fy}$$

Steel Fatigue Design:

Fatigue Moment:

$$M_f(z) := \Delta M(z)$$

Design Cycle:

$$nf := 5.29 \cdot 10^8$$

$$\gamma_{ss} := 1.265$$

$$\Delta\sigma_y := 310 \text{MPa}$$

Initial Cycle:

$$N_0 := 10000$$

Slope of the curve:

$$m := 4$$

Yielding Moment: $M_{fs}(z) := \Delta\sigma_y \cdot S(z)$

Extrapolated Yielding Moment: $M_{ss}(z) := M_{fs}(z) \cdot \sqrt[m]{N_0}$

Number of Cycles at Applied Moment: $N_f(z) := \left(\frac{M_f(z) \cdot \gamma_{ss}}{\Delta\sigma_y \cdot S(z) \cdot \sqrt[m]{N_0}} \right)^{-m}$

$fat(z) := \frac{nf}{N_f(z)}$

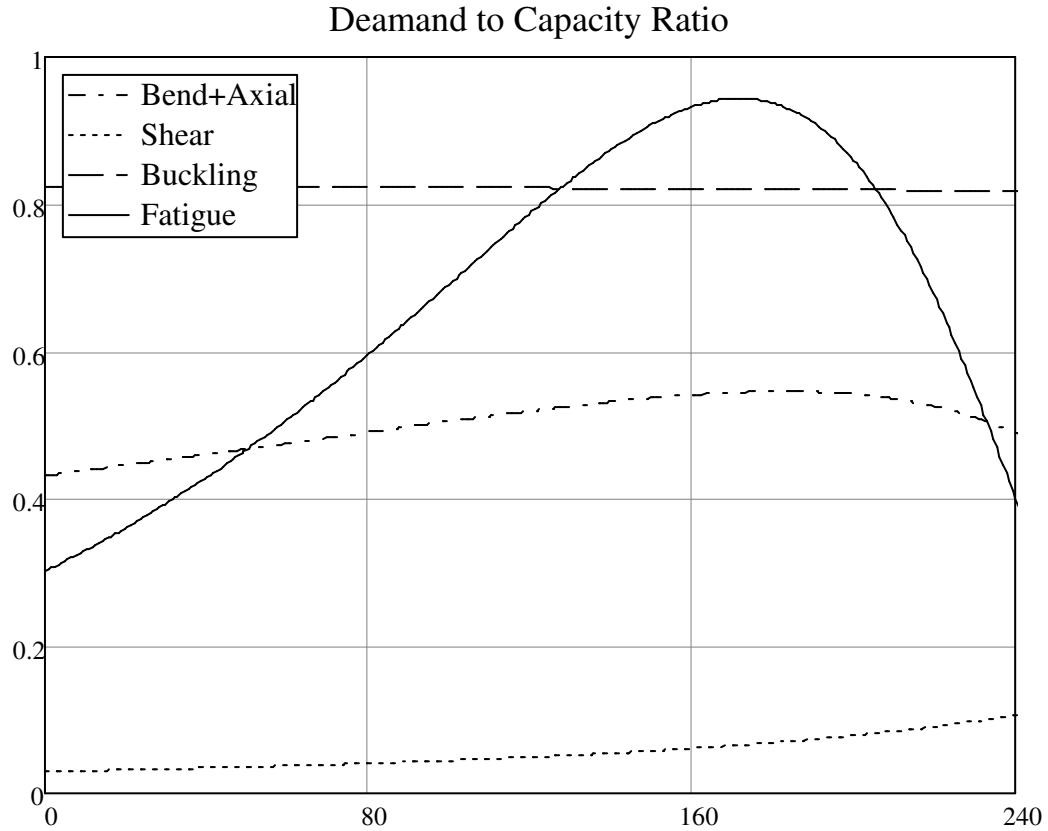


Figure C-4: Demand to capacity ratio.

APPENDIX D

D. DYNAMIC ANALYSIS

APPROACH

To properly determine the dynamic behavior of the proposed tower, a proper model has to be constructed. There are a lot of methods and numerical models available for choosing and using a wrong approach can either sacrifice accuracy or falsely represent the dynamic properties of the tower. Two different approaches were taken to provide a better understanding of the tower behavior under dynamic loading; the first method is modal analysis of a simplified lumped mass system, the second is a finite element method. The next paragraph states the assumptions that apply for the two models, individual approximations concerning a specific model will be stated separately.

The wind turbine will be modeled as stationary mass on top of the tower. Concrete used for the design have a 28 day compressive strength of 8 (*ksi*) and a modulus of elasticity of 5422 (*ksi*). Wilson damping was used for all the models, constant at 2% for each node. All models have a linear elastic response that allows the use of modal superposition.

LUMPED MASS MODEL

This section covers the first approach taken when modeling the tower; it considers the tower as a number of lumped masses concentrated at discrete nodes which are connected by massless bending element. Discretizing the tower into nodes was easy as a result of the tapered profile of the tower. As shown in Figure D-1, the tower was divide into four segments each has its own weight plus the weight of the turbine on top, which gives five masses and connecting elements. Table D-1 shows the properties of the lumped mass model for both towers.

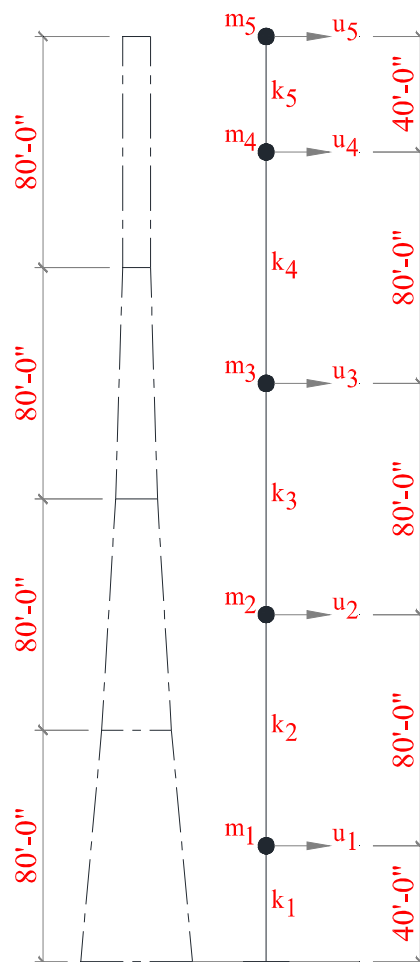


Table D-1: Lumped mass model properties.

Figure D-1: Lumped mass model.

Seg.	Triangular		Circular	
	Mass (kip-s ² /in)	Inertia (in ⁴)	Mass (kip-s ² /in)	Inertia (in ⁴)
1	2.51	312 x 10 ⁶	3.96	485 x 10 ⁶
2	1.93	133 x 10 ⁶	2.44	159 x 10 ⁶
3	1.58	44 x 10 ⁶	1.52	34 x 10 ⁶
4	1.46	20 x 10 ⁶	1.22	10 x 10 ⁶
5	1.79	20 x 10 ⁶	1.79	10 x 10 ⁶

Table D-2: Modal properties.

System	Triangular (proposed)				Circular (current)			
Mode	1	2	3	4	1	2	3	4
Natural period (s)	2.37	0.39	0.14	0.09	2.56	0.43	0.17	0.10
Mode Shapes								
Effective modal masses and heights								
Top deflection contribution	98 %	1.3 %	0.3 %	0 %	98 %	1.7 %	0.08 %	0 %
Base shear contribution	65 %	22.2 %	9.4 %	3.4 %	55.4 %	25.7 %	12.6 %	6.3 %
Base moment contribution	84 %	12.1 %	3.0 %	0.8 %	76.7 %	16.6 %	4.8 %	1.9 %

Analysis of the model was done using modal analysis where the total response is the superposition of the five modal responses. The modal properties were determined and the modal contributions for each mode were calculated. Table D-2 provides a comparison of both towers modal properties. It is to be noted that the fifth mode was not included in the comparison as it didn't contribute to the response. The two systems have very similar mode shapes. The circular system has slightly higher periods than the triangular one which means that it is more flexible. As for modal contribution, the first mode contribute more to the triangular system's response due to the higher effective modal mass and base straining actions contribution, however the rest of the modes contribute more to the circular system's response.

After calculating the modal properties, a time history analysis was performed to determine the response histograms of the model when subjected to the ground motion of El Centro earthquake 1940 North South Component (Peknold Version). Two models for each system were constructed to increase the level of confidence in the results; the first using a MATLAB code along with a numerical method to solve for each time step, the second using SAP 2000 and imputing the earthquake acceleration as a time history function.

The numerical method implemented in this study is "Central Difference Method". It is based on a finite difference approximation of the time derivatives of displacement, i.e. velocity and acceleration. Taking constant time steps and solving for the time derivatives each step by using the difference from the preceding and succeeding time step. This

method was chosen due to its accuracy and simplicity. Figure D-2 and Figure D-3 show the modal and total top deflection of both systems under the seismic acceleration. Table 2 shows the total responses from MATLAB and SAP.

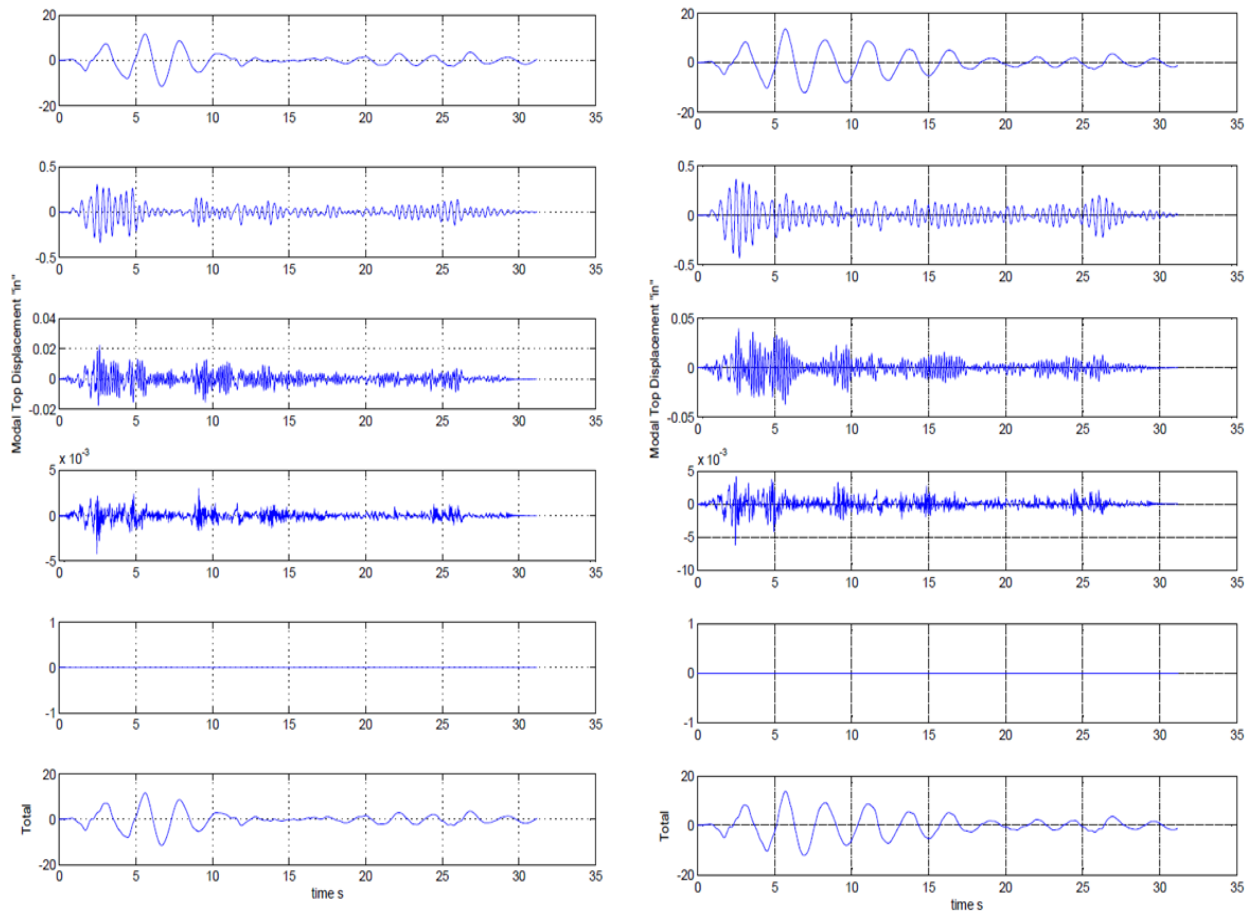


Figure D-2: Modal and total top deflection for triangular (left) and circular (right) tower.

(MATLAB model)

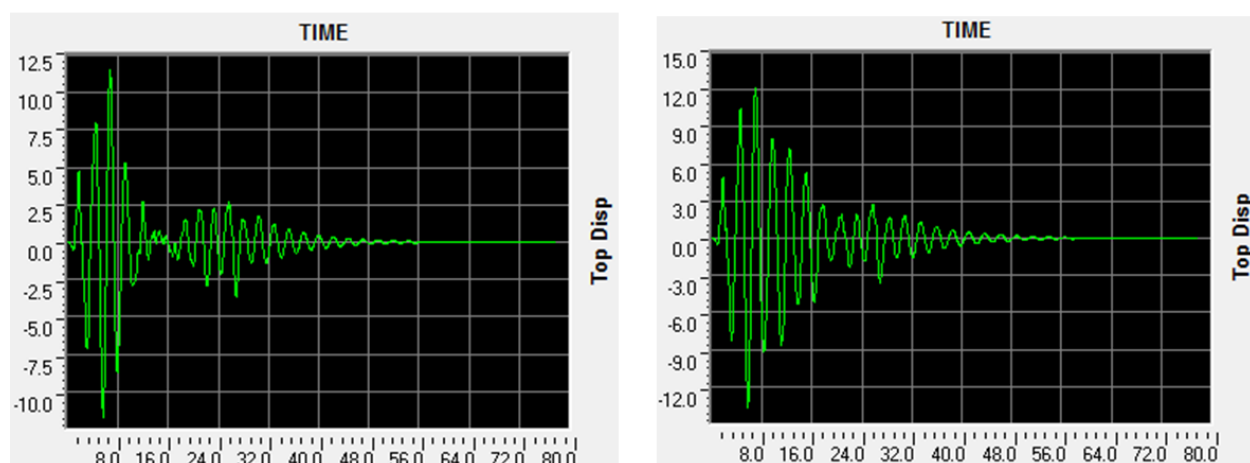


Figure D-3: Modal and total top deflection for triangular (left) and circular (right) tower.

(SAP model)

Table D-3: MATLAB and SAP result comparison.

Seg.	Triangular			Circular		
	Top Displacement (in)	Base Shear (Kip)	Base Moment (kip-ft)	Top Displacement (in)	Base Shear (Kip)	Base Moment (kip-ft)
MATLAB	11.73	839.9	12×10^4	13.70	1076.6	14×10^4
SAP 2000	11.72	959.4	12×10^4	13.70	1134.0	14.4×10^4

As shown in Table D-3 the two models are working as expected providing close results.

It is to be noted that the peak modal contribution to any response happens at the same time as the peak acceleration; however the peak total response happens at a different time instants. Moreover the peak of different responses also happens at different time instants; i.e. the peak base shear doesn't happen at the same time as the peak base moment which has to be considered in design.

Due to the fact that the circular system is more flexible than the triangular system, the latter has a better overall response in terms of deflection, vibrations and base straining actions. As a result the triangular system will perform better than the circular one when subjected to the same dynamic motion.

FINITE ELEMENT METHOD

This method is a finite element analysis in SAP 2000, using the time history function to solve for the response at every time step. This three dimensional model will consider all the interaction between the columns and the panels and will give the most accurate results. Figure D-2 shows the finite element model and the discretization of the tower. Figure 9 shows the first different mode shapes of the tower.

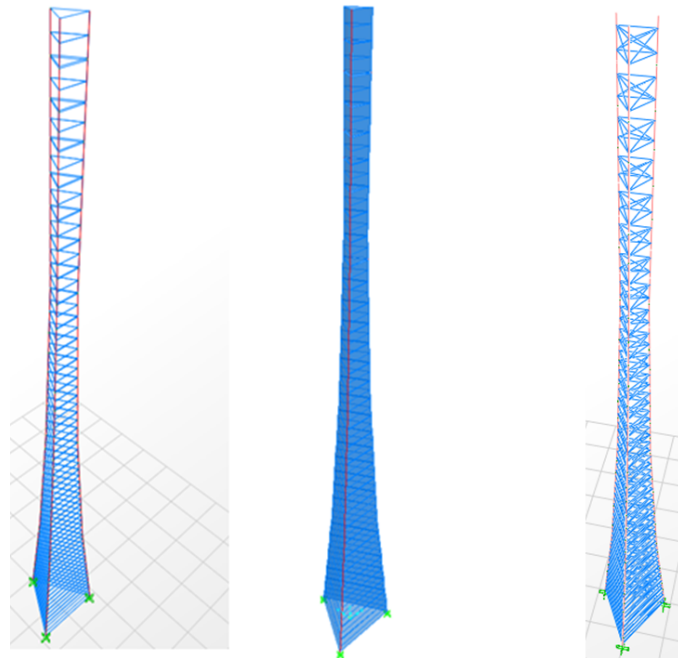


Figure D-4: SAP model for the triangular system.

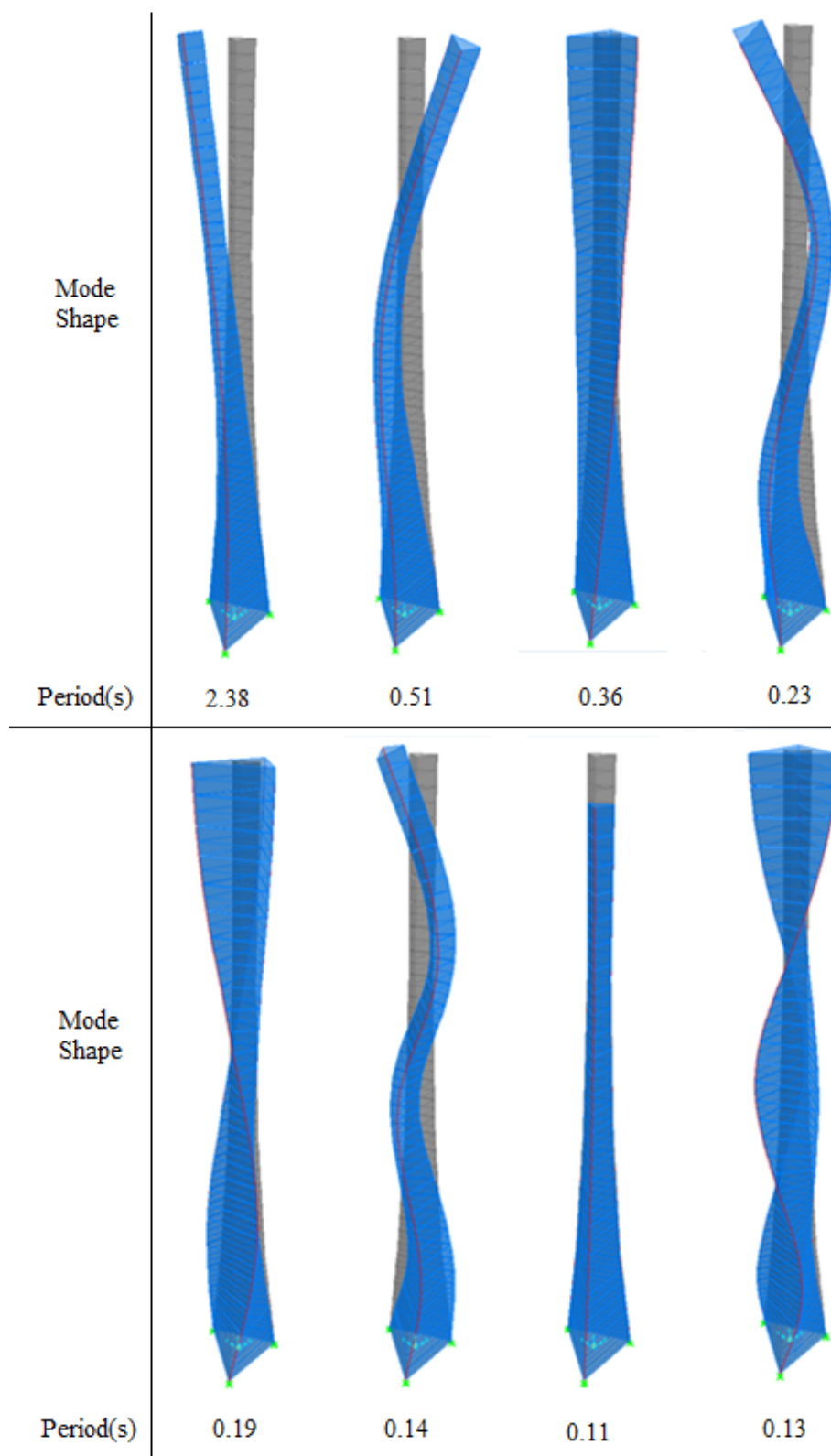


Figure D-5: Mode shapes and periods for the triangular system.